

1997

Modeling of fading dynamics for the indoor microwave channel

Mangeet Singh
Edith Cowan University

Follow this and additional works at: https://ro.ecu.edu.au/theses_hons



Part of the [Signal Processing Commons](#)

Recommended Citation

Singh, M. (1997). *Modeling of fading dynamics for the indoor microwave channel*. https://ro.ecu.edu.au/theses_hons/1015

This Thesis is posted at Research Online.
https://ro.ecu.edu.au/theses_hons/1015

Edith Cowan University

Copyright Warning

You may print or download ONE copy of this document for the purpose of your own research or study.

The University does not authorize you to copy, communicate or otherwise make available electronically to any other person any copyright material contained on this site.

You are reminded of the following:

- Copyright owners are entitled to take legal action against persons who infringe their copyright.
- A reproduction of material that is protected by copyright may be a copyright infringement. Where the reproduction of such material is done without attribution of authorship, with false attribution of authorship or the authorship is treated in a derogatory manner, this may be a breach of the author's moral rights contained in Part IX of the Copyright Act 1968 (Cth).
- Courts have the power to impose a wide range of civil and criminal sanctions for infringement of copyright, infringement of moral rights and other offences under the Copyright Act 1968 (Cth). Higher penalties may apply, and higher damages may be awarded, for offences and infringements involving the conversion of material into digital or electronic form.

**MODELING OF FADING DYNAMICS FOR
THE INDOOR MICROWAVE CHANNEL**

BY

Manjeet Singh

BEng (Honours)

**Edith Cowan University
Faculty of Science, Technology and Engineering
Department of Computer and Communications
Engineering**

Date of Submission: 30 January 1997

**EDITH COWAN UNIVERSITY
LIBRARY**

ABSTRACT

This report outlines the multipath fading phenomenon and its relationship to wireless system design. The work was conducted for the academic year of 1996. This report provides the reader with an insight into the phenomenon called fading and its relevance when designing wireless systems. Fading is an important consideration when wireless systems are to be designed. Because fading is very unpredictable and it cannot be totally eliminated in a wireless system, systems engineers have a hard time trying to design and commission efficient communication systems for a particular environment.

Over the years, there has been an existing need worldwide to design wireless systems which perform efficiently under fading conditions which is introduced into the propagation channel.

As Wireless Local Area Networks (WLAN) and Wireless Private Branch Exchanges (WPBX) have become increasingly popular, along with a whole other range of wireless systems such as Personal Communication Systems and cellular systems, the need to provide effective and efficient systems which perform well under fading conditions and also other conditions which degrade a system, has been the utmost challenge faced by systems and communications engineers.

With all this research going into designing efficient systems for communication being conducted worldwide, when the opportunity was presented by my supervisor to conduct similar research into indoor wireless systems within the microwave region, I was very excited as to the prospect of conducting research in these fields of interest.

This report outlines the background theory, which the reader will find most helpful and then presents the measurements conducted, and finally the results and analysis of the conducted measurements and its important relationship to wireless systems design within the ISM band of 2.4 to 2.5 GHz. This study investigates the various aspects of fading which affect a wireless channel under the introduction of controlled motion for a set measurement period.

The empirical data base consists of twenty five 20 second recordings of the continuous wave envelope fading waveforms with both antennas in a stationary position.

Measurements were conducted in a cluttered laboratory setting at 2.4 GHz with two quarter wave monopole antennas with transmitter and receiver separation ranging from 2 to 5 meters.

Effects of controlled degrees of motion with 2 individuals walking briskly around the antennas was investigated. The report results are presented with statistical properties such as the number of crossings at a particular level, the level crossings rates and the average duration of fades being investigated on the fading envelopes of the measurements. These results and statistical analysis can be used in designing wireless computer communication applications, such as WLAN's and also the results can be used to simulate wireless channels which use intelligent antenna systems to reduce fading.

DECLARATION

I certify that this thesis does not incorporate without acknowledgment any material previously submitted for a degree or diploma in any institution of higher education; and that to the best of my knowledge and belief it does not contain any material previously published or written by another person except where due reference is made in the text.

Manjeet Singh

30/1/97

ACKNOWLEDGMENTS

The completion of this report would not have been possible without the support and encouragement of a few people. Firstly, I would like to thank Dr. Tadeusz Wysocki for giving me the guidance, direction and opportunity to get involved in this project and also being ever so patient with me, when it came to finishing off this report. Next, I would like to thank Ted Walker for his enormous input, encouragement, experience and direction towards this report. There have been lots of times during this project completion, when the support and inspiration shown and given by Ted Walker has been invaluable. I extend my most gracious thanks and gratitude to Ted Walker. Finally, I would like to thank all the people who have contributed to the accomplishment of this project, no matter how small their input. Once again, thank you all.

TABLE OF CONTENTS

ABSTRACT	i
DECLARATION	iii
ACKNOWLEDGMENTS	iv
1. INTRODUCTION	1
1.1 Overview.....	1
1.2 Outline of the Project.....	3
2. PROJECT DEFINITION	5
2.1 Aims.....	5
2.2 Purpose.....	5
2.3 Strategy	6
3. WAVE PROPAGATION	8
3.1 Discussion.....	8
3.2 Electromagnetic Radiation.....	9
3.2.1 Electromagnetic waves	9
3.2.2 Free Space Propagation.....	11
3.2.3 Polarisation	12
3.3 Propagation losses due to environmental properties.....	15
3.3.1 Reflection of waves	16
3.3.2 Refraction of waves	19
3.3.3 Diffraction of waves	21
3.3.4 Interference of waves.....	27
3.3.5 Scattering of waves.....	28
3.4 Line of Sight Propagation (Space Wave Propagation)	29
3.5 Summary of Propagation Mechanisms	31
4. MULTIPATH FADING	33
4.1 Introduction.....	33
4.2 Multipath Propagation	34
4.3 Fading	36
4.4 The Characteristics of Multipath Fading	39
4.4.1 Types of fading	41
4.4.2 Frequency selective fading.....	41
4.5 Mathematical Modelling of the Channel	43
4.6 Multipath Fading Distributions.....	48
4.6.1 Rayleigh Distribution.....	48

4.6.2 Rician Distribution.....	50
4.6.3 Nakagami m-Distribution	51
4.6.4 Weibull Distribution	52
4.6.5 Lognormal Distribution	53
4.6.6 Suzuki Distribution.....	53
4.7 Fading Envelope Statistics.....	54
4.7.1 Level Crossing Rate (LCR).....	54
4.7.2 Average Duration of Fades	55
5. MEASUREMENTS	57
5.1 Measurement Introduction.....	57
5.2 Measurement Environment.....	58
5.3 Measurement Equipment	60
5.3.1 Antenna.....	61
5.3.2 Vector Signal Analyser and RF Section	64
5.3.3 Marconi Instruments Modulation Analyser	66
5.3.4 Aphex Systems Voltage Control Attenuator.....	67
5.3.5 3NX Computer.....	68
5.3.6 Coaxial Cables	68
5.4 Measurement System	68
5.5 Measurement System Calibration.....	72
5.6 Measurement Procedure.....	74
6. RESULTS AND ANALYSIS	77
6.1 Introduction.....	77
6.2 Procedure and Software Code.....	77
6.3 Results of The Statistical Analysis: Fading Envelopes and Statistical Data.....	82
6.3.1 Transmitter Position E and Receiver position A	83
6.3.2 Transmitter position D and Receiver position A	86
6.3.3 Transmitter position C and Receiver position A	88
6.3.4 Transmitter position B and Receiver position A	90
6.3.5 Transmitter position F and Receiver position A.....	92
6.3.6 Transmitter position H and Receiver position A	94
6.3.7 Transmitter position E and Receiver position C.....	96
6.3.8 Transmitter position G and Receiver position C	98
6.3.9 Transmitter position G and Receiver position D	100
6.3.10 Transmitter position G and Receiver position E.....	102
7. SIGNIFICANCE OF RESULTS.....	104
7.1 Introduction.....	104
7.2 Graphical Representation of the Number of Crossings	104
7.3 Graphical Representation of the Level Crossing Rates	108
7.4 Mean Statistical Parameters for Combined Fading Envelopes.....	111
7.5 Discussion of Fading and Bit Error Rates.....	115

8. CONCLUSION	118
REFERENCES.....	121
APPENDIX.....	125

Chapter 1

INTRODUCTION

1.1 Overview

The past decade has seen a phenomenal growth in wireless communications. Wireless technology is permeating business and personal communications across the globe, and the demand is driving availability and performance to new levels. Consumers are demanding small hand-held or pocket communicators, to meet their wireless voice and data communications needs. The demand for omnipresence communications has led to the development of new wireless systems, like the Personal Communication Systems (PCS), Wireless Local Area Networks (WLAN), Wireless Private Branch Exchanges (WPBX) and parasitic cellular systems [25]

Indoor radio communication covers a wide variety of situations ranging from communication with individuals in offices, homes, supermarkets, factories to fixed stations like WLAN or WPBX inside office buildings, airports, banks and other locations where flexible, reconfigurable computer networks are needed on demand [3] [8].

Due to the portable (mobile) nature of radio transceivers, the need for extensive cabling in buildings using either twisted pair, coaxial, or optical fibre cables can be eliminated. This is highly desirable where user mobility is needed. The communication that is presently being offered by indoor radio systems include transmission of voice, data and video services [31].

The main thrust of this report is focused on the indoor microwave channel and the affects of multipath fading which effects propagation within the channel. The understanding of this channel degradation affect is paramount in designing indoor wireless systems. Theoretical and also the practical nature of fading is presented to give a better understanding of multipath fading in indoor environments.

Assignments and technical standards on an international basis are set by two committees. These two committees being the International Telegraph and Telephone

Consultative Committee (CCITT) and the International Radio Consultative Committee (CCIR). The two committees in turn function under the authority of the International Telecommunications Union (ITU). The electromagnetic frequency spectrum is divided into various frequencies by the ITU.

The microwave spectrum has been a popular choice for wireless propagation due to its relatively broad bandwidth, which is a desired aspect of emerging wireless communications. The frequency range from about 300 MHz to about 60 GHz is often referred to as the “*microwave*” band. The bands of the microwave spectrum are referred to as Ultra High Frequency (UHF), Super High Frequency (SHF) and Extremely High Frequency (EHF).

In Australia the Spectrum Management Agency (SMA) regulates and controls the various frequencies used in transmission technologies. Users of microwave technologies must pay a licence fee depending on the equipment being used [12]. The SMA has allocated frequency ranges in the Industrial, Scientific and Medical (ISM) bands pertaining to systems operating within these bands, based on the frequencies designated by the ITU for use as fundamental ISM frequencies. This is based on the standards AS/NZS 20641:1992 and AS/NZS 2064.2:1992 set by Standards Australia. There are various frequency ranges allocated for ISM equipment, but the frequency range of interest is in the 2.4 - 2.5 GHz frequency range for wireless systems. The maximum radiation limit produced by equipment within the 2.4 - 2.5 GHz frequency range is dependent only on safety regulations.

The focus of this project is concerned with the effects of multipath fading in a temporally varying environment. Through introduction of controlled motion, we can see how a system reacts to this motion and what are the affects of this introduced motion to a wireless system. The gathered results and statistical analysis, can be used in designing wireless systems in relation to combating fading. Hopefully, my project results can be used to assist in the design of a wireless system and also to assist in producing simulations of a typical cluttered office environment using intelligent antenna systems and diversity techniques to see how feasible these simulation results are when

compared to the physically measured results conducted for the various antenna positions.

1.2 Outline of the Project

Chapter 1 is the introduction of this report and deals with the emerging needs for wireless communication worldwide and the effect multipath fading has on wireless systems. The relevant standards which are set worldwide by governing bodies are mentioned briefly.

Chapter 2 introduces the aims of the project, its purpose in relation to wireless systems and the strategy used to accomplish this project.

Chapter 3 deals with wave propagation within a channel. The factors which affect waves and cause multipath fading in wireless systems is presented in length. The factors include the reflection, refraction, diffraction, interference and scattering of waves.

Chapter 4 deals with the phenomenon of multipath fading. The multipath nature of waves are presented and the phenomenon of fading is also described. The types of fading which are evident in indoor communication channels are also presented. Finally, the statistical analysis needed for the results is also mentioned and explained.

Chapter 5 deals with the measurements conducted. The measurement environment is mentioned, the measurement equipment is presented along with their specifications, the measurement system and the measurement procedure is also presented. System calibration is also discussed and the calibration curve is presented.

Chapter 6 presents the important results and statistical analysis of these results. Statistical analysis considered includes the number of crossings at each level, the level crossing rates and the average duration of fades.

Chapter 7 investigates the significance of the results and the statistical analysis. It also shows graphical representations of the number of crossings and the level crossings rates for each fading envelope which is presented in chapter 6. The relationship between fades and bit error rates is also investigated.

Chapter 8 presents the conclusion of this report and summarises the entire report.

Chapter 2

PROJECT DEFINITION

2.1 Aims

The aim of the project was to perform a series of measurements in order to gather results necessary to derive a statistical model for the temporal variations of the indoor microwave channels attenuation for the ISM band. Analysis of these measurements will provide fading statistics pertaining to the indoor environment, so that a better understanding of channel fading for the ISM band can be grasped. By following this approach a better understanding of sources which contribute to fading in indoor wireless systems can be understood for the ISM frequency band and can be used to design wireless systems

2.2 Purpose

The intentions of this project is to gather experimental results and to statistically analyse these results for fading characteristics for the ISM band. The contributions from these results and statistical analysis can then be used towards designing wireless systems which perform efficiently under fading condition. Fading results were carried out for the ISM band because no fading results to date have been collected for the 2.4 GHz frequency band. Gathering experimental results was done in a planned fashion, whereby measurements were taken at a specified location being the Australian Telecommunications Research Institute (ATRI) / Cooperative Research Centre (CRC) laboratory, located at Curtin University. Measurements were carried out in a controlled environment whereby multipath fading was strongly present at every instant due to motion. This measurement environment showed the various sources which cause multipath fading and also clearly show to what extent they influence and degrade a communication channel.

Although multipath fading is only one of the attenuation factors which effects a communication channel, it is by no means the least considered factor when designing wireless communications. Multipath fading basically arises when a radio wave is reflected, diffracted or scattered by an obstruction which is in its path. Obstructions can be either man-made (buildings, cars, aeroplanes) or natural (mountains, clouds, hills).

Although multipath fading is a randomly occurring phenomenon, it can severely degrade a communication system. Therefore, in designing wireless communication systems, we must incorporate this phenomenon to minimise bit error rate degradation of a system. Through the results and their statistical analysis on fading envelopes for the measurements, we can design smarter antenna systems which can decrease the BER introduced into a wireless system by the improvement of the S/N ratio between terminals.

2.3 Strategy

This project report followed a sequence of steps whereby the aims could be achieved within the required time span allocated for the academic year of 1996. These steps were mainly dependant on hardware availability, time availability and booking requirements. The end result was that these requirements were satisfied and thus, lead to the successful accomplishment of the project. The strategy which was used to achieve the project aims was as follows:-

1. Literature review on the subject matter was conducted, so that a good understanding of the subject matter can be achieved.
2. A suitable location was decided on, being the ATRI/CRC laboratory.
3. Determine the availability of all hardware needed in carrying out the project measurements correctly.
4. Measurements for the different transmit and receive antenna positions were finalised.
5. The measurement system was then setup to carry out the measurements.
6. System testing and calibration was conducted at the start of each measurement.
7. After system calibration was completed, the 20 second measurement period for the chosen transmit and receive antenna positions were initiated with controlled motion in progress during the measurement period.
8. The 20 second fading measurements were stored onto a computer for post analysis.
9. Any additional measurements if required were investigated at this point. Once, we were satisfied we had enough measurements, statistical analysis of the fading envelopes was then carried out.

10. Statistical analysis of fading results for all the measurement positions were then conducted extensively.
11. Finalisation of the project report .

The strategy was strictly adhered to, and the successful accomplishment of the report on time was achieved with minimal problems. Step 10, proved to be the most time consuming step in this strategy as there were large amounts of data which needed to be processed within a relatively short time frame.

Chapter 3

WAVE PROPAGATION

Due to fact that this project deals with wireless communications, a brief discussion of the nature of microwave propagation is examined so that a better picture can be imaged when it comes to describing multipath fading. General characteristics of electromagnetic wave propagation is examined along with the factors which cause multipath fading in a channel. From this background information, when it comes to dealing with multipath fading a good understanding will be available. Before I go any further, I will reiterate that this is only a brief tutorial on aspects of radio wave propagation.

3.1 Discussion

The effect of the atmosphere on the propagation of energies in the microwave frequencies has been studied extensively in the past. The study of the effects of propagation on line-of-sight (LOS) paths began with the introduction of FM systems in the early 1950's [16]. The dominant mode of propagation at frequencies in the VHF band and higher is LOS. For terrestrial communication systems, the transmit and receive antennas must be in direct LOS with relatively little or no obstructions in its path [23]. LOS propagation is limited by the curvature of the earth. Due to this restriction, antenna towers must be mounted on high towers or buildings to receive LOS propagation [23]. LOS propagation will be discussed later on this chapter.

Microwave propagation necessitates line-of-sight (LOS) propagation due to its frequency characteristics. Microwave energy travels through free space in a straight line in the same manner as a light beam. This should not be a surprise as microwaves are forms of electromagnetic energy. Microwaves can propagate through space like light and heat, where they spread out as they move further and further from the source. Microwaves travel through a vacuum at the speed of light, the same for all forms of electromagnetic energy [6].

Due to the inherent LOS nature of microwave propagation, obstructions or structures in the way of signals radiated between transmit and receive antennas will be affected. Due to this obstructions in the path of propagation, it is likely that the signals will be reflected from the ground to the receiving antenna. This is especially a problem under severe weather conditions. This received signal arrives via many different paths along with the LOS path and constitutes *multipath propagation*, a detailed discussion about the nature of multipath is presented in section 4.2. The loss or gain of a signal due to the atmosphere is uniform across the radio channel bandwidth, under many propagation conditions [16].

A discussion of the nature of electromagnetic waves will now be conducted and following this, the mechanisms which govern radiowave propagation will be conducted. These mechanisms are vital to the understanding of fading in a propagation channel.

3.2 Electromagnetic Radiation

When electric power is applied to a circuit, voltages and currents are set up within it, with certain relations governed by the properties of the circuit itself. Similarly, power which is escaping into free space is governed by the characteristics of free space. Such power which escapes intentionally is said to have been radiated, and propagates in free space in the shape of what is known as an *electromagnetic wave* [17].

Free space is space which is ideal because it does not interfere with normal radiation and propagation of radio waves. Thus, it does not have any magnetic or gravitational fields, no solid bodies and no ionised particles. Although free space does not exist in the ‘real world’, it is used to approximate the propagation of waves, since it is possible to calculate the conditions if the space were free and then predict the effect of its actual properties [17]. Free space propagation is discussed in the following sub-section.

3.2.1 Electromagnetic waves

Electromagnetic waves are invisible. Waves in general are just means of transporting energy or information. Electromagnetic waves propagate through free space at a

velocity of light, c , which is about 3×10^8 metres per second [17]. The velocity of the wave slows in dense media. In pure water, the speed of the wave is about 1/9 the free space speed [4]. Typical examples of electromagnetic waves include radio waves, TV signals, radar beams and light rays. All forms of electromagnetic waves share three fundamental characteristics [28],

1. all electromagnetic waves travel at high speeds (as stated above)
2. they assume the properties of waves
3. they radiate outward from a source, without the benefit of any discernible physical vehicles.

Electromagnetic waves consists of two mutually perpendicular oscillating fields travelling together, as shown in Figure 3.1 [4],

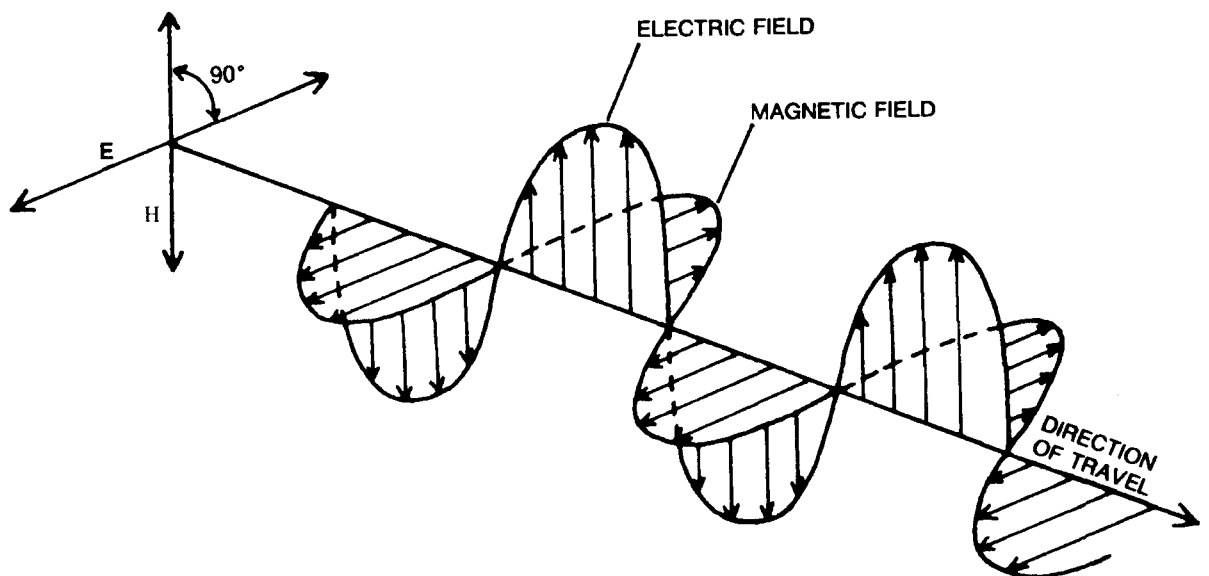


Figure 3.1 Electromagnetic wave consisting of right angle electric and magnetic fields. [4]

One of the fields is the electric field E and the other is the magnetic field H . The direction of the electric field and the magnetic field are mutually perpendicular in the electromagnetic wave [17]. This means, the fields lie in a plane that is transverse or

orthogonal to the direction of wave propagation. Each of the E and H is called a uniform plane wave because E (or H) has the same magnitude throughout any orthogonal or transverse plane [28]. The polarisation, of an electromagnetic wave is defined as the direction of the electric field E [4]. This designation is especially convenient as it tells us the type of antenna used, either vertical or horizontal polarised. For more on polarisation, see section 3.2.3.

3.2.2 Free Space Propagation

According to [17], since there are no interferences or obstacles in free space, an electromagnetic wave will spread out in all directions from a point source at a constant rate. An analogy of this point, is when we switch on a light bulb and it radiates light in all directions. Figure 3.2 shows a spherical wavefront originating from a isotropic source.

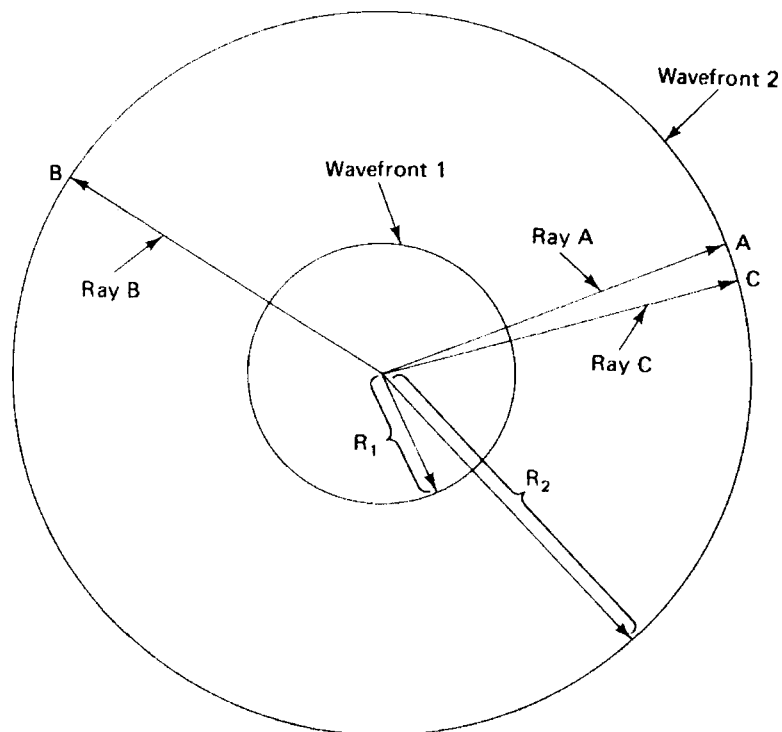


Figure 3.2 A spherical wavefront from an isotropic source [30]

Such a source is called an isotropic radiator. Although a true isotropic radiator does not exist, it can be closely approximated by an omnidirectional antenna [30]. A spherical

wavefront is produced by an isotropic radiator with radius R . All points which are a distance R from the source lie on the surface of the sphere and have equal power densities. For example, in Figure 3.2 points A and B are equal distance from the source, which means that their power densities are equal [30]. At any instant of time, the total transmitted power P_t is uniformly distributed over the entire surface of the sphere (assuming a lossless transmission medium).

This results in the power density at any point on the sphere is the total transmitted power divided by the total area of the sphere [30].

This is mathematically represented by,

$$\mathcal{P} = \frac{P_t}{4\pi R^2} \quad (3.1)$$

where,

\mathcal{P} = power density at a distance R from an isotropic source

P_t = total transmitted power

R = radius of the sphere

This power density decreases as the wavefront propagates further from the source. This is why a signal gets weaker when the receive antenna is moved further away from the transmitter [6]. The total distributed power over the surface remains the same. According to [30], because the area of the sphere increases in direct proportion to the distance from the source squared, the power density is inversely proportional to the square of the distance from the source. This is the inverse-square law, which applies to all forms of radiation in free space [17].

3.2.3 Polarisation

Up to now, we have dealt with radio propagation as if it were pure energy. Polarisation is a property of electromagnetic waves, which depends on the angle of rotation (orientation) of the transmitting antenna [6]. An antenna can be either linearly polarised

or circularly polarised. Linearly polarised antennas can be either horizontal or vertical depending on whether the antenna elements lie in a horizontal or vertical plane [30]. An example of linear polarisation using a dipole rod antenna is illustrated in Figure 3.3.

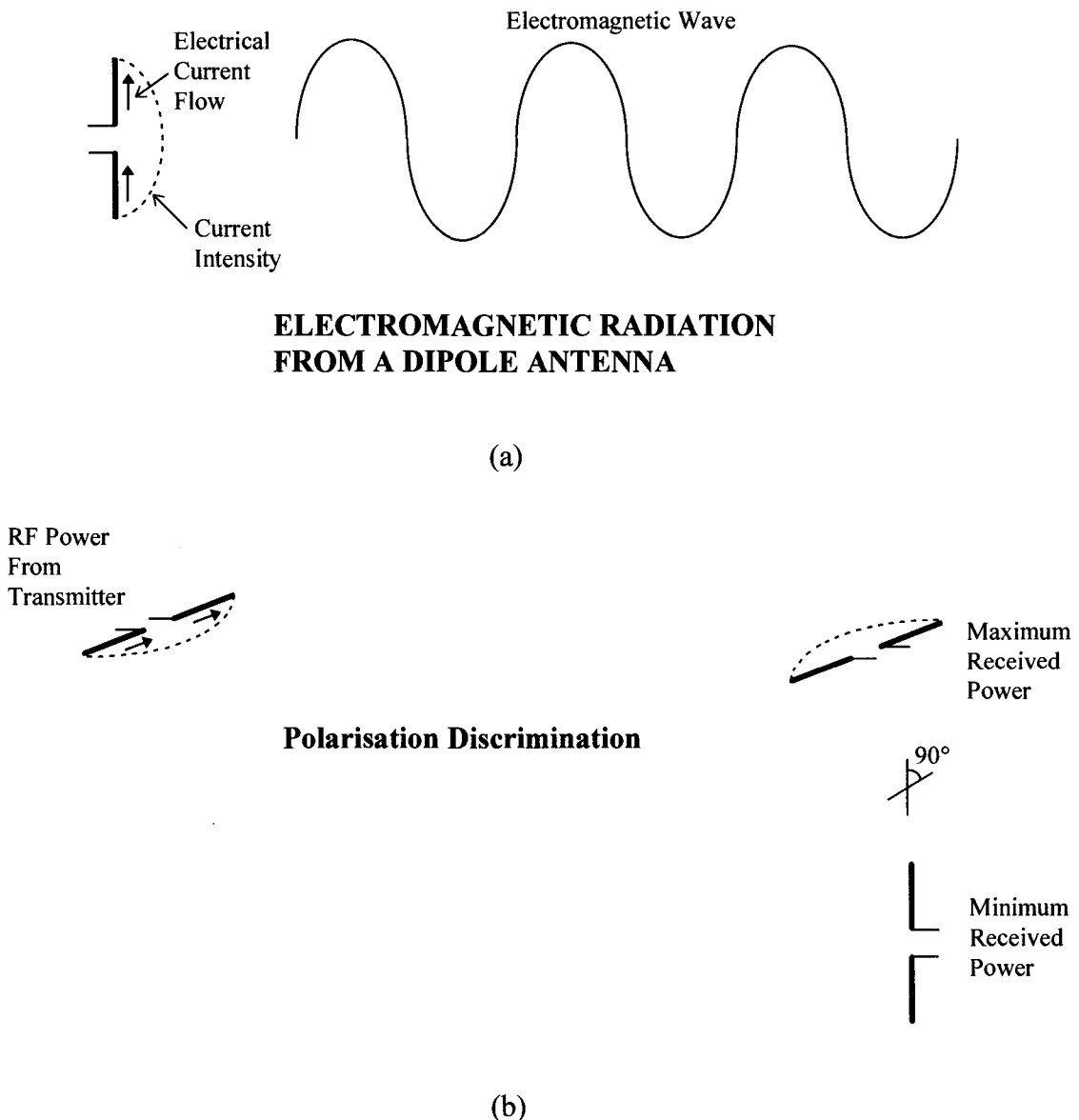


Figure 3.3 Properties of linear polarised dipole rod antennas: (a) vertically polarised; (b) horizontally polarised [6]

From Figure 3.3 (a), the electrical current from the transmitter flows along the dipole antenna rod in an upwards and downwards direction, oscillating at the transmission frequency. As a result, the alternating current in the dipole rods produce an

electromagnetic wave which propagates off into space. The electrical currents in the rods cause the electromagnetic wave to have its electric vector component lined up in the same direction, which is vertical for this illustration [6]. Thus an antenna which radiates a vertically polarised electromagnetic wave is said to be vertically polarised [30].

Horizontal linear polarisation is produced when the dipole is rotated 90° , so that the direction of the electric current is horizontal. This thus produces a horizontal electromagnetic wave radiating off into space, as shown in Figure 3.3 (b). A reception occurs when the electric component of the incoming wave produces a current in the receiving antenna.

From this illustration, we can see that if the conductors of the receiving antenna are improperly aligned, then the reception of the incoming wave will not occur [6]. Horizontally polarised transmitting and receiving antennas provide for the maximum amount of power to be carried (coupled) between them. The antenna pairs are said to be co-polarised. A vertical polarised receiving antenna, which is perpendicular to and therefore cross-polarised with the transmitter, produces minimum amount of coupled energy [6].

The other type of polarisation is circular polarisation. Circular polarisation can be produced by combining two linearly polarised waves [26]. These two linearly polarised waves can be represented by vectors, where the direction of the vector is in line with the electric component. In circular polarisation, these two vectors are out of phase by 90° with respect to each other. This is done by first splitting the transmit signal in two at the source and delaying one of them by a quarter period before radiating them through an antenna. The resultant vector rotates like a corkscrew, as it propagates through free space [6]. The rotation can either be clockwise (right-handed) or counterclockwise (left-handed), depending on which direction of rotation of the electric field vector is seen by an observer looking in the direction of travel of the propagation wave [15]. Figure 3.4, shows a clockwise rotation of the electric component during circular polarisation.

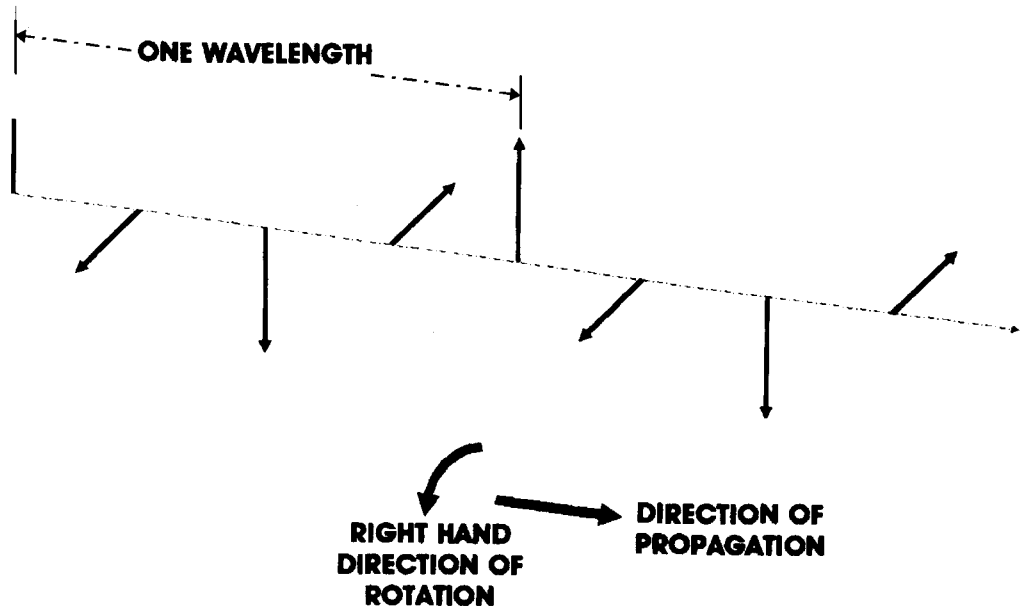


Figure 3.4 Rotation of the electric component during the propagation of a circularly polarised signal [6]

3.3 Propagation losses due to environmental properties

When near earth propagation is dealt with, several factors which did not exist in free space propagation must be considered [17]. These atmospheric phenomena which can be random or time varying, causes a loss in the propagation path. When taken in consideration, these losses can and will reduce the strength of the received signal by causing its level to vary over time which can lead to signal fading [6].

Thus, electromagnetic waves propagated from a transmitter will be reflected by obstacles such as buildings, mountains or the ground. These waves will also be refracted as they pass through different layers of the atmosphere due to the difference in densities or differing degrees of ionisation. The electromagnetic waves can be diffracted around tall, massive obstructions such as mountains or hilly terrains. Waves can also interfere with one another after two or more waves which have travelled from the source meet. The energy of these waves can also be absorbed by the atoms or molecules in the atmosphere, which leads to a reduction of power densities. These

environmental effects will now be discussed in more detail, so that a good background is established when it comes to dealing with the fading phenomena.

3.3.1 Reflection of waves

Electromagnetic wave reflection occurs when an incident wave (transmitted wave) strikes a boundary of two media and some or all of the incident power does not enter the second media. Basically, any wave that does not penetrate the second media is reflected [30]. There is much similarity between the reflection of light by a mirror and the reflection of electromagnetic waves by a conducting medium [17]. Figure 3.5, shows the concept of reflection between two media [30].

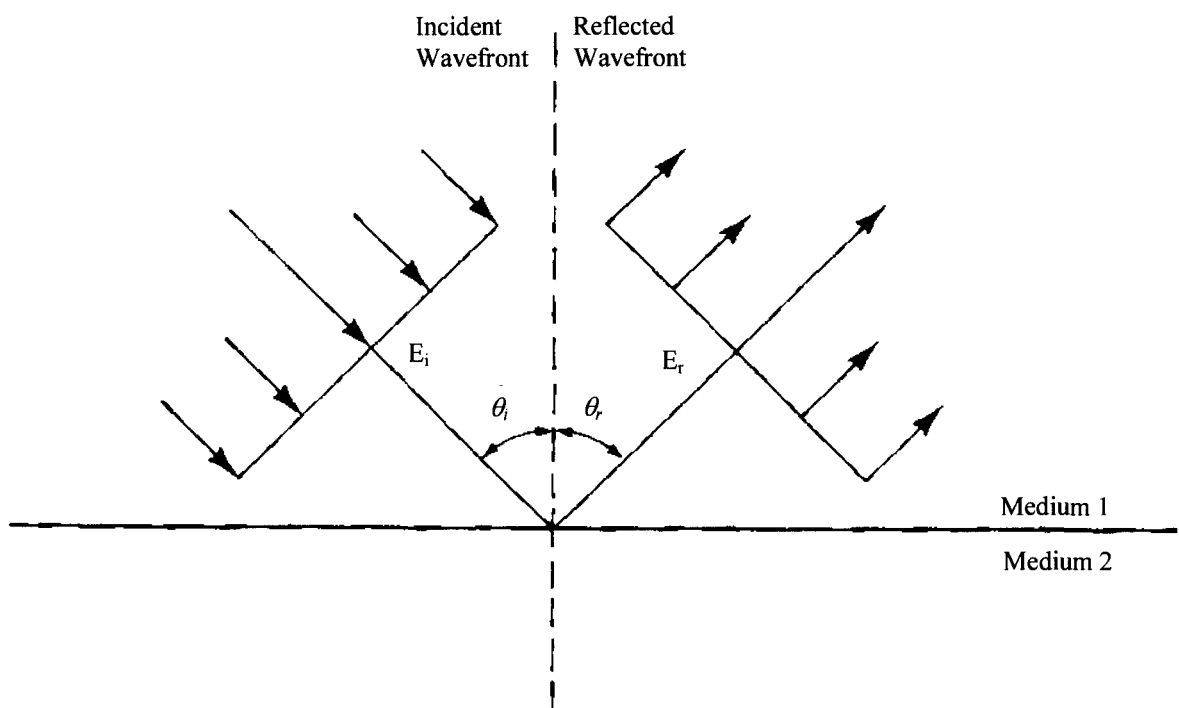


Figure 3.5 Reflection of an electromagnetic wave at a plane boundary of two mediums

As can be seen from the diagram, because all the reflected waves remain in medium 1, the velocities of the incident and reflected waves are equal. Consequently, the angle of incidence and the angle of reflection are also equal ($\theta_i = \theta_r$) [30]. This proof of the

equality of the angles of reflection and incidence follows the corresponding proof of the second law of reflection for light [17].

When a signal is transmitted or reflected off a partition, wall or object, the amount of phase change and signal attenuation depends on the complex transmission coefficient T and reflection coefficient R . These coefficients are computed from the permittivity of the materials ϵ , the signal encounters. Other factors which affect the transmission and reflection of the signal are the angle of incidence and the relative polarisation (see section 3.2.3).

The complex transmission coefficient is defined as the ratio of the transmitted to the electric field strengths E_t / E_i [29], it is the portion of the total incident power which is not reflected [30]. For a perfect conductor, T is equal to zero. The reflection coefficient is defined as the electric intensity of the reflected wave to that of the incident wave E_r / E_i . The reflection coefficient is used to indicate the relative amplitude of the reflected and incident fields and also the phase shift which occurs at the point of reflection [30]. For a perfect conductor or reflector the reflection coefficient is equal to 1. For other practical conducting surfaces the reflection coefficient is less than 1, the difference is due to the abortion of energy of the wave by the imperfect conductor [17]. The transmission and reflection coefficients will be discussed further in section 4.5, when a mathematical model is presented.

If a reflecting surface is not plane (ie.,it is curved) the curvature of the reflected wave is different to the curvature of the incident wave. When the reflective surface is plane and the wavefront of the incident wave is curved, the curvature of the reflected wavefront is the same as that of the incident wavefront [30].

Reflection which occurs at irregular or rough surfaces can destroy the shape of the wavefront. When an incident wavefront strikes a rough surface the wavefront is scattered in many directions, resulting in a diffused reflection. Specular reflection is when waves are reflected from a perfectly smooth surface, like a mirror. Semirough surfaces are surfaces which fall between specular and diffused reflections. Semirough

surfaces will not completely destroy the shape of the reflected wavefront, but there will be a reduction in the total power. The Rayleigh criterion states that a semirough surface will reflect as if it were a smooth surface, as long as the angle of incidence (θ_i) is greater than $\lambda/8d$ [17]. Figure 3.6 shows reflection from a semirough surface.

The Rayleigh criterion can be shown mathematically as [30],

$$\cos \theta_i = \frac{\lambda}{8d} \quad (3.3)$$

where,

d = depth of surface irregularity

λ = wavelength of the incident wave

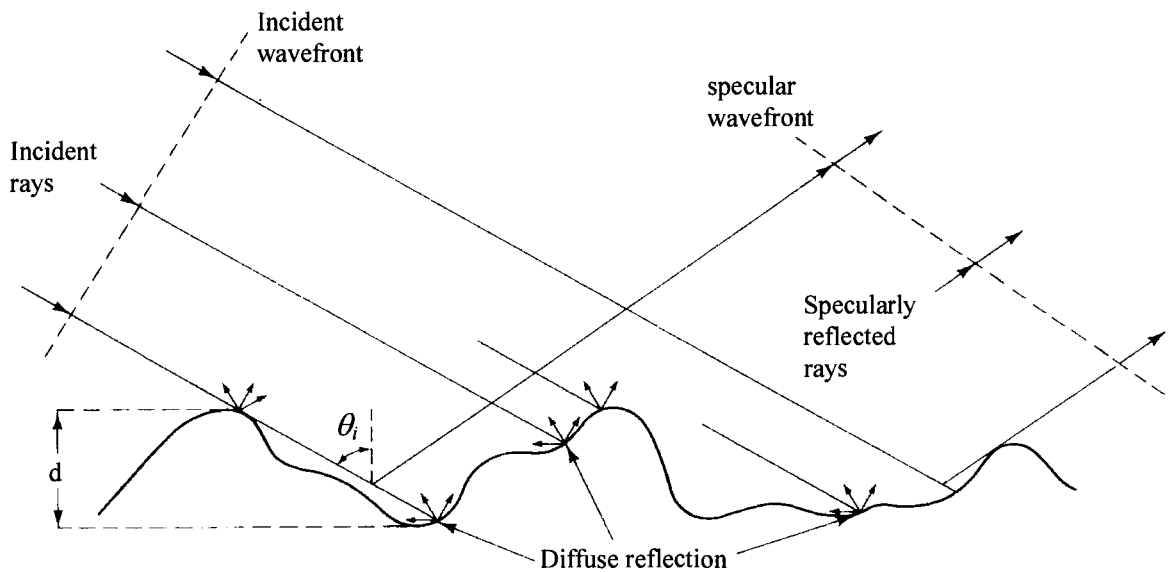


Figure 3.6 Reflection from a semirough surface [30]

3.3.2 Refraction of waves

Refraction is the change in direction of a ray when it passes from one propagating medium to another medium which has a different density. This causes the wavefront to change to a new direction in the second medium and is brought about by a change in the wave velocity [17] [30]. Figure 3.7 shows refraction of a wavefront at a plane between two different mediums with different densities [30].

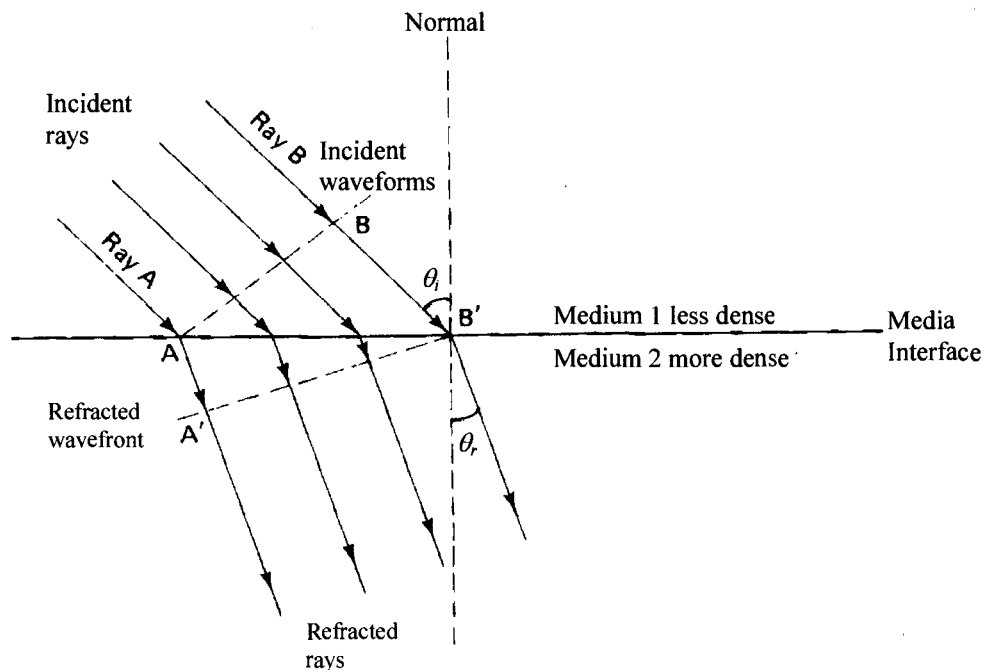


Figure 3.7 Refraction at a plane between two media [30]

From Figure 3.7, it can be seen that ray A enters the denser medium 2, before ray B. Consequently, ray B propagates slower than ray A and travels the distance B-B' during the same time ray A travels the distance A-A', this results in a bend of the wavefront A'B' in a downward direction. Whenever, a ray is passed from a less dense to a more dense medium, it effectively bends toward the normal. If a ray passes from a more dense medium to a less dense medium, it effectively bends away from the normal. The angle of incidence θ_i is the angle formed between the incident wave and the normal, and the angle of refraction θ_r is the angle formed between the refracted wave and the normal [30]. The amount of bending or refraction of a wavefront depends on the refractive

index of the two materials. The refractive index is the ratio of the velocity of propagation of light in free space to the velocity of propagation of light in a given medium [30].

Mathematically this ratio is represented as [30],

$$n = \frac{c}{v} \quad (3.4)$$

where,

n = refractive index

c = speed of light in free space

v = speed of light in a given material

The effect of how an electromagnetic wave reacts when it is incident on a surface of two transmissive materials which have different refractive indices, can be explained with Snell's Law. The angle of incidence is equal to the angle of reflection, according to Snell's Law. Snell's Law states that [30],

$$n_1 \sin \theta_i = n_2 \sin \theta_r \quad (3.5a)$$

and

$$\frac{\sin \theta_i}{\sin \theta_r} = \frac{n_2}{n_1} \quad (3.5b)$$

where,

n_1 = refractive index of material 1

n_2 = refractive index of material 2

θ_i = angle of incidence

θ_r = angle of refraction

Also, since the refractive index is equal to the square root of its dielectric constant, equation (3.5b) can be shown as,

$$\frac{\sin \theta_i}{\sin \theta_r} = \sqrt{\frac{\epsilon_2}{\epsilon_1}} \quad (3.6)$$

where,

ϵ_1 = dielectric constant of medium 1

ϵ_2 = dielectric constant of medium 2

If a boundary between two mediums are curved, refraction still takes place [17]. For example, if a transmission medium is more dense at the bottom and less dense at the top, then the rays which are travelling at the top travel faster than the rays at the bottom and consequently the wavefront will tilt in a downward direction as it progresses through the medium [30].

3.3.3 Diffraction of waves

Diffraction occurs when the path between the transmitter and receiver is blocked by an impenetrable object [1]. Diffraction is the phenomenon that allows radio waves to propagate around corners [30]. When we discussed reflection and refraction of wavefront previously, we assumed that the dimensions of surfaces were very much larger in respect to the wavelength of the signal. However, when a signal passes near an obstruction or surface which has similar dimensions as the wavelength, simple geometrical analysis cannot be used to explain the results. We must therefore use Huygens' principle to explain the results produced by these wavefronts [30].

Huygens' principle states that every point on a spherical wavefront can be regarded as a source of electromagnetic waves from which other wavefronts are radiating outward. Huygens' principle is illustrated in Figure 3.8 [30].

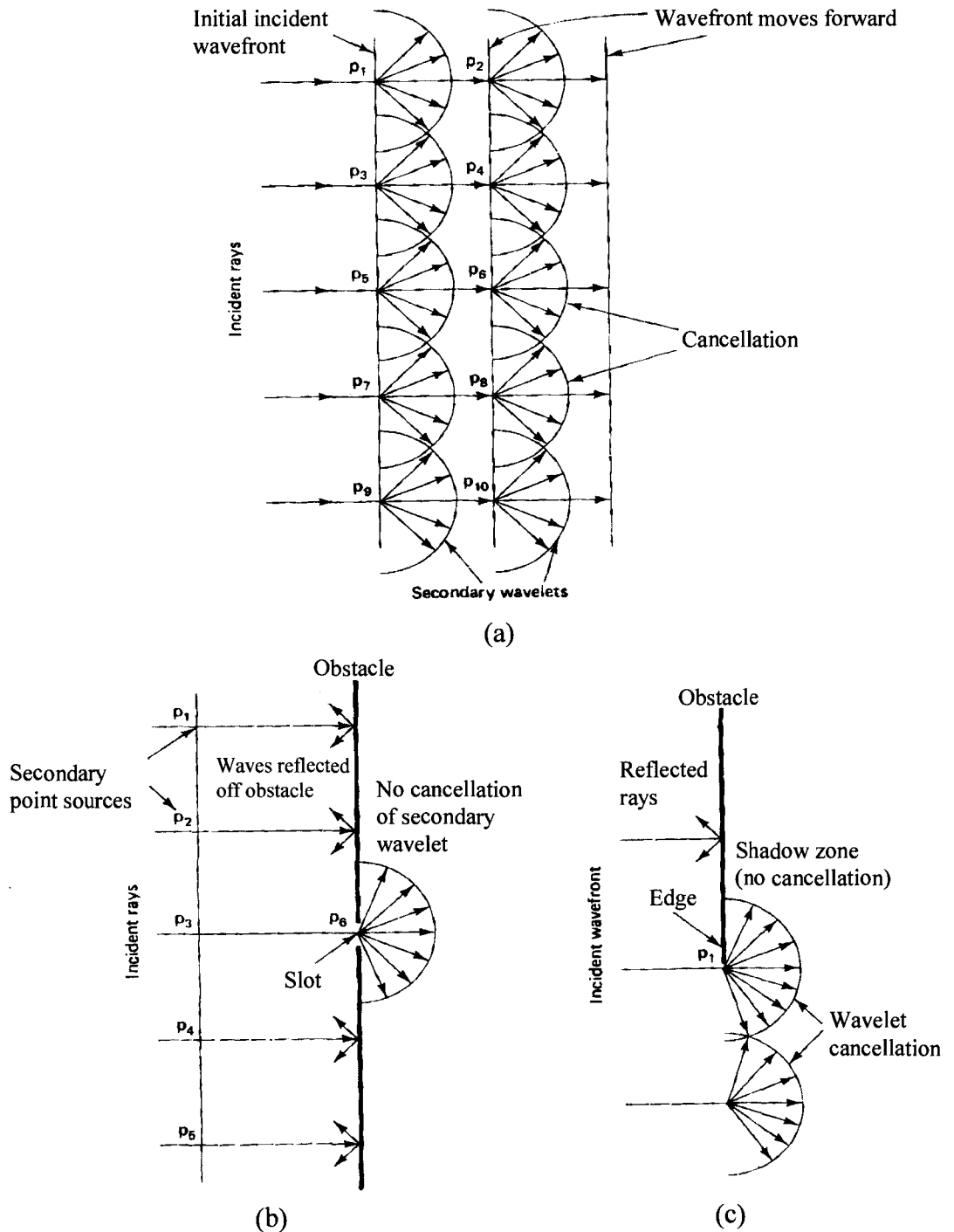


Figure 3.8 Diffraction: (a) of a plane wavefront; (b) of a finite wavefront through a small slot; (c) around the edge of an obstacle [30]

The total field which is at successive points away from the source is then equal to the vector sum of these secondary wavelets [17]. As shown in Figure 3.8 (a), when considering a plane wavefront energy is radiated in an outward direction from each secondary point source (p_1 , p_2 , p_3 , etc.). However, due to the cancellations of the

secondary wavelets which happens in all directions except forward causes the wavefront to continue in its original direction rather than spread out. Therefore, the wavefront remains plane.

When a finite wavefront is considered, the cancellation in spurious direction is no longer noticeable, however the wavefront must be small, which is produced by a small slot in a plane. As shown by Figure 3.8 (b), instead of being pushed through the slot, the wavefront spreads or scatters out past the small slot. This scattered wave now acts as Huygens' point source and proceeds in all directions [17]. This scattering effect is called diffraction [30].

Figure 3.8 (c), shows diffraction by a sharp edge of an obstacle. Only partial wavelet cancellation occurs. Diffraction occurs around the edge of the obstacle, which allows the secondary waves to progress around the corner of the edge into what is called the shadow zone. A similar phenomenon is experienced when a door is opened into a dark room, where light rays diffract around the door's edge and light up the area behind the door [30]. Due to shadowing RF energy can travel into rural and also urban environments without a LOS path. [1]. The degree of diffraction affects in any given case is a function of the wavelength of the signal, the size of the obstruction and its electromagnetic properties [4].

When the ray diffracts around corners from the transmitter and reaches the receiver, we can represent this mathematically as [13],

$$|E_i|^2 = \frac{Z_0 P_e \prod_m D^2(\alpha_m)}{4\pi \sum_m L_n \prod_m L_n} \quad (3.7)$$

where,

- E_i = electric field intensity of the i th ray
- Z_0 = freespace wave impedance
- P_e = effective transmitted power
- L_n = length of the ray path between diffracting sites

$D(\alpha_m)$ = diffraction coefficient for a ray bending through an angle α_m at an absorbing screen

The diffraction coefficient $D(\alpha_m)$ can be represented mathematically as [13],

$$D(\alpha_m) = \frac{1}{\sqrt{2\pi k}} \left[\frac{1}{2\pi + \alpha_m} - \frac{1}{\alpha_m} \right] \quad (3.8)$$

The summation term in the denominator of equation (3.7), accounts for the vertical spreading of the ray, while the product term in the denominator accounts for the horizontal spreading. At each corner of an obstacle, a ray bends through an angle α_m . Diffraction is also significant for wavefronts reaching receiver sites around corners at the end of long hallways or rooms [13].

Fresnel Zones Phenomenon

As mentioned above diffraction occurs when wavefronts encounter opaque objects in their path. The degree of diffraction and its harmful effects on a wavefront is frequency related.

There is a minimum clearance which is required to prevent attenuation from diffraction. Calculations of the required clearances comes from the Fresnel wave theory [4]. This is the additional clearance which is added to an obstacle to maintain a strong receive signal at the receive antenna.

Energy is assumed to propagate from the transmitting antenna to the receiving antenna along a straight path called the direct path. A wavefront expands when it travels, resulting in reflection, refraction, diffraction and phase changes as it passes over an obstacle. This in turn causes an increase or decrease in the signal level received. The regions where these path losses takes place are called Fresnel zones. For instance, about half of the signal reaching a receiver antenna passes through the first Fresnel zone.

Consequently, terrain features which do not intrude into the first Fresnel zone cannot significantly change the level of the received signal [16]. As can be seen from Figure 3.9, the first Fresnel zone is the locus of points in space for which all indirect paths differ by half a wavelength ($\lambda/2$) at most from the direct path length.

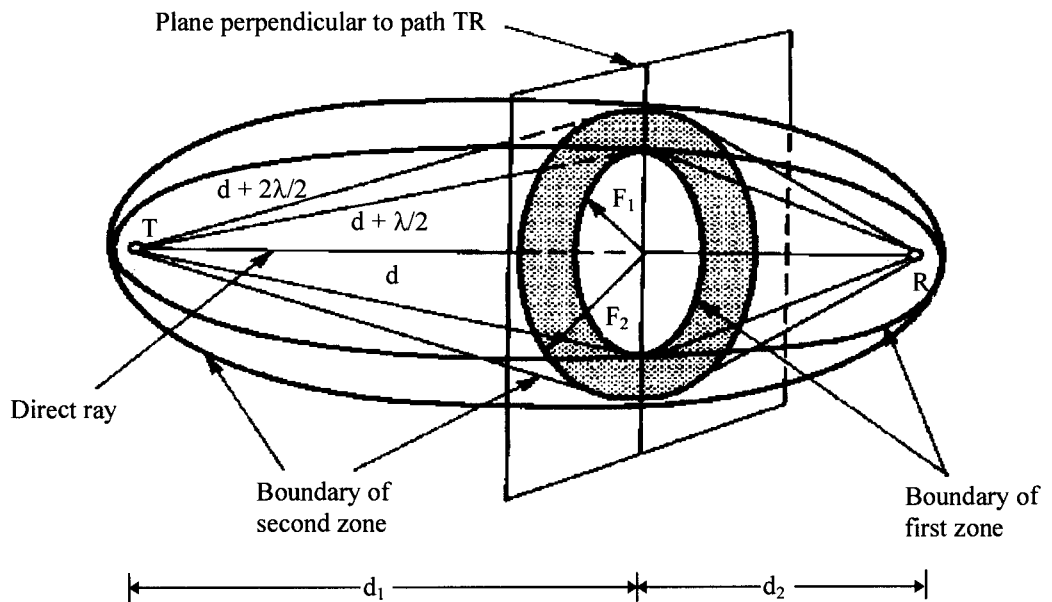


Figure 3.9 Three dimensional representation of the first two Fresnel zones of a direct path propagation ray [16]

The first Fresnel zones boundary is an ellipsoid, with the two antennas at the focal points. Higher order zones are also defined in a similar manner [16]. The second Fresnel zone contains all points that define a two segment path by which its length is greater than the direct path by more than $\lambda/2$, but less than $2(\lambda/2)$ [16]. It is found in practice that only signals reflected within the first Fresnel zone have large enough amplitudes to produce significant interference. However, precautions are taken to keep these zones free of any obstacles.

The radius of the n th Fresnel zone at a point defined by the geometry of figure 3.9 [21],

$$R_n = \sqrt{\frac{n\lambda d_1 d_2}{d_1 + d_2}} \quad (3.9)$$

where,

d_1, d_2 = the terminal distances from the obstruction

n = is an integer

λ = wavelength of the wave

In radio propagation, the receiver field R, is influenced by the obstacles which lie in, or close to the LOS path as shown in Figure 3.10. If the straight-edge obstacle which is between the transmitter (T) and receiver (R) does not encroach into the first Fresnel zone than the field at R is unaffected. However, if the height is increased the field strength at R oscillates with increasing amplitude. The point where the obstructing edge is just in line with T and R, the strength of the field at R is 6 dB below the free-space value. If the height of the obstruction is increased further, so that the LOS path is actually blocked, the oscillations cease and the field strength decreases steadily with height [21].

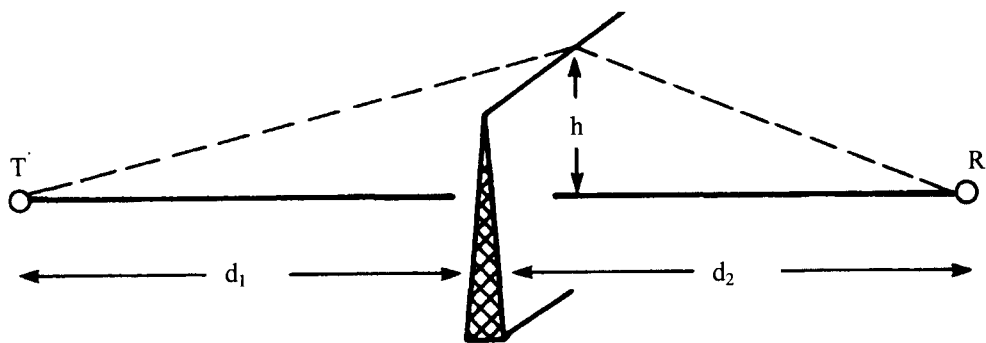


Figure 3.10 Knife-edge diffraction geometry [21]

3.3.5 Interference of waves

Interference occurs when two or more waves combine or add up in such a way that the performance of a systems is degraded. The resultant waveform is strongly dependent on the phases of the interfering waves. Interference is based on the principle of linear superposition of electromagnetic waves and occurs when two or more waves occupy the same point simultaneously in space. The principle of superposition, as mentioned by [26], states that when several waves combine at a point, the displacement of any particle at any given time is simply the vector sum of the displacements that each individual wave acting alone would give [26]. With free space propagation, a phase difference may exist due to the electromagnetic polarisation of two waves differ. Depending on the phase angles of these two wave vectors, either addition or subtraction will result [30].

Consider two sinusoidal waves of equal wavelength and amplitude, travelling in the x direction. One wave has a phase constant of ϕ , while the other has a phase constant $\phi = 0$. Figure 3.11 shows the effects of waves interfering constructively and destructively. Figure 3.11(a), shows the resultant waveform of two waves ($y_1 + y_2$) which are nearly in phase (ϕ nearly equal to zero). Figure 3.11(b), shows the resultant of the two waves ($y_1 + y_2$) which are nearly out of phase (ϕ nearly 180°). By merely adding the individual displacements at each x in Figure 3.11(a), we see that there is nearly complete reinforcement of the two waves and the resultant wave has nearly doubled the amplitude of the individual components of the two waves. Whereas in Figure 3.11(b), we see that there is almost complete cancellation at every point and the resultant amplitude is close to zero [26]. Figure 3.11(a) shows constructive interference, while Figure 3.11(b) shows destructive interference.

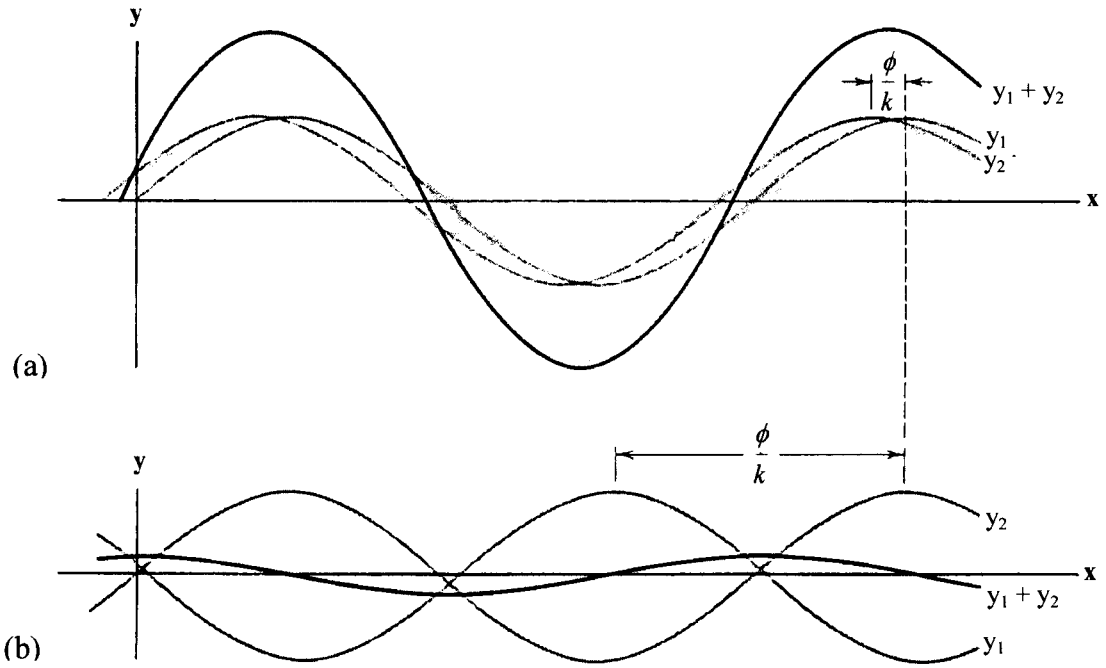


Figure 3.11 (a) Constructive interference of two almost in phase waves
 (b) Destructive interference of two almost 180° out of phase waves [26]

If the phase difference, $\Delta\phi = (\phi_2 - \phi_1)$, between two waves is exactly zero, this means the two waves have the same phases everywhere. This leads to total constructive interference, whereby the crest of one wave falls exactly on the crest of the other and the valley of one wave falls on the valley of the other. The resultant amplitude is just twice that of either wave alone. On the other hand, if the phase difference is close to 180° , the resultant amplitude will be nearly zero (as shown in Figure 3.11(b)). However, if the phase difference of any two waves is exactly 180° , then the crest of one wave falls exactly on the valley of the other wave. This leads to a resultant amplitude of zero, which corresponds to total destructive interference [26].

3.3.6 Scattering of waves

Scattering of waves occurs when the dimensions of the object interacting with the microwave is on the order of the impinging wave's wavelength or less. Following the physical principles of diffraction, scattering causes the energy from the transmitter to be

re-radiated in many different directions [1]. Scattering of waves in built-up areas depends on the geometry and terrain, and the radio channel between a transmitter and a receiver therefore has randomly time-varying characteristics [21]. Microwaves which can be effected by water droplets causes the signal to be scattered in many direction. This reduces the LOS path power level, whereby some of the signal can be sprayed back towards the source [6].

Scattering has proven be the most difficult propagation loss mechanism to predict in emerging wireless communication systems. For example, in urban microcellular systems, lamp posts, street lights and buildings scatter energy in many directions. Consequently, providing RF coverage to areas which do not receive energy via reflection or diffraction [1].

3.4 Line of Sight Propagation (Space Wave Propagation)

There are four major propagation path characteristics: surface wave, space wave, tropospheric and sky-wave propagation [4]. Space waves and surface waves are both 'ground waves' but behave differently, so they are split up into separate propagation considerations. Because microwaves follow space wave propagation paths we will discuss this propagation path and ignore the other three propagation paths.

According to [17], space waves behave with merciful simplicity. Space waves depend on LOS conditions and they are limited in their propagation by the curvature of the earth. Their mode of behaviour is forced onto them because the ground wave disappears very close to the transmitter and their wavelengths are too short to be reflected by the ionosphere [17]. The space wave follows the ground wave phenomenon, but it radiates from an antenna many wavelengths from the earth's surface [4]. It travels in the lower few kilometres of the earth surface and no part of the space wave normally touches the surface [4][30]. Space waves include two components, which are both the direct and ground reflected waves as shown in Figure 3.12 [30].

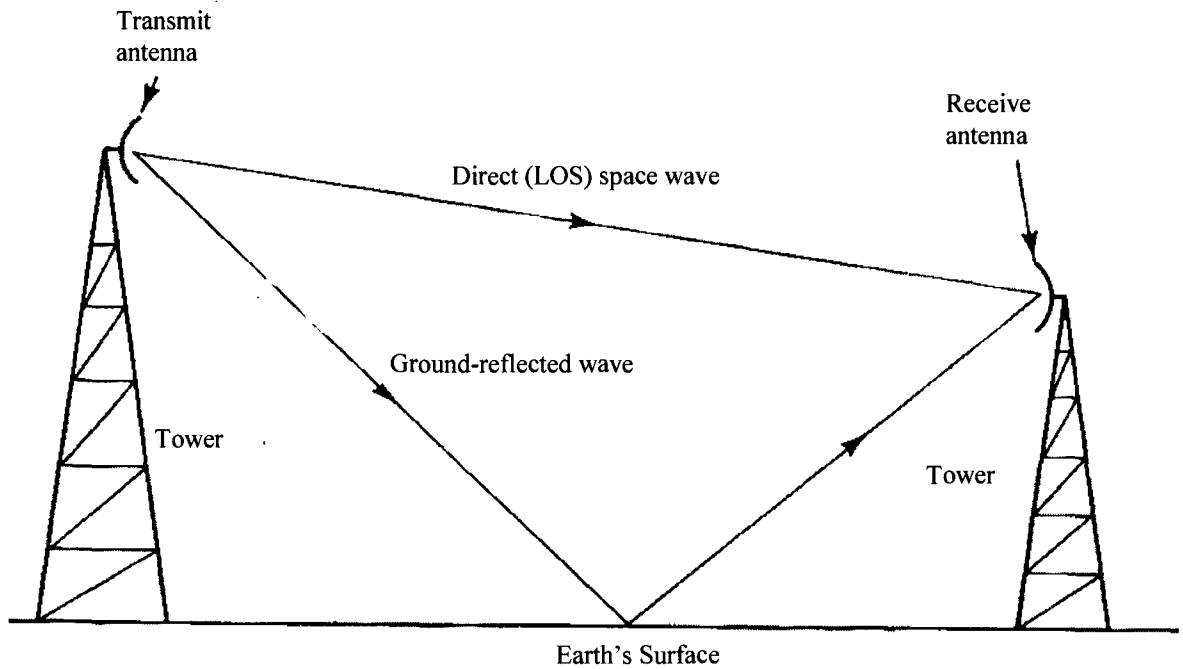


Figure 3.12 Multipath propagation which shows the direct and reflected waves of space wave propagation [30]

The direct wave is the wave which travels in a straight line between transmitter and receiver. Ground reflected waves are waves which are reflected by the earth's surface or other obstructions as they travel between transmitter and receiver [30].

Space waves are affected by factors such as: wavelength, height of both transmit and receive antennas, distance between antennas, terrain and weather along the transmission path. If both the direct and reflected waves arrive at the receiver they will add algebraically to either increase or decrease the signal strength. There is also a phase shift between the two components because the two signal paths have different lengths. Additionally, there may also be a 180° phase reversal at the point of reflection. As a general rule, a phase-shift of an odd number of half wavelengths causes constructive interference (see section 3.3.4). A phase shift of an even number of half wavelengths causes destructive interference. Phase shifts which are other than half wavelengths add or subtract according to relative polarity and amplitude. The reflected signal constitutes both amplitude and phase changes. The phase change is typically 180 degrees and the amplitude change is a function of frequency and the nature of the reflecting surface [4].

Figure 3.12, also illustrates the nature of multipath propagation, whereby the signal arrives via a direct path and also an ensemble of secondary paths that are reflected from the ground terrain. The reflected path arrives, as mentioned, at the receiver with various delays and thus constitutes multipath propagation. The multipath signal components generally have different carrier phases offsets and, hence, the waves may add destructively at times, resulting in the phenomenon called signal fading. A more elaborate discussion on the topic of multipath propagation and signal fading will be discussed in section 4.2 and 4.3, respectively.

3.5 Summary of Propagation Mechanisms

Many of the propagation mechanisms discussed earlier can be present in a transmission path at the same time and it is very difficult to predict which specific mechanism is producing the change in the signals strength. Figure 3.13, indicates which mechanisms affect the parameters of a signal on a communication link [15].

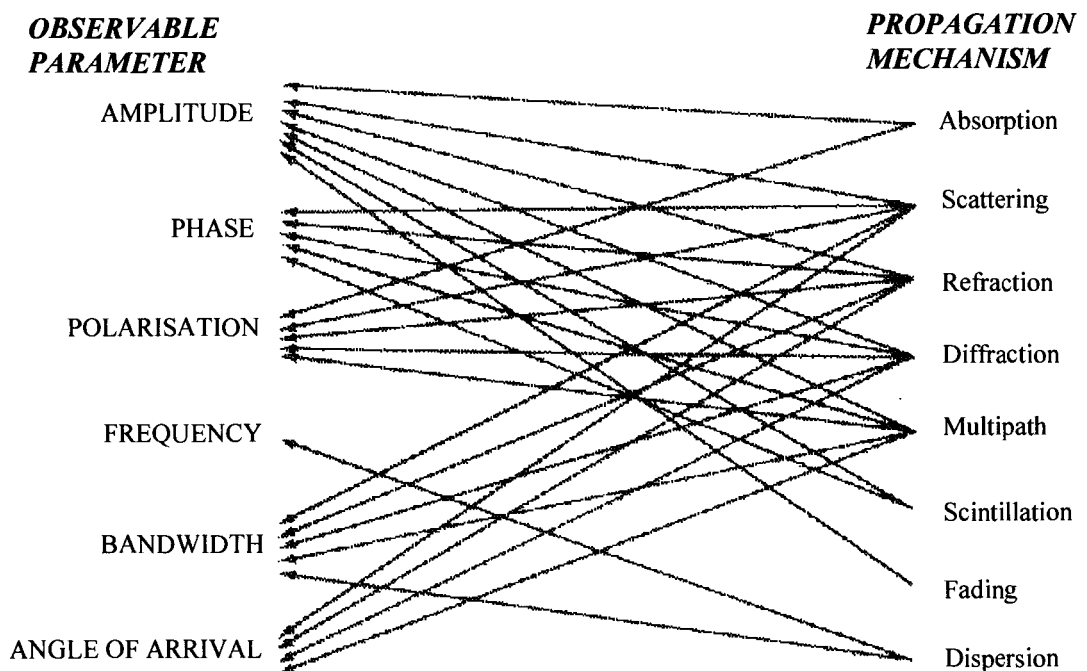


Figure 3.13 Radiowave propagation mechanisms and their impact on a communication signals parameters [15]

Each of these mechanisms, if present in the signal path, will affect one or more of the signals parameters. If a reduction in signal amplitude is received then a number of these mechanisms could have caused it. These include absorption, diffraction, fading, multipath, refraction, scattering, scintillation, or even a combination of the above. Therefore, when there is a variation in the signal parameters, one or several propagation mechanisms could be present in the link [15].

Finally, a glossary of the standard terms and definitions used in this chapter to explain propagation of waves in presented in the Appendix. These standards and terms are based on The New Institute of Electrical and Electronics Engineers (IEEE) Standard Dictionary of Electrical and Electronics Terms.

Chapter 4

MULTIPATH FADING

4.1 Introduction

This chapter concerns itself with the main thrust of this project, which is fading in the indoor environment. The indoor environment is not affected by terrain features of the outdoor environment and atmospheric conditions, such as rain, snow, hail, fog, ice or clouds. But, because of the geometry of buildings such as size, shape, structure, layout of rooms and the type of construction materials used, electromagnetic wave propagation within buildings are more complex multipath structures than terrestrial radio channels [29]. Besides the basic building structures (such as walls, floors and ceilings), furnishings and people serve as scatterers of radio waves [13].

This report considered multipath propagation characteristics between transmit and receive antennas, on the same floor of the ATRI laboratory which is situated on the ground floor of the New Technologies building (building no. 304) at Curtin University. The geometry of the laboratory includes features which can be treated separately. These features include, firstly, the vertical clear space between floor and ceiling, or between objects and the ceiling. The second feature, consists the walls and objects at which reflection and transmission of the signal takes place in the horizontal plane (see section 3.3.2 and 4.5). Lastly, depending on the geometry of the objects and walls, it is also possible for waves which diffract around corners of obstacles to reach the receive antenna (see section 3.3.3) [13].

In this chapter we will discuss the nature of the indoor propagation channel and the affects of multipath fading which influences the signal propagated between transmit and receive antennas. Descriptions of fading channel characteristics will also be discussed, this is important because we will then have a better understanding of the significance of the fading results when they are presented in chapters 6.

4.2 Multipath Propagation

Multipath propagation is affected by objects and motion of people within buildings. Multipath propagation occurs when the transmitted signal arrives at the receiver antenna via one or more paths other than the direct line of sight (LOS), each with its own degree of attenuation and delay. The LOS is the main wave and other waves are either reflected, diffracted or scattered by structures such as walls, floor, ceilings, people and furniture. A two path model of multipath propagation was shown in Figure 3.11 (see section 3.4). The number of identifiable paths recorded in the measurements at given points in space depend on the shape and structure of a building and the resolution of the measurement setup [10]. Figure 4.1, shows a picture of multipath propagation inside an empty room [29].

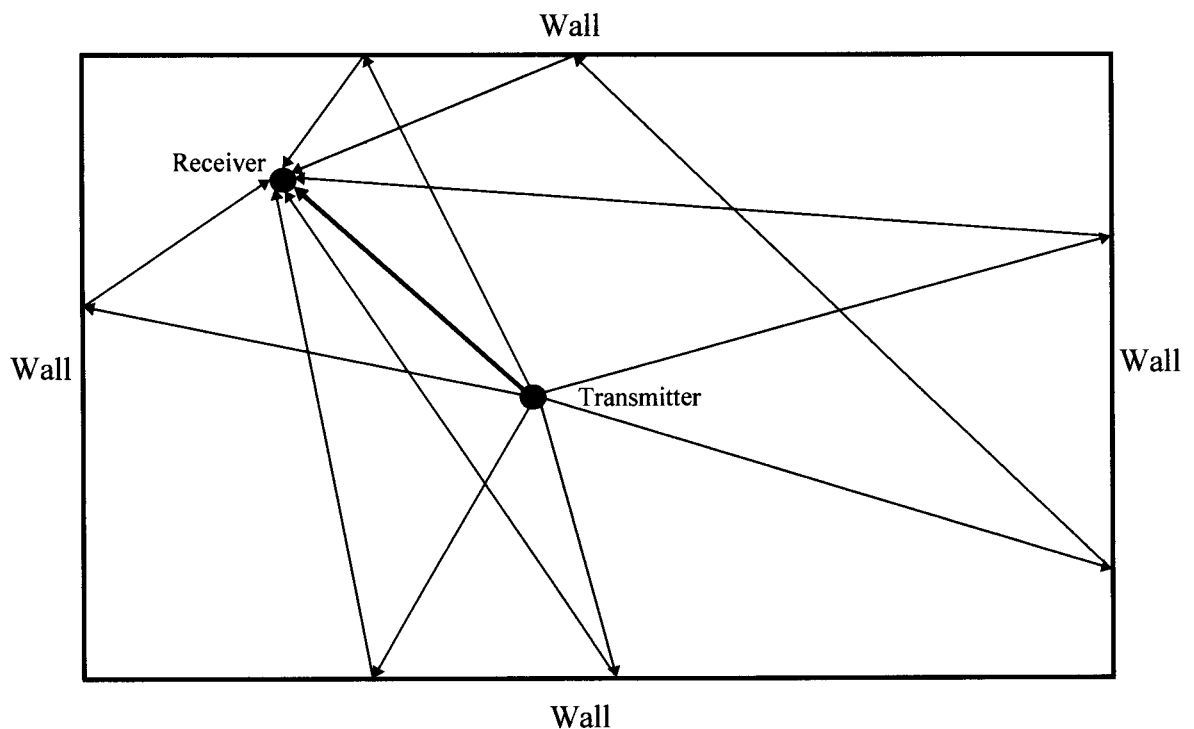


Figure 4.1 Multipath propagation inside a room [29]

As shown in the example Figure 4.1, the waves which reflect off some interface or object, experiences a longer path than the direct line of sight path (bold line in Figure 4.1) from the transmitter to the receiver. This means that the reflected signal is delayed relative to the direct path transmission [27]. This results in the waves combining

vectorially at the receiver antenna to give a resultant signal which can be either small or large depending upon whether the transmitted signal combines constructively or destructively [21]. A receiver at one location may only experience a signal strength several tens of dB different from a similar receiver which is located only a short distance away. As a receiver is moved to several different locations or rooms within a building, the phase relationship between the various incoming waves change. Hence, there are substantial amplitude fluctuations and the signal received is said to be subject to fading [21] (see section 4.3).

If the transmission of waves takes place only over two major propagation paths (one direct path and one reflected path), we then refer to this as specular multipath. An example of specular multipath propagation was shown in Figure 3.13 (see section 3.4). Consequently, if there are multiple reflections with differing delays (one direct path and multiple reflected paths), we then refer to this multipath propagation as diffuse multipath. It is much easier to reduce the effects of specular multipath using filters (called equalisers) than it is to reduce the effects of diffuse multipath [27]. In narrowband transmission the multipath medium causes phase fluctuations and also received signal envelope fluctuations. Whereas, in wideband pulse transmission the multipath medium produces a series of delayed and attenuated pulses (echoes) [10].

An unwanted effect of multipath is that it leads to intersymbol interference (ISI), since the delayed version of the waveform will extend into the next sampling interval. The multipath effect is well known in a television set, where it manifests itself as ghost images [27]. These ghost images are caused by the difference in the phase of the direct and reflected rays. This situation is worse near a transmitter than at a distance, due to the fact that the reflected rays are stronger nearby [17]. These ghost images can also occur in cable systems if proper attention is not paid to line terminations [27].

There are many affects of multipath propagation on systems. The affect of multipath reception, for:-

- A fast moving user is rapid fluctuations of the signal and phase (fading).
- A Wideband (digital) signal is dispersion and intersymbol interference.

- An analog television signal is “ghost” images (shifted slightly to the right).
- A multicarrier signal is different attenuation at different sub-carriers and at different locations.
- A stationary user of a narrowband system is good reception at some locations and frequencies, while poor reception at other locations and frequencies.
- A satellite positioning system is strong delayed reflections, which may cause a severe miscalculation of the distance between user and satellite, and may lead in a wrong “fix”.

4.3 Fading

Fading is the variation of the amplitude of a radio wave caused by changes in the transmission path. Fading can either be long-term or short-term, flat or frequency-selective [17]. Fading is caused directly by the multipath nature of waves in an indoor environment. The fading phenomenon is primarily a result of the time variations in the phases of waves arriving at the receive antenna.

Section 3.4, mentioned this point whereby the waves which have been reflected, diffracted or scattered by obstacles arrive at the receiver terminal and thus may add algebraically to either increase or decrease the signal strength. Due to these phase shifts, two or more waves will interfere either constructively or destructively, depending on whether a phase shift of an odd or even number of wavelengths is encountered. When waves add destructively by vector addition, the resultant received signal is very small or practically zero [23]. At other times, the waves add constructively, which leads to a resultant received signal which is large. Therefore, these amplitude variations in the received signal, is termed *signal fading*, and is due, as mentioned above, to the time-variant multipath characteristics of a channel.

The reflected signal constitutes both amplitude and phase changes. The phase change is typically 180 degrees and the amplitude change is a function of frequency and the nature of the reflecting surface [4]. It is worth noting that, whenever there is relative motion in wireless channels, there exist a Doppler shift in the received signal. This Doppler shift being a manifestation in the frequency domain of the envelope fading in the time

domain. Fading and the Doppler shift (spread) are not separable, since they are both manifestations of the same phenomenon.

If we consider a ‘static multipath’ environment, where the receiver and transmitter are stationary, the different propagation paths are distinguishable from one another if their electrical path lengths are such that the various delayed versions of a signal radiated from the transmitter can be recognised by the receiver in a sequentially manner. Figure 4.2, shows the two resolvable paths where the differential time delay is greater than the reciprocal of the signal bandwidth [21].

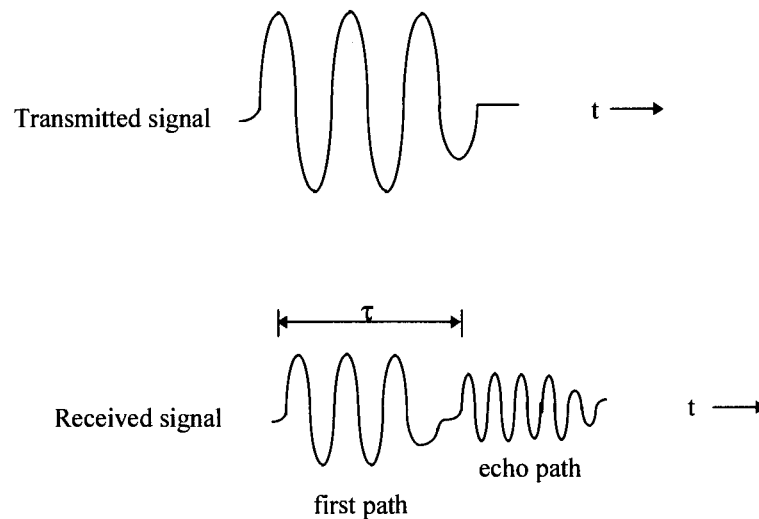


Figure 4.2 The two resolvable paths with time delay (τ) greater than the reciprocal of the signal bandwidth [21]

If we considered the transmission of an unmodulated carrier signal in a narrowband channel, then we would get several versions still arriving sequentially at the receiver. But, the effect of the differential time delays will be to introduce phase shifts between the component waves, and superposition of different components will then lead to constructive or destructive summation (at one instant of time) depending on the relative phases (see section 3.3.4).

A ‘dynamic multipath’ environment, is where there is a continuous change in the electrical length of every propagation path, caused by motion of either antenna or

people, and also the relative phase shifts between them change as a function of spatial location. Figure 4.4, shows an example of how the received amplitude of a signal varies in the simple case of two incoming paths with different phases [21]. This figure shows part of an enlarged multipath fading envelope.

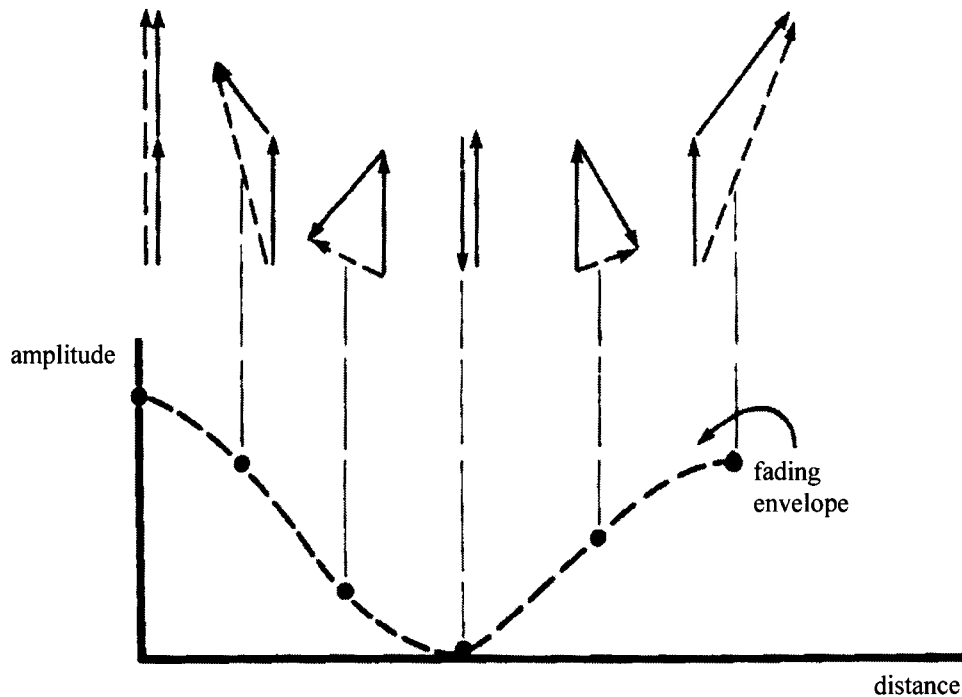


Figure 4.3 Illustration of envelope fading as two incoming signals combine with varying phases [21]

As we can see from Figure 4.3, there are some positions where constructive addition takes place and at other positions we see complete cancellations. In practice a more realistic envelope fading pattern is encountered as shown in the results of chapter 6 of this report. But, for now a clear understanding of the nature of multipath fading patterns is more important to be recognised.

The dynamic changes or time variations in the propagation path lengths can be related directly to motion of people and indirectly to the Doppler effects that arise. This time variations of the channel occur if the antenna or components of its environment are in motion.

The rate of change of phase, caused by motion, is apparent as a Doppler frequency shift in each propagation path, and this arises due to the fact that the phase changes $\Delta\phi$ and the change in the path length Δl are related by [21],

$$\Delta\phi = \frac{2\pi}{\lambda} \Delta l \quad (4.1)$$

where,

λ = carrier wavelength

Fortunately, the degree of time variations within an indoor system is much less than that of an outdoor mobile system. Given the conditions of a typical indoor wireless system, frequency spreading (Doppler shift) should be virtually nonexistent [10]. But, Doppler spreads of 0.1 - 6 Hz have been reported by some researchers. The change in the length of the path will depend on the spatial angle between any component wave and the direction of motion, and it is apparent that waves which arrive from directly ahead or behind the receiving antenna are subjected to the maximum rate of phase change [21].

In practical situations, the receive antenna will have several incoming paths, where the individual phases as experienced by the receive terminal will change continuously and randomly. This also means that the fading envelope and the RF phase will therefore also be random variables and a mathematical model is needed to describe the relevant statistics of the multipath fading channel [21]. A mathematical model of the multipath fading channel will be described in section 4.5.

4.4 The Characteristics of Multipath Fading

According to [20], it is possible to distinguish between three mutually independent and multiplicative propagation phenomena, which is multipath fading, shadowing and large-scale path loss. This report is solely concerned with the affects of multipath fading in the indoor wireless environment, therefore, we shall discuss the nature of multipath fading and its direct relationship with the channel.

We have read, in previous sections, about the nature of multipath propagation and what basically affects the nature of waves propagated through wireless channels. We have also read about the affect of the multipath medium on waves which arrive at the receive terminal and thus produce fading. All, the basic characteristics mentioned above about multipath propagation and fading, thus combine to give the phenomenon called multipath fading of a wireless channel.

Multipath propagation leads to rapid fluctuations (fading) of the phase and amplitude of the signal [20]. Fast and deep fading to a depth of less than 20 dB is frequent. Deeper fade depths, in excess of 30 dB is although less frequent, but not uncommon. For stationary terminals within buildings, measurements carried out by researchers have shown that ambient motion by people through the building causes Rician fading, with the ratio of specular signal power to multipath signal having a value of about 10 dB. This results in a typical variation of less than 15 dB for 99.9% of the time [1].

Multipath fading seriously degrades the performance of communication systems operating inside buildings. *Temporal variations* which are due to the motion of people and equipment around the antennas (fixed or mobile) results in multipath disturbances and fading effects [11]. Temporal variations within the channel produces a significant variation to the received radio frequency signal power. This variation of the received signal envelope results in a changing signal-to-noise ratio (S/N) at the sampling instant for the received data, and thus a non-constant BER probability [31].

These temporal variations studies conducted by some researchers, in office buildings where there are many separate rooms within the buildings have shown that fading occurs in 'bursts' lasting tens of seconds with a dynamic range of about 30 dB [11]. Unfortunately, one can do little to eliminate multipath disturbances and fading effects [10]. More comparisons concerning the measurement environment (see section 5.2) will be discussed and compared once the results of this project have been presented and analysed in chapters 6 and 7.

4.4.1 Types of fading

There are two distinct types of fading which are evident in the indoor environment, these being *frequency selective fading* and *flat fading*. *Frequency selective fading* occurs when a transmitted signal follows several different paths (each arriving at the receiver antenna at different times), resulting in a dispersion of the received signal in time [7]. Frequency-selective fading caused by multipath delay spread degrades the communication channel by causing intersymbol interference (ISI), thus resulting in an irreducible bit error rate (BER) and imposing an upper limit on the data symbol rate.

Flat fading occurs when a transmitted wave scatters off many obstacles which are close to the mobile unit. As a result, the phase and amplitude of each ray arriving at the receive antenna is different. Assuming a number of rays arrive at the receiver antenna at the same time, the combined effect is that these rays may add up constructively or destructively from reinforcement to total cancellation or fading [7].

In most indoor environments frequency selective fading accounts for the majority of fading in a channel. Flat fading is much, much less, but is present when the LOS is blocked due to intermittence caused by obstructions such as people or objects in the propagation path. This intermittence can cause severe or total loss of the received signal in extreme circumstances [31]. Thus for the indoor environment fading is directly caused by these two fading types.

Knowledge of fading behaviour in indoor wireless channels allow bit error rate (BER) probabilities to be calculated based on the dynamically changing received S/N ratios.

4.4.2 Frequency selective fading

Lets expand on the topic of frequency selective fading in more detail. Measurements have shown that very small movements of the transmit or receive antenna, in the order of a few centimetres, results in a wide range of receive power levels due to frequency selective fading. By observing the received power spectrum, verification that the fading was indeed frequency selective rather than flat can be concluded [31].

Frequency selective fading occurs when two different frequencies which are separated by a finite frequency range propagating in a medium do not observe the same fading. This fading is closely related to the time-delay spread Δ . If the time-delay spread equals zero than no selective fading exists [19].

If this two frequencies are close together, then the different propagation paths have approximately the same electrical length for both components, and the amplitude and phase variations of the frequencies will be very similar. However, as the frequency separation increases, the behaviour of one frequency can become uncorrelated with the other frequency. This is because the differential phase shifts along the various propagation paths are different at the two frequencies [21].

The extent of this decorrelation depends on the time-delay spreads, since the phases shifts arise from the excess path lengths. Large delay spreads, can cause the incoming components phase to vary over several radians even if the frequency separation is quite small. Signals which occupy a bandwidth greater than that over which spectral components are affected in a similar way will become distorted. This is due to fact, since the amplitude and phase of the spectral components in the received signals are not the same as they were in the transmitted signal. Basically, this phenomenon is called frequency selective fading. The bandwidth which the spectral components are affected in a similar way is called the coherence bandwidth [21].

For the two fading amplitudes to vary uncorrelately, the frequency separation should be greater than the coherence bandwidth,

$$\Delta f > B_c = \frac{1}{2\pi\Delta} \quad (4.2)$$

where,

B_c = coherence bandwidth

Δf = $|f_1 - f_2|$, two frequency difference

Δ = time delay spread

The coherence bandwidth will vary depending on the geometry of the indoor environment. Obstructions will have an impact on the time-delay spread of the bandwidth.

4.5 Mathematical Modelling of the Channel

According to [31], due to the multipath nature of waves in indoor environments, waves encounter many surfaces when propagating through the channel. These surfaces consist of walls, floor, ceiling and other objects such as furniture and people. At these surfaces the amount of energy which is transmitted through and reflected from the material is a function of the materials physical constants which are conductivity (σ), permittivity (ϵ) and permeability (μ), as well as frequency and the angle of incidence between wave propagation direction and surface material.

Two main classes of indoor propagation modelling which have been used by different researchers of the indoor environment, are statistical and site-specific. Both classes have strengths and weakness when applied to design and installation of indoor wireless systems. Site-specific propagation models depend on the electromagnetic wave propagation theory to characterise the indoor environment. They depend a great deal on the indoor environment to obtain accurate predictions of signal propagation. Ray tracing methods are used to calculate the signal strength, impulse response, rms delay spread and other related parameters [29].

In statistical modelling, on the other hand, depends on the extensive measurements and data collation [29]. A general statistical impulse response model for the multipath fading channel was first suggested by G. L. Turin (in 1956). The statistical impulse response model has been an approach used by many researchers to model the indoor wireless channel over the years. More recently the impulse response model has been used either directly or indirectly to model the indoor propagation channel [10]. We shall, therefore, use the impulse response model method to describe the nature of indoor propagation.

The multipath nature of the indoor channel can be fully described by its time and space varying impulse response. This impulse response approach to characterise the channel has been conducted by many researchers. More recently, the impulse response approach has been used either directly or indirectly by researchers in the indoor radio propagation channel modelling [10]. It is mainly used in indoor measurements and modelling efforts. The impulse response for the indoor channel gives a measure of the severity of multipath propagation within the channel [31].

Radio waves can be modelled at discrete paths resulting in a multipath model. The complicated and time-varying indoor radio propagation channel can be modelled by the impulse response. According to [3], the complex envelope baseband equivalent for the impulse response of such a channel at range r , between transmit and receive antennas can be mathematically modelled as,

$$h(\tau, r) = \sum_{i=0}^N E_i(r) e^{-j2\pi f_c \tau} R_i \delta(t - \tau_i) \quad (4.3)$$

where,

$i = 0$, is for the direct signal path (generally line of sight) between the transmitter and receiver.

τ_i = represents the propagation delay of the i th signal component.

E_i = the electric field intensity of the i th received signal component.

R_i = the reflection coefficient of the i th received component.

f_c = carrier frequency of bandpass channel.

To fully calculate the impulse response at any range, the values of E_i and R_i for the i th multipath radio signal needs to be known. R_i can be representative of one or more reflections from one or more different surfaces resulting in a final composite value for R_i . The i th multipath ray may be involved in one or more reflections as its total propagation delay is proportional to the distance the signal travels.

From [3], the value of $E_i(r)$ is given by,

$$E_i(r) = \frac{\sqrt{P_T}}{(r + \Delta \tau_i c)} \quad (4.4)$$

where,

$E_i(r)$ = electric field intensity of the i th received signal component

r = range between transmitter and receiver

P_T = transmitter power level

c = speed of light

$\Delta \tau$ = delay for the discrete paths $i = 1 \dots n$ with respect to that of the direct component (r/c)

The value of E_i has been shown and extensively proven by [31] to be the same value given for the received electric field intensity i th path, equation (4.4). P_T is the transmitter power level, c is the speed of light and equation (4.4) can be substituted into equation (4.3) of the impulse response to get the electric field intensity of the i th received signal component $E_i(r)$ [31].

In the introduction of this chapter (section 4.1), we mentioned that reflection and transmission of signals takes place in the horizontal plane or vertical plane. In the horizontal plane, when rays are incident on walls or obstacles they produce specularly transmitted and reflected rays, as well as diffuse scattering. This diffuse component is significant in determining the local variations to the field in the scattering site vicinity. However, the amplitude of the diffusing component decreases more rapidly with distance travelled. The diffused scattered fields are reduced by subsequent reflections or scatterings. The diffuse scattering component does contribute to the rapid local variations making up the interference patterns. We shall discuss more about the reflected and transmitted nature of the rays [13].

Section 3.3.1, briefly mentioned the transmission and reflection coefficients of a medium. We will expand on the discussion of the reflection coefficient R_i because it is needed in the computation of the impulse response. Figure 4.6, shows the two cases

when electric field intensity E is perpendicular to the plane of incidence and when it is parallel to the plane of incidence, which depends on whether the antenna is horizontally or vertically polarised [29]. The reflection coefficients are real and depend on the E of the wave impinging on the surface, (being either perpendicular or parallel to the surface), they also depend on the incidence angle and upon the relative dielectric constant of the material (ϵ_r) [3].

Considering the reflection coefficient of the i th received component R_i , for dielectric walls, floors, and ceilings of a building, the reflection coefficient is real at high frequencies where the angular frequency ω is large [31]. Figure 4.6(a), shows the case when the electric field intensity E , of a signal wave is perpendicular to the plane of incidence. Therefore, the complex coefficient of reflection R_i for horizontal polarisation is [31],

$$R_i = \frac{\cos \theta_i - \sqrt{(\epsilon_2 / \epsilon_1) - \sin^2 \theta_i}}{\cos \theta_i + \sqrt{(\epsilon_2 / \epsilon_1) - \sin^2 \theta_i}} \quad (4.5)$$

Figure 4.6(b), shows when E of a signal is parallel to the plane of incidence, for vertical polarisation the reflection coefficient R_i is [31],

$$R_i = \frac{(\epsilon_2 / \epsilon_1) \cos \theta_i - \sqrt{(\epsilon_2 / \epsilon_1) - \sin^2 \theta_i}}{(\epsilon_2 / \epsilon_1) \cos \theta_i + \sqrt{(\epsilon_2 / \epsilon_1) - \sin^2 \theta_i}} \quad (4.6)$$

where,

θ_i = angle between the incident radio wave and the normal to the surface

ϵ_1 = permittivity constant of the first medium (generally air)

ϵ_2 = permittivity constant of the second medium being the walls, floor and ceilings

Equation (4.5) or (4.6) can be used depending on which discrete path i is being worked on and the polarisation used (i.e., electric field intensity E either perpendicular or parallel to the plane of incidence) either equation can be substituted into equation (4.3)

to get the reflection coefficient of the i th received component R_i [31]. In the case where the E of a wall incident wave is perpendicular to the plane of incidence, then the reflection coefficient is as equation (4.5) and the reflection coefficients of the floor and ceiling of a room is as equation (4.6). From figure 4.6, E_i , E_r and E_t are the incident, reflected and transmitted electric field intensities, respectively [29].

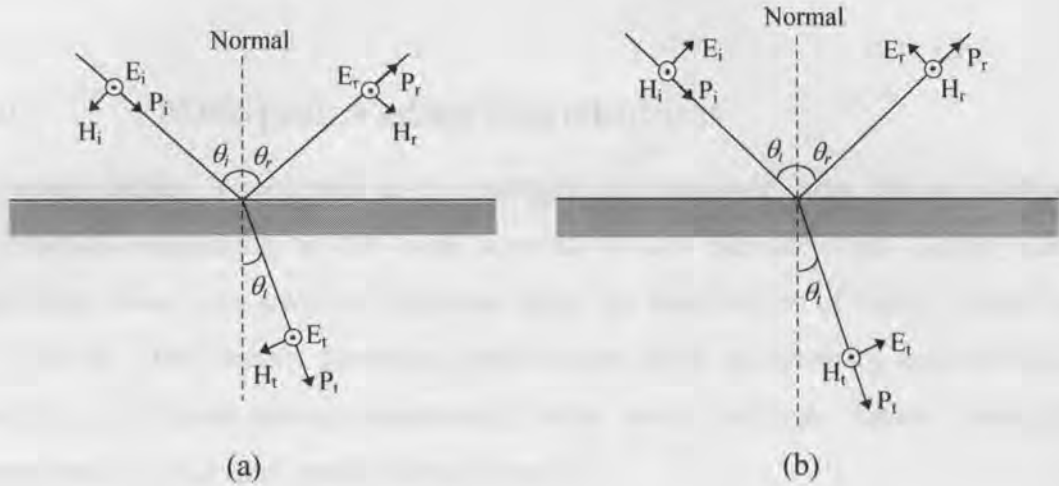


Figure 4.6 A signal wave incident obliquely on a plane:
 (a) E perpendicular to plane of incidence
 (b) E parallel to plane of incidence

The impulse response model equation (4.3) would represent a perfect 7 path propagation model if only 7 propagation delay paths exist when waves are transmitted from the transmit antenna and received as 7 different multipath waves at the receiver antenna in an empty room. The seven rays would be a direct LOS path, reflections from each of the side walls of a building or room, reflections from the end walls, one reflection from the ceiling and one reflection from the floor. This model was discussed and used by [3] in the measurements of impulse response for three separate buildings, but in real situations waves are reflected, diffracted and scattered and reach the receiving antenna by many paths (multipath propagation).

The impulse response model, equation (4.3), is a good approach for channel characterisation and along with the rms delay spread we can further evaluate the channel performance and its link with BER and the severe error burst caused by impairments to the channel. Although the impulse response and rms delay spread are not dealt with in this project, it can certainly be a topic of research by another party in the near future to further evaluate the wireless channels characteristics.

4.6 Multipath Fading Distributions

Envelope fading waveforms in a multipath environment may follow different distributions depending on the area covered by the measurements. These fading waveforms show how temporal variations effect the distributions of waves received by the antenna. There are six theoretical distributions which are normally encountered in describing multipath fading phenomenon, these being Rayleigh, Rician, Nakagami, Lognormal, Weibull and Suzuki distributions [5].

Depending on which frequency band we use, researches have indicated either a Rayleigh or Rician distribution is a good fit for the temporal fading data depending on the LOS component being present or not [3]. A brief discussion of the distributions is given in this section, as the Cumulative Distribution Function (CDF) of the results presented in Chapter 6, will be compared to the known distributions to determine which distribution is the best fit for the recorded data.

4.6.1 Rayleigh Distribution

A well accepted model for small-scale fading in the absence of a strong received component is the Rayleigh fading distribution. A strong received component may be the LOS path or a path which goes through much less attenuation when compared to the other arriving components [10]. This has been stated and proven by many researchers.

This distribution has been closely related to the central chi-square distribution [23]. The Rayleigh probability density function (pdf) is given by [10],

$$p(r) = \frac{r}{\sigma^2} \exp\left\{-\frac{r^2}{2\sigma^2}\right\}, \quad r \geq 0 \quad (4.7)$$

where,

$$\sigma^2 = \text{variance of the random multipath (Rayleigh parameter)}$$

The mean of this distribution is $\sqrt{\pi/2}\sigma$ and the variance is $(2 - \pi/2)\sigma^2$. The Rayleigh distribution is widely used to describe multipath fading because of its occasional empirical justifications and its elegant theoretical explanation. To explain it theoretically, we consider an unmodulated carrier transmitted by terminal i . It is assumed that the transmitted signal reaches the receiver via N directions, where the i th path having a complex strength $r_i e^{j\theta_i}$ that can be described by a phasor with an amplitude r_i and a phase θ_i . The received signal $r_i(t)$ is given by [10],

$$r_i(t) = \sum_i r_i e^{j\theta_i} \quad (4.8)$$

The path phase θ_i is very sensitive to path length, changing by 2π when the path length changes by a wavelength. This shows that, the phase is uniformly distributed in the interval $[0, 2\pi)$. Quadrature I and in-phase components Q of the received signal are independent and by the central limit theorem, are Gaussianly distributed random variables. Lord Rayleigh, first investigated the joint distribution of r_i and θ_i . These two variables can be shown to be [10],

$$\begin{aligned} r_i &= \sqrt{I^2 + Q^2} \\ \theta_i &= \arctan[Q / I] \end{aligned} \quad (4.9)$$

It has been shown that even as few as six sine waves with uniformly distributed and independently fluctuating phases are combined, the resulting amplitude and phase very closely follow the Rayleigh and uniform distributions, respectively [10].

4.6.2 Rician Distribution

The Rician distribution occurs when a significant or strong path (such as the LOS path) exists in addition to the low level scattered paths. The Rician distribution is related to the non-central chi-square distribution [23]. When a strong path exist, the received signal vector can be considered to be the sum of two vectors: a scattered Rayleigh vector which has a random amplitude and phase, and a vector which is deterministic in amplitude and phase, representing the fixed path. The received signal vector $r e^{j\theta}$ is the phasor sum of the two signals, which is the random component $u e^{j\alpha}$ (with u being Rayleigh and α being uniformly distributed) and the fixed component $v e^{j\beta}$ (v and β are not random).

S. O. Rice, who was an outstanding engineer at Bell Telephone Laboratories [5], showed that the joint pdf of r and θ to be [10],

$$p(r) = \frac{r}{2\pi\sigma^2} \exp\left\{-\frac{r^2 + v^2 - 2rv \cos(\theta - \beta)}{2\sigma^2}\right\},$$

$$r \geq 0, \quad -\pi \leq (\theta - \beta) \leq \pi \quad (4.10)$$

The length and phase of the fixed path usually change, therefore β is itself a random variable which is uniformly distributed on $[0, 2\pi)$. Randomising β causes r and θ to become independent, θ having a uniform distribution while r has a Rician distribution given by the pdf [10],

$$p(r) = \frac{r}{\sigma^2} \exp\left\{\frac{-r^2 + v^2}{2\sigma^2}\right\} I_0\left(\frac{rv}{\sigma^2}\right), \quad r \geq 0 \quad (4.11)$$

where,

I_0 = zeroth-order modified Bessel function of the first kind

v = magnitude of the strong component

σ^2 = proportional to the power of the “scatter” Rayleigh component

The zero-order modified Bessel function can be shown mathematically as [19],

$$I_0(z) = \sum_{n=0}^{\infty} \frac{z^{2n}}{2^{2n} n! n!} \quad (4.12)$$

For $z \gg 1$, equation (4.12) can be expressed by [19],

$$I_0(z) = \frac{e^z}{\sqrt{2\pi z}} \left(1 + \frac{1}{8z} + \frac{9}{128z^3} + \dots \right) \quad (4.13)$$

If v in equation (4.11) goes to zero (or if $v^2/2\sigma^2 \ll r^2/2\sigma^2$), the strong path is thus eliminated and the amplitude distribution then becomes Rayleigh, as expected. This shows, that the Rician distribution contains the Rayleigh distribution as a special case [10]. The Rician K -factor is defined as, $K = v^2/2\sigma^2$. The Rician K -factor of about 7 dB ($K = 5$) adequately describes most microcellular channels [20].

4.6.3 Nakagami m -Distribution

The Nakagami distribution, which contains many other distributions as special cases, has generally been neglected, as most of Nakagami's works are written in Japanese [10]. The Nakagami- m is a two parameter distribution, namely, involving the parameter m and the second moment Ω . As a consequence, this distribution provides more flexibility and accuracy in matching the observed signal statistics. This distribution can be used to model fading conditions which are either more or less severe than the Rayleigh distribution. When we described the Rayleigh distribution we assumed that the length of the scatter vectors were equal and their phases to be random. A more realistic model, proposed by M. Nakagami in 1960, also permits the length of the scatter vectors to be random.

Using the same notation for $r_i(t)$ as shown in equation (4.8), the Nakagami derived formula for the pdf of r is [10],

$$p(r) = \frac{2m^m r^{2m-1}}{\Gamma(m)\Omega^m} \exp\left\{-\frac{mr^2}{\Omega}\right\}, \quad r \geq 0 \quad (4.14)$$

where,

$\Gamma(m)$ = Gamma function

Ω = $E(r^2)$

$m = \frac{\Omega^2}{E[(r^2 - \Omega^2)]}$, $m \geq \frac{1}{2}$. It is called the fading figure [23]

The Nakagami distribution is a general fading distribution that reduces to a Rayleigh distribution for $m = 1$ and to a one-sided Gaussian distribution for $m = 1/2$. It also approximates with high accuracy the Rician distribution and approaches the Lognormal distribution under certain conditions [10].

4.6.4 Weibull Distribution

The Weibull Distribution has a pdf given by [10],

$$p(r) = \frac{\alpha b}{r_0} \left(\frac{br}{r_0}\right)^{\alpha-1} \exp\left[-\left(\frac{br}{r_0}\right)^\alpha\right], \quad r \geq 0 \quad (4.15)$$

where,

α = shape parameter

r_0 = rms value of r

$b = [(2/\alpha)\Gamma(2/\alpha)]^{1/2}$ is a normalisation factor

There is no theoretical explanation for encountering this distribution, according to [10]. However, the Weibull distribution contains the Rayleigh distributions as a special case, for $\alpha = 1/2$. For $\alpha = 1$, it reduces to an exponential distribution. The Weibull distribution has provided good fit to some mobile radio fading data [10].

4.6.5 Lognormal Distribution

To explain large scale variations of the signal amplitude in a multipath fading environment, the Lognormal distribution has often been used. The pdf is given by [10],

$$p(r) = \frac{1}{\sqrt{2\pi}\sigma r} \exp\left\{-\frac{(\ln r - \mu)^2}{2\sigma^2}\right\}, \quad r \geq 0 \quad (4.16)$$

where,

μ = mean

σ = standard deviation

With this distribution, $\log r$ has a Gaussian distribution. A heuristic theoretical explanation for encountering the Lognormal distribution is, due to multiple reflections in a multipath environment, fading can be characterised as a multiplicative process. Multiplication of the signal amplitude gives rise to a Lognormal distribution [10].

4.6.6 Suzuki Distribution

The Suzuki distribution is a mixture of the Rayleigh and Lognormal distributions. It was proposed by Suzuki to describe the mobile channel. It has the pdf [10],

$$p(r) = \int_0^{\infty} \frac{r}{\sigma^2} \exp\left(-\frac{r^2}{2\sigma^2}\right) \frac{1}{\sqrt{2\pi}\sigma\lambda} \cdot \exp\left[-\frac{(\ln \sigma - \mu)^2}{2\lambda^2}\right] d\sigma \quad (4.17)$$

This distribution although complicated in form, has an elegant theoretical explanation: one or more relatively strong signals arrive at the general location of the portable. The main wave, which has a Lognormal distribution, is broken up into subpaths at the portable site due to scattering by the local objects. Each subpath has random uniformly distributed phases and approximately equal amplitudes. The subpaths arrive at the

portable unit with approximately the same delay. The envelope sum of these components has a Rayleigh distribution with a Lognormal distributed parameter σ , giving rise to the mixture distribution of (4.17) [10]. The Suzuki distribution explains the transition between the local Rayleigh distribution and the global Lognormal distribution. However, it is complicated for data reduction since the pdf is given in an integral form.

4.7 Fading Envelope Statistics

The probability density function (pdf) and the cumulative distribution function (CDF) are both first-order statistics. By definition they are both not functions of time. Second-order statistics on fades which are functions of time, consist of level crossing rates (LCR), average duration of fades (ADF) and fade depth [19]. A general discussion of these statistics will be presented in this section. These statistics will be used to analysis the results of chapter 6, to see how the fading patterns vary under different measurement parameters.

4.7.1 Level Crossing Rate (LCR)

The level crossing rate (LCR) $N(R)$ is the average number of times per second that the signal crosses a specified threshold or level, R , with a positive slope [21].

It is represented mathematically as [21],

$$N(R) = \int_0^{\infty} \dot{r} p(R, \dot{r}) d\dot{r} \quad (4.17)$$

where, $p(R, \dot{r})$ is the joint pdf of r and \dot{r} at $r = R$, and the dot indicates the time derivative. According to [19], the total number of crossings C over a T -second length of data divided by T seconds becomes the LCR:

$$N(R) = \frac{C}{T} \quad (4.18)$$

The LCR of a typical fading signal can be calculated and is shown in Figure 4.7.

4.7.2 Average Duration of Fades

The average duration of fades (ADF) below the specified level $r = R$ is also of interest, as an indoor communication system is also sensitive to the duration of time that the signal stays below the given threshold level [11]. Let τ_i be the duration of the i th fade. Then the probability that $r \leq R$ for a total time interval of length T is [19],

$$P[r \leq R] = \frac{1}{T} \sum \tau_i \quad (4.19)$$

The average fade duration τ is [19],

$$\tau = \frac{1}{TN(R)} \sum \tau_i = \frac{P[r \leq R]}{N(R)} \quad (4.20)$$

where,

$N(R)$ = level crossing rate

τ_i = i th individual fade

T = time interval

The average duration of fades is also shown in Figure 4.7 [19].

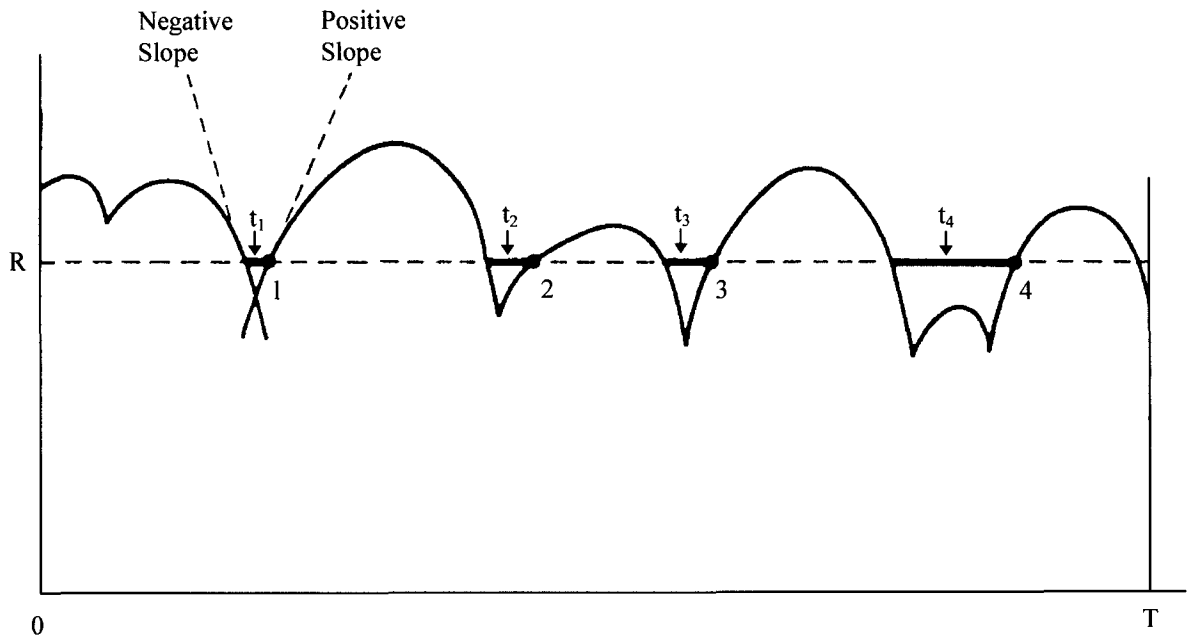


Figure 4.7 Level crossing rate and the average duration of fades [19]

This thus concludes the discussion on multipath fading and its important characteristics. The statistical analysis and the theoretical distribution have been discussed in length and will be used when analysing the fading envelope waveforms in section 6. The next section deals with the measurements conducted at the ATRI laboratory.

Chapter 5

MEASUREMENTS

5.1 Measurement Introduction

The measurement plan for this project consisted of collecting and analysing data for a specific location, which was the ATRI laboratory at Curtin University. The specific aim was to gather results which were influenced by temporal variations of the indoor environment and to statistically analyse these results, so that accurate and relevant multipath fading channel models could be developed [12].

A sufficient number of measurements were collected around the laboratory to ensure that a statistically accurate and warranted model could be developed. These measurements were conducted over a period of a week, due to some uncontrollable constraints, such as time and equipment demand. This did prove to be a bonus, because a slowly and carefully conducted measurement procedure was achieved without any mistakes.

As, the majority of the measurement equipment was placed on a trolley (except for the computer), it was easy to take measurements at antenna positions which were further away from the initial trolley position (near the computer terminal). The measurement environment is presented in section 5.2.

One of the measurement equipment, the Apex Systems Voltage Control Analyser had to be ordered and installed, as it was a vital solution to the measurement system. The rest of the equipment was readily available at the time of connecting up the measurement system and did not pose a big problem. The quarter-wave monopole antennas had to be constructed and calibrated at the ATRI laboratory to the specifications of CSIRO Australia. The antenna measurements covered the 2.3 - 2.5 GHz range only, as this was the measurement band being considered for this project. A constant frequency band of 2.4 GHz was used throughout the measurements.

The following sub-sections describe the measurement environment used for the measurements, the measurement equipment features and specifications are noted, the measurement system is explained in depth, the system calibration is noted and measurement procedure is outlined and discussed.

5.2 Measurement Environment

Measurements were conducted at the Australian Telecommunications Research Institute (ATRI) laboratory, located in the new technologies building (building 314, level 1) at Curtin University, Bentley Campus. The measurements were carried out at the main laboratory, which is located on the ground floor of this three story building. The building is a fairly new colourful brick building, which is about 3 years old. Located on the ground floor of this building are, office cubicles, a spacious reception area, a kitchen, 2 conference rooms, hallways and the big central laboratory.

The laboratory is a rectangularly shaped room in a central position, and has other office rooms to its sides along the central hallway. The dimensions of the laboratory are 7.8 x 9.95 meters. There is also, an adjoining store room which is located beside the laboratory, the store room and laboratory are separated by a door. Also closely located to the store room in a single concrete pillar, which is part of the building structure. The interior walls of the laboratory consist of smooth Gyprock plasterboard's on metal studs. The floor is carpeted, and it is constructed of concrete over corrugated steel panels. The ceiling which is made of non-metallic tiles has fluorescent lights and air-conditioning ducts, and is about 3 meters in height.

Within the laboratory, there are benches along the four sides of the laboratory walls and also a central bench located in the middle of the laboratory. There are computers, test and measurement equipment and various other accessories which are placed on these benchtops and on trolleys. The movement of people in this laboratory depends on the particular day and on the equipment or accessories being used or sort after. The floor plan of the laboratory is shown in Figure 5.1 (the Figure is not to scale).

This measurement environment was chosen due to the availability of the laboratory and the relatively easy excess to equipment which is needed to carry out the measurements. The laboratory is a good choice because there is a lot of furniture within the laboratory and occasional movement of people walking in and out of the laboratory is present. In Figure 5.1, the black circles represent the transmitter and receiver positions for the measurements which were conducted in the laboratory. The antenna positions were elected at random, with the intention that the whole laboratory space was covered or represented.

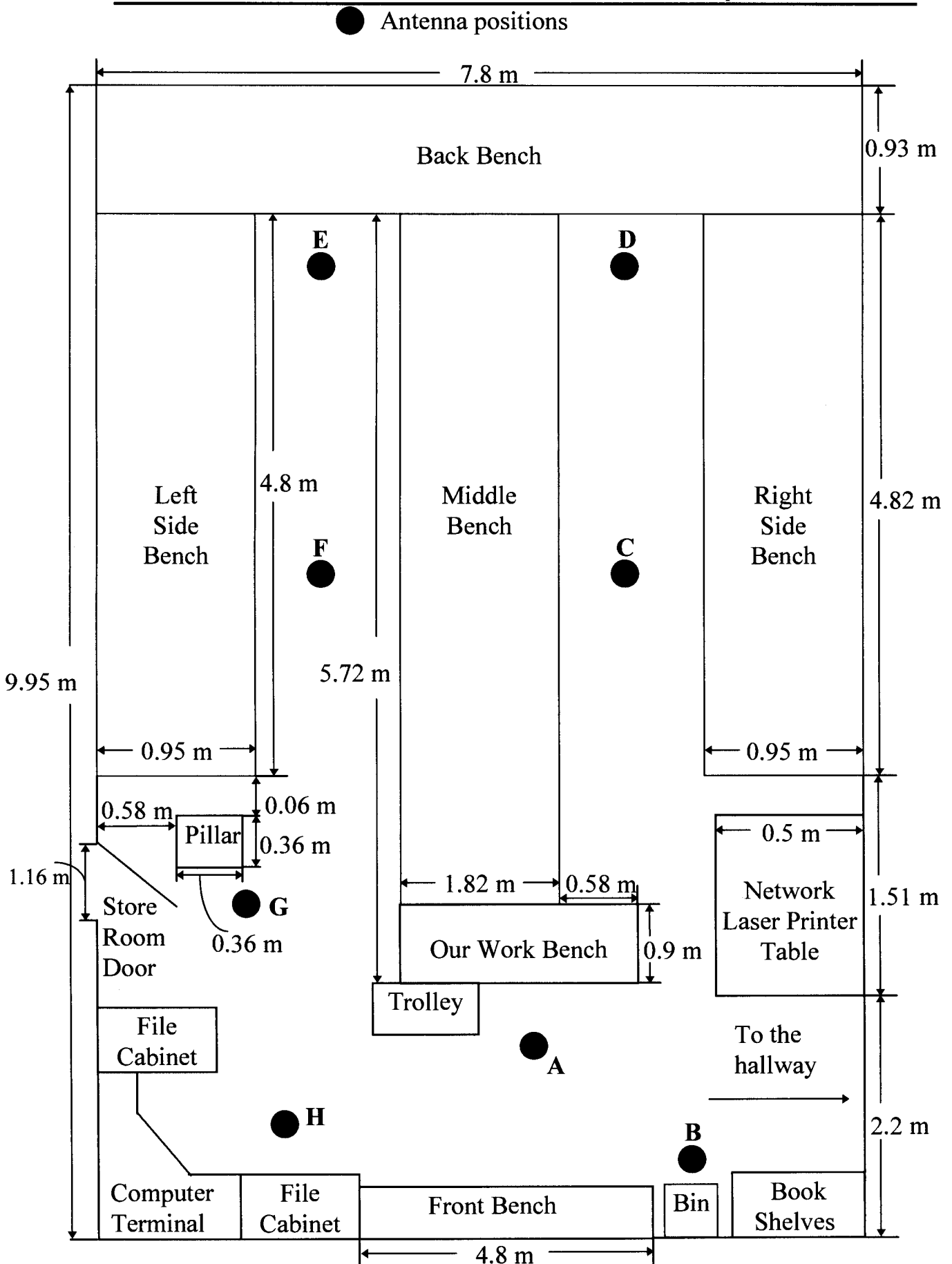


Figure 5.1 Floor plan of the ATRI laboratory at Curtin University

5.3 Measurement Equipment

The equipment which was used to gather the results for this report was chosen because they were available at the time and were relatively easy to use. The equipment used to gather the results consisted of,

- 2 x Monopole Test Antenna
- 1 x Hewlett Packard (HP) 89441A Vector Signal Analyser (VSA)
- 1 x Hewlett Packard (HP) 89441A Radio Frequency (RF) Section
- 1 x Two Way Splitter
- 1 x Marconi Instruments TF 2300A FM/AM Modulation Analyser
- 1 x Aphex Systems VCA1001 Voltage Control Attenuator (VCAtt)
- 1 x AWA Crystal Oscillator
- 1 x 3NX IBM Compatible PC, with Creative Labs Sound Blaster card installed

These equipment made up the measurement system (see section 5.4) for this project. These equipment at the time of taking the measurements, provided the best solution for gathering raw fading results so that the appropriate statistical analysis could be conducted using available software.

Setting up the equipment prior to system calibration and measurement did not pose a big dilemma, as the only equipment which was used frequently by people in the laboratory, was the HP vector signal analyser, its RF section and the 3NX computer. The other equipment belonged to my colleague, Ted Walker, who assisted me in conducting the measurements. As the majority of the equipment, except for the computer, was placed on a trolley, it was easy to move the entire test setup to various locations within the laboratory for the different antenna positions. This proved to be a very big advantage.

A brief discussion on the equipment used in this project will be mentioned in the following sub-sections. Specifications and features of the equipment used in this project will be outlined.

5.3.1 Antenna

The antennas used in the measurements are identical laboratory constructed quarter-wave monopole reference antennas, constructed to CSIRO Australia model specifications for the frequency range of 2.3 - 2.5 GHz. The quarter-wave monopole antenna is an antenna which consists of one half of a half-wave dipole antenna, which is located on a conducting ground plane. This ground plane is assumed to be infinite and perfectly conducting. The monopole antenna is perpendicular to this ground plane [28]. The antennas were fed to coaxial cables connected to their bases. Figure 5.2 shows a basic picture of the laboratory constructed antenna (not to scale).

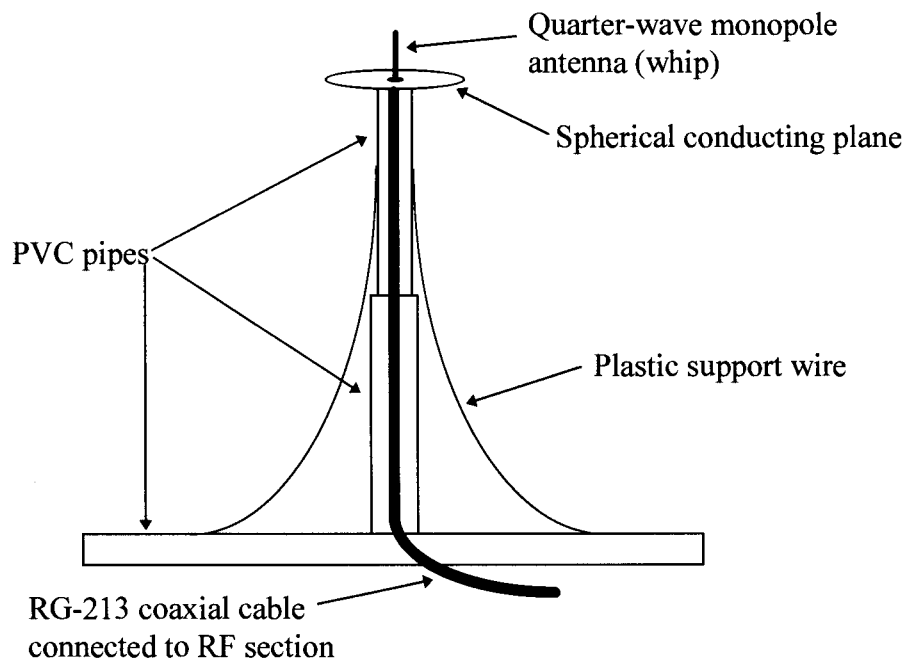


Figure 5.2 Side-view of the laboratory constructed quarter-wave monopole antenna

The antennas are omnidirectional radiators and either antenna can be used for transmitting or receiving signals because they obey the Law of Reciprocity. The omnidirectional measurements served to determine the nature of the radiating waves in the wireless channel environment between the two antennas. With obstacles located in different locations around the antennas, the omnidirectional nature of the measurements, showed the multipath nature of the received waves in the form of fading. This

measurements were good because they showed the expansion of the RF wave in “all directions” from the transmit antenna and passed through the channel being reflected, diffracted and scattered of obstacles and moving people located in different positions around the antenna.

The features and specifications of the antennas used in the measurements are shown in table 5.1,

Table 5.1: Features and Specifications of Quarter-wave Monopole Antenna

FEATURES	
CSIRO monopole test antenna	
Omnidirectional	
Vertical polarisation	
Assembled and calibrated using HP S-parameter test set at ATRI laboratory	
Rugged and flexible construction	
Lightweight design	
SPECIFICATIONS	
Frequency Range	2.3 - 2.5 GHz
Gain	Unity
VSWR	1.67:1
Radiation Pattern	See Figure 5.3
Maximum Power Output	
Construction Height (from ground to spherical conducting plane)	1.5 m
Antenna Whip Height	31.25 mm
Diameter of Spherical Conducting Plane	125 mm
Whip and Conducting Plane Material	Stainless steel
Support Pipe Material	Poly-vinyl Chloride (PVC)

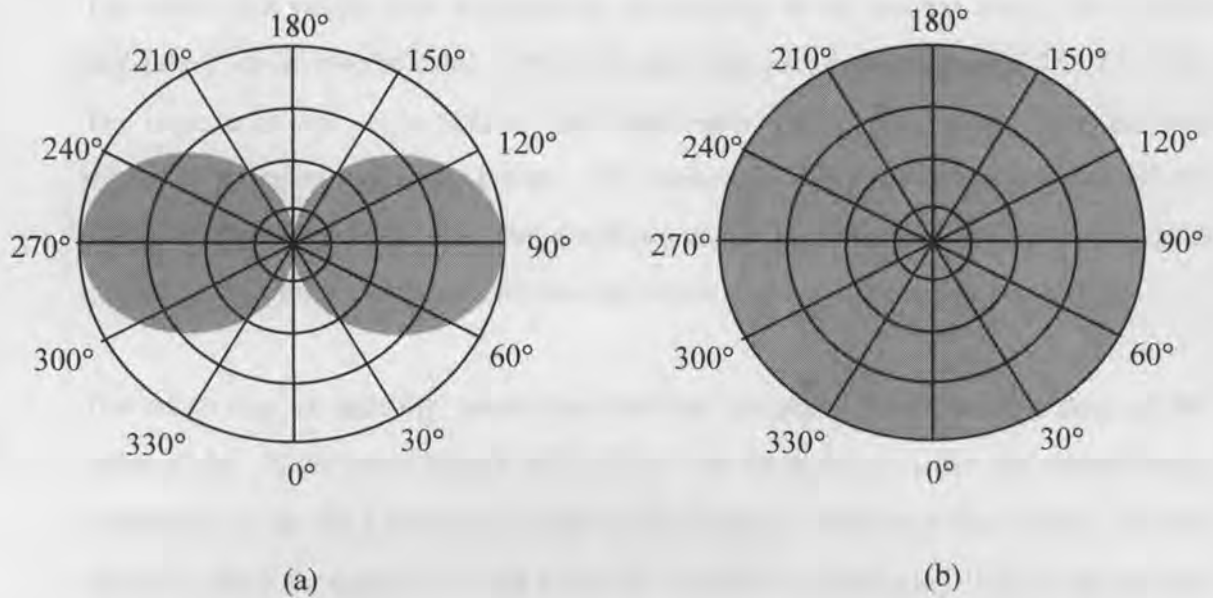


Figure 5.3 Radiation pattern for quarter-wave monopole antenna:

- (a) Vertical pattern (side view)
- (b) Horizontal pattern (top view)

The calibration of the antenna was conducted at the laboratory using the Hewlett Packard Network Analyser with the S-parameter test set option. Allowing for the 50Ω calibration cable RG-213 at 1.2 dB, the quarter-wave monopole antenna was measured for return loss using the S-parameter test set. The cable calibration to determine the loss (attenuation) of the cables, which are the same cables used in these measurements, was carried out by [12]. For the details on the method used to calibrate the cables, refer to [12]. Figure 5.4 shows the measurement setup used to measure values of the return loss for the frequency range of 2.3 - 2.5 GHz.

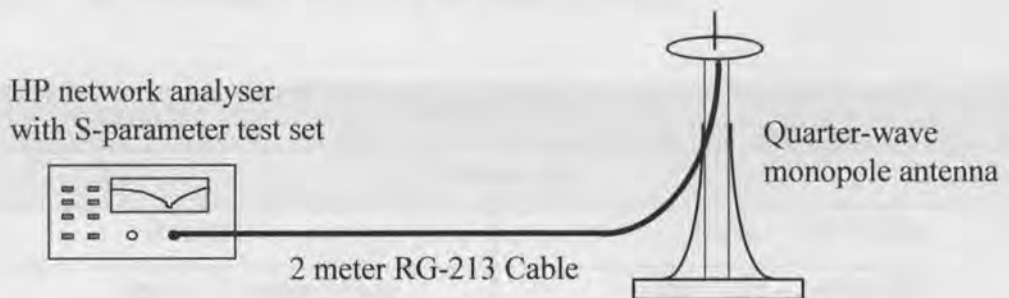


Figure 5.4 Return loss measurement setup (not to scale)

The return loss values were measured by connecting up the antenna unit to the test set using the 2 meter coaxial cable. Next, the span was set for the range of 2.3 to 2.5 GHz. The impedance was set to 50Ω on the S-parameter test set and the measurement was started by pressing the sweep button. The measured values for the return loss for the specified frequency range was then displayed on the S-parameter test set. From these values the best return loss value for our laboratory constructed antenna is -30 dB.

The return loss, is basically, where two loads are compared to see whether they are the same or not. In the measurement setup above, we are trying to match the characteristic impedance of the 50Ω calibration cable to the antenna, which acts like a load. We are trying to match the antenna, so that it closely resembles a 50Ω load. This is because we don't want any unwanted reflected power returning back to the system and being wasted. A perfect radiating antenna would have a Voltage Standing Wave Ratio (VSWR) of 1. Our VSWR for the quarter-wave monopole antenna is 1.67, as compared to 1. But this is an acceptable value for the antenna, as a fairly good antenna would have a VSWR of 1.3:1.

5.3.2 Vector Signal Analyser and RF Section

The Hewlett Packard 89441A Vector Signal Analyser (VSA) and its Radio Frequency (RF) Section was used in performing measurements for the fading data. Table 5.2, presents some very basic specifications of the Vector Signal Analyser. To find out the full specifications of the VSA, please refer to the technical data handbook.

Table 5.2: Specifications of the HP Vector Signal Analyser

SPECIFICATIONS (RF)	
Frequency	
Range	2 MHz - 2650 MHz
Span (i) Scalar Mode (ii) Vector mode	(i) 1 Hz - 2.648 GHz (ii) 1 Hz - 7 MHz
Resolution Bandwidth (RBW)	312 μ Hz - 3 MHz

Amplitude	
Input Range	-50 dBm to +25 dBm
Input port Impedance	50 Ω (75 Ω with option 1D7)
Source	
Types	CW (fixed sine), random noise, periodic chirp, arbitrary
Frequency Range	2 MHz - 2650 MHz
Maximum offset from center frequency	3.5 MHz
Amplitude (CW source type)	
(i) Range	(i) -40 dBm to +13 dBm
(ii) Typical Maximum Amplitude	(ii) +17 dBm
(iii) Amplitude Resolution	(iii) 0.1 dB
Source Port Connector	Type-N
SPECIFICATIONS (Baseband)	
Frequency	
Range	dc - 10 MHz
Span	1.0 Hz - 10 MHz
Center Frequency Tuning Resolution	0.001 Hz
Resolution Bandwidth (RBW)	312 μ Hz - 3 MHz
Amplitude	
Input Range (50 Ω input)	-30 dBm to +24 dBm
Input port Impedance (IF section only)	50 Ω / 75 Ω
Connector	BNC
Source	
Scalar mode types	CW (fixed sine), arbitrary
Vector mode types	CW, random noise, periodic chirp, arbitrary
Source Frequency Resolution	25 μ Hz
Return loss (IF section only)	>20 dB

5.3.3 Marconi Instruments Modulation Analyser

The TF2300A modulation analyser is primarily used for measurements of FM deviation but it also measures AM depth. With its wide range of deviation frequency, modulation bandwidth and carrier frequency, this instrument is suitable for applications to fixed and mobile point-to-point communications, broadcasting, telemetry and multi-channel link equipment in the HF, VHF and UHF. The Marconi analyser can be operated from the mains power or a nominal 24 V battery for mobile purposes. The specifications of the modulation analyser are shown in table 5.3,

Table 5.3: Specifications for the modulation analyser

SPECIFICATIONS	
RF Input	
Frequency Range	4 MHz - 1000 MHz
Maximum Input	3 V rms (200 mW)
Center Frequency Tuning Resolution	Nominally 50 Ω
Local Oscillator	
Variable Frequency Operation	5.5 - 11 MHz and 22 - 44 MHz
Calibration Accuracy	$\pm 3\%$
IF Output	
Frequency	1.5 MHz
Amplitude	approx. 250 - 750 mV EMF
Output Impedance	Nominally 10 k Ω
Power Requirements	
AC Mains	190 V - 260 V
External Battery	21.5 - 30 V DC
Dimensions and Weight	
Height	19 cm
Width	47 cm
Depth	36 cm
Weight	13.6 kg

5.3.4 Aphex Systems Voltage Control Attenuator

The Aphex Systems VCA1001 ultra-low distortion VCAtt is the nearest device to a variable potentiometer. The VCA1001 operates as a class “A” amplifier at all times and all parameters are exceptionally stable against temperature changes. The VCAtt, which was ordered from America, was primarily needed to change the DC voltage from the Marconi Instruments Modulation Analyser to an AC voltage because the sound blaster only accepts AC voltage due to its blocking capacitor within its circuitry. Table 5.4, shows the features and specifications for the VCA1001 VCAtt,

Table 5.4: Features and specifications for the VCA1001 Voltage Control Attenuator

FEATURES	
Ultra low noise	
Reduced external parts count	
Ultra low noise	
Super low control feedthrough	
Wide bandwidth	
Bipolar power supplies	
Wide dynamic range	
Wide attenuation range	
SPECIFICATIONS	
AC Electrical Characteristics	
Maximum Input Level	-21 dBu
Slew Rate	120 V/ μ s
Output at Clipping	0+21 dBu
Noise (20 Hz -20 KHz)	-90 dBu
DC Electrical Characteristics	
Recommended Supply Volts	Bipolar 15 V DC
Positive Supply Current	7.65 mA
Negative Supply Current	7.75 mA

5.3.5 3NX Computer

The computer which was used to sample and store the data was a 3NX 80486 computer. The Creative Labs sound blaster card was installed in the computer to sample the amplitude modulated 100 Hz sinusoid for all the relevant fading data, produced for the 20 second measurement period.

5.3.6 Coaxial Cables

The coaxial cables used in this project consisted of,

- 2 x 2m RG-213 Coaxial Cables
- 1 x 20m RG-213 Coaxial Cable

One 2 meter cable was used as the calibration cable, while the other 2 meter RG-213 cable was used in the measurements and was connected to the receive antenna. The RG-213 cables were chosen due to their flexibility and the minimal cost associated with their purchase [12].

The 20 meter cable was chosen because of its relatively long length which was needed due to the topology of the laboratory, that would have rendered the 2 meter cable unsuitable. The 20 meter cable was connected to the transmit antenna and this antenna was placed at various positions across the laboratory (see Figure 5.1), so that the fading measurements can be conducted easily. This proved to be a bonus, as the trolley and its equipment did not have to be moved consistently around the laboratory.

5.4 Measurement System

The measurement method or setup for the fading measurements was implemented using the equipment represented in Figure 5.5. This is the block diagram of the 2.4 GHz band measurement system. Measurements were conducted using this measurement setup. Before any measurements were started, the system was calibrated using one of the 2 meter RG-213 coaxial cables with known attenuations losses connected to the cable on either end. More on the system calibration will be mentioned in section 5.5.

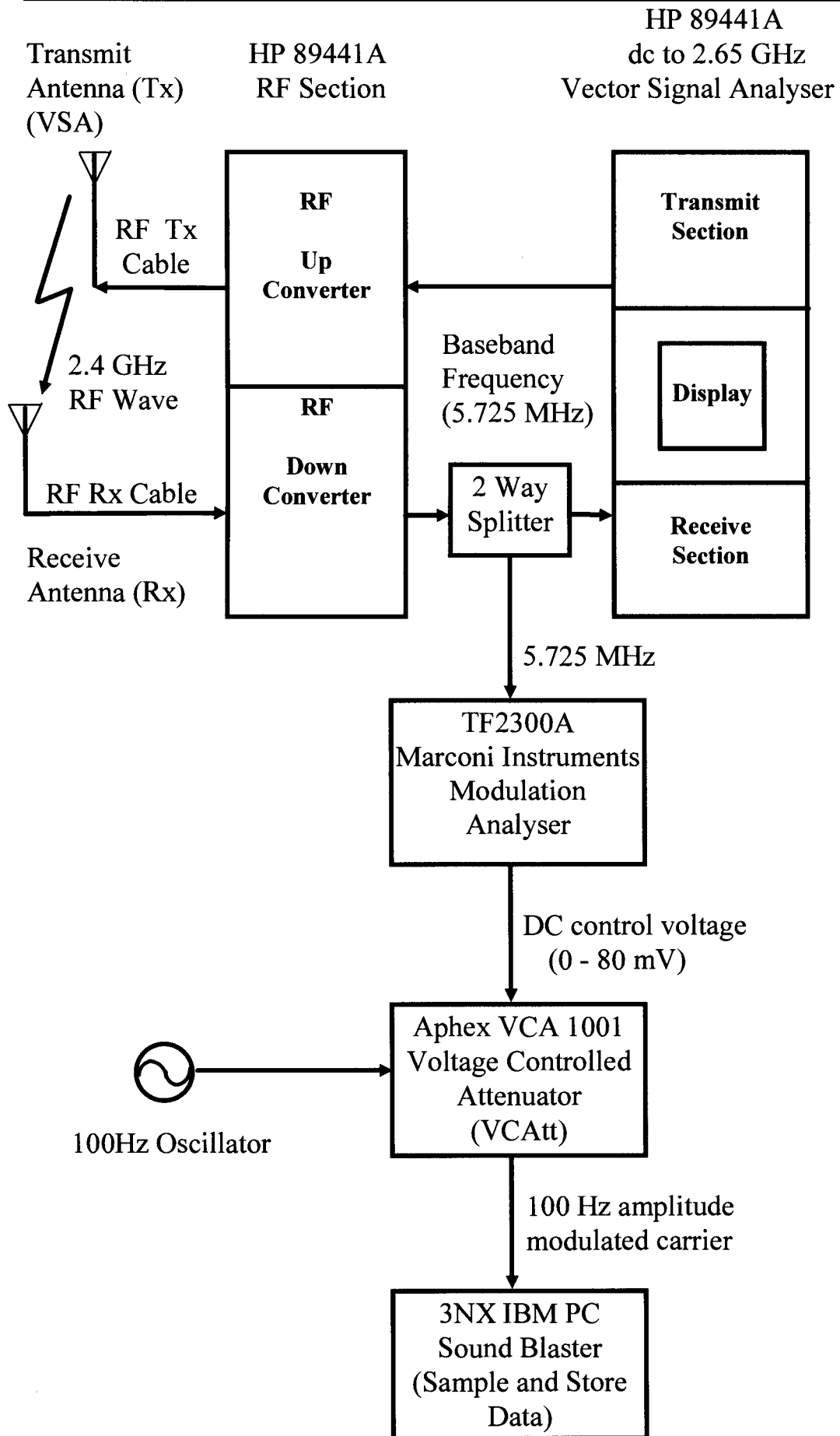


Figure 5.5 Block diagram of the 2.4 GHz band measurement system

After thorough calibration of the system, the measurements were started for the 20 second measurement period. The span on the Vector Signal Analyser (VSA) was set to 10 MHz, the resolution bandwidth was set at 300 KHz and the source type was a fixed sine (CW). The transmit section of the VSA is used to send a 5.725 MHz baseband signal (IF signal) into the RF section up converter, which basically up converts this signal frequency into the frequency which is to be transmitted, being 2.4 GHz. Next, the unmodulated 2.4 GHz carrier frequency (RF signal) is transmitted from the transmit antenna through the multipath propagation channel and is received at the receive antenna. The transmit power used during the measurements is set to provide a mean receive signal power of about -67 dBm. The transmit power was around -10 dBm to -15 dBm. Both the transmit and receive antennas (gain is unity) being used are quarter-wave monopole antennas, which is specified by CSIRO Australia. The display on the VSA shows the signal spectrum produced when movements occur near the antennas. The receive signal fluctuates when more movement or less movement occurs.

Because the transmit and receive sections of the VSA are co-located, the need for carrier recovery from the transmitted signal is eliminated. This ensures a noise free phase estimate which is free from fluctuations and full coherent reception [31].

From the receive antenna the 2.4 GHz signal is then down converted at the RF section, back to the original baseband frequency of 5.725 MHz and this frequency is then fed into a two way splitter. The splitter halves the receive power (3 dB loss), where one half of the receive power goes to the receive section of the VSA and the other half is fed to the Marconi Instruments Modulation Analyser. The purpose of the splitter is to see what the carrier is doing (i.e., carrier to noise) in the VSA and to take sample readings of error tables, eye patterns, vector constellation diagrams and other useful information.

The baseband frequency is then fed into the Marconi Instruments Modulation Analyser (MIMA) which has a IF output frequency of 1.5 MHz. On the MIMA, the RF input level knob was turned all the way to the maximum level, the tune oscillator and adjust level was set to 1. The MIMA, basically, acts as a peak detector, whereby it detects the levels of the propagated RF signal and gives this signal a DC control voltage (0 - 80 mV), which is directly proportional to the RF signals amplitude. This DC control

voltage results from the envelope detection of the down converted baseband signal by the MIMA. The MIMA changes the AC voltage fluctuation to a DC voltage through its internal circuitry. When the RF signal amplitude increases this produces a higher output DC amplitude and when the RF signal amplitude is decreased, this produces a lower output DC amplitude. This DC voltage is then used to control the Voltage Control Attenuator (VCAAtt).

This DC voltage is fed into the Apex Systems VCA1001 VCAAtt, before it goes into the sound blaster within the computer. The VCAAtt's main purpose is to respond to the DC voltage fed into it. The VCAAtt attenuates and amplifies the DC control voltage, which is assigned to pin 9 (VC) on the VCAAtt chip. The VCAAtt changes the DC amplitude fluctuations, from the MIMA, back into an AC amplitude fluctuation because the sound blaster card which is used to sample and store the data, only accepts AC voltage due to its blocking capacitor within its circuitry. At the same time a 100 Hz sinusoidal carrier from an AWA oscillator is assigned to pin 2 (input 1) on the VCAAtt chip. The DC control voltage amplitude modulates the 100 Hz sinusoid, when they are assigned to their respective pins. The amplitude modulation is achieved by assigning the DC control voltage to pin 9 and the 100 Hz sinusoid to pin 2 of the VCAAtt chip, and the output which is assigned to pin 17 on the chip, outputs the 100 Hz amplitude modulated carrier. This 100 Hz amplitude modulated signal is then fed into the sound blaster. This amplitude modulated 100 Hz carrier accurately reflects the fading of the 2.4 GHz carrier wave, when propagated between the transmitter and receiver.

Finally, the 100 Hz signal (from pin 17) is fed into the sound blaster which samples the data and this data is stored on the computers hard disk for post analysis. The sound blaster accepts frequencies in the range of 30 Hz - 20 kHz. The 100 Hz carrier is over-sampled at 11.025 kHz rate. The sampling rate was chosen at 11025 samples/s, because the period for the 100 Hz is, $T = 0.01$ seconds. This means, that there are 111 samples in one period of 0.01 seconds. This are more than enough samples to carefully track all the peaks and troughs of the sinusoid (99% accuracy), which is represented by the 100 Hz carrier. A higher sampling rate could have been chosen (40 kHz), but then we would have more samples within each period and this directly results in more data being produced. Due to the limited capacity of the computers hard disk, we could not choose

a higher sampling rate. A lower sampling rate (4 kHz) may not have been sufficient enough to carefully track all the peaks and troughs of the sinusoid. Therefore, the 11.025 kHz sampling rate was chosen keeping in mind the limited capacity of the hard disk and more importantly, the number of samples (sampling rate) needed to carefully represent the fading.

The audio option was chosen, and the left and right channel gains were set to 1 on the sound blaster. Next, the start button was pressed and temporal fading data was recorded for the 20 second measurement period. Once, the recording of the data is finished, we can view the fading signature on the monitor. The sound blaster produces a wave signature and waveform graph which can be seen by enlarging a particular area on the wave signature. The sound blaster is a good indicator of the effects of movement which causes fading through temporal variations. The data was saved on the hard disk in the sound blaster format, which was a .wav file format.

5.5 Measurement System Calibration

The measurement system was calibrated thoroughly prior to taking any measurements for the day. The 2 meter RG-213 calibration coaxial cable was connected to attenuators at the input and output ports of HP 89441A RF section. A 10 dB attenuator was connected to the input port, while a 40 dB attenuator was connected to the output port at the RF section. This is a realistic reference to start from when antennas are not used. These attenuators are connected for calibration purposes, so that, a realistic situation is created, whereby the attenuators give the system attenuation losses. These are similar losses which are experienced by the system when the monopole antennas are connected up to the input and output ports of the RF section via their respective coaxial cables, with the propagation path inserted.

With the calibration cables and the attenuators connected to their respective ports, the system was ready for calibration measurements. Initially the source was set to provide a mean receive signal power of -63 dBm as shown on the vector signal analyser (VSA), because this level is yet to be affected by noise and interference as can be seen in Figure

5.6. After setting up the source level and other measurement settings, the start button on the sound blaster was pressed and the measurement was taken for a period of 1.5 to 2 seconds for the specific source level.

After the first measurement, the next measurement was taken for the same period of time, but for a different receive level being -64 dBm. The next measurement was taken when the receive level was set to -65 dBm. Following this level, the next level was set to -67 dBm and the measurement taken. This same procedure was followed by incrementing the source level by 1 or 2 dBm, for measurements down to -92 dBm. As shown in Figure 5.6, at -88 dBm the calibration data is deeply affected by noise and interference. Figure 5.6 gives us a window of opportunity because by setting the source on the VSA around the -65 to -70 dBm mark, we can ensure that the received fading data is not greatly affected by noise. Therefore, most of our fading measurements had a source setting of -67 dBm.

Figure 5.6 was produced by writing a few lines of code in a high-performance numeric computation and visualisation software package called Matlab, version 4.2c.1 created by The Mathworks Inc. Section 6.2, shows and explains the procedure which was followed and the software which was written to produce Figure 5.6 and also the fading patterns, which are shown in section 6.3 for the different antenna positions. The procedure used to obtain the system calibration data and its associated software code written to produce Figure 5.6 in section 6.2, is the same procedure which is used to produce the fading patterns as shown in section 6.3.

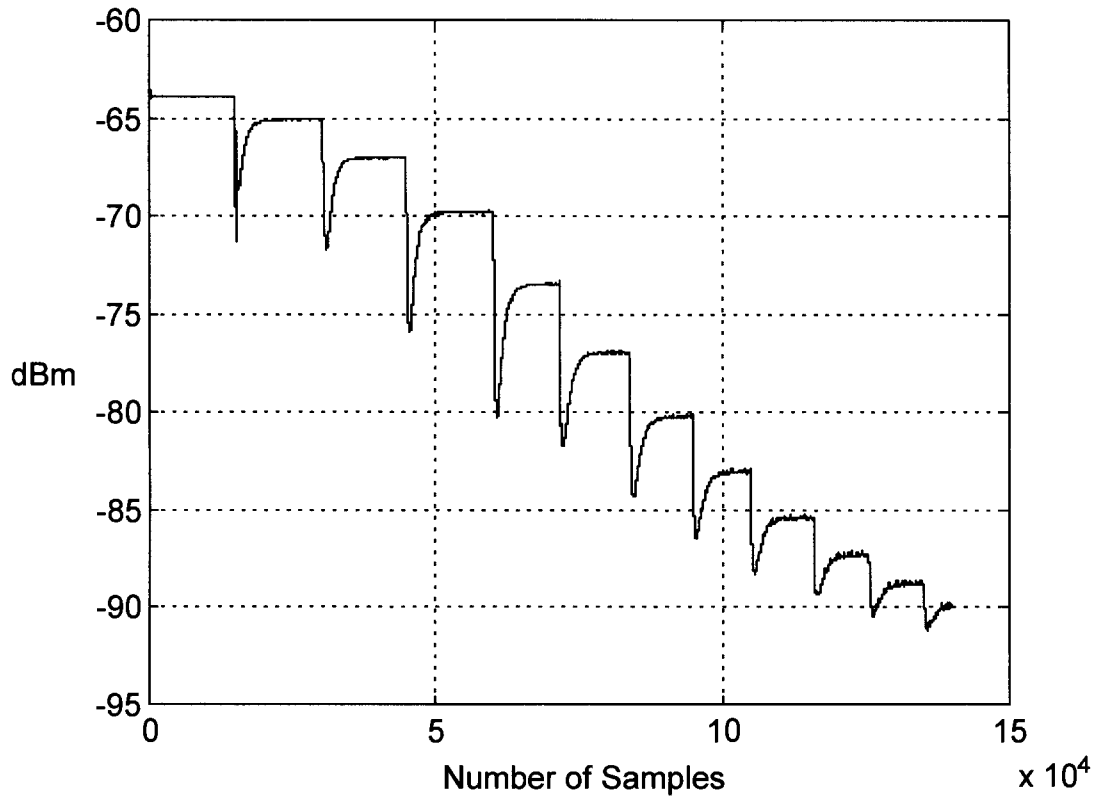


Figure 5.6 System calibration data for fading measurements

5.6 Measurement Procedure

The measurements were conducted over a week to collect all the data samples for the 25 fading measurements. At first, different antenna positions were considered, but were then discarded because these antenna positions did not represent the entire laboratory space. Finally, after some deliberation with my colleague the measurements were conducted for the antenna positions as shown in Figure 5.1 (see section 5.2).

After deciding on the location of the antennas within the laboratory, the measurements were ready to be taken. On arrival at the laboratory on any specific day, the equipment was setup (as shown in Figure 5.5). Next, the system was calibrated. Finally, the antennas were connected to the measurement system and the measurements were ready to be commenced.

The antenna positions for obtaining the fading data were conducted as follows. Firstly, the measurement for a specific position for the transmit and receive antenna was conducted (eg. Tx = B, Rx = A). For the next measurement, the receiver position remained the same (eg. A), while the transmitter was moved to a new position (eg. C). Following this measurement, the same pattern was conducted, whereby the receiver remained in the same position (eg. A), but the transmitter was moved to a new position (eg. D). This same pattern was followed until all the positions were covered by the transmit antenna, these being positions B, C, D, E, F and G. After this, the receiver was moved to a new position (eg. B) and the transmitter was positioned at the other positions, A, C, D, E, F and G, and the measurements were performed for these new locations. This procedure was followed until all the positions were represented by the receiver (from A - G) and its subsequent transmitter positions. The distance between the transmit and receive antenna positions were about 2 to 5 meters, depending on where the transmit and receive antennas were positioned. An extra position H was incorporated as one of the measuring positions, as there was activity present around this positions as it was near a computer terminal.

The basic procedure for attainment of the fading data was as follows:-

1. The system was setup and calibrated.
2. The transmit and receive antennas were placed in their respective positions (as mentioned above).
3. After everything was ready, the start button on the sound blaster was pressed.
4. A controlled environment was initiated (where temporal variations are known, people ranging from 1 to X persons are moving around the receive antenna in close proximity).
5. The measurement was taken for a period of about 20 seconds (shown on the sound blaster).
6. At the 20 second mark, the measurement was stopped and the sampled data was stored on the hard disk for post analysis.
7. Steps 2 - 6 are repeated until all the antenna positions have been covered for that particular day.
8. Steps 1 - 6 are commenced, if the measurements are conducted on a different day.

It should be noted, that step 1 only needed to be commenced if the measurements were being commenced on a different day. All the measurements were not conducted in a single day, due to time constraints, demands placed on the equipment by other people and the lengthy nature of the measurement procedure.

Each recording described above corresponds to 20 seconds of channel temporal variations. During each 20 seconds, care was taken to have a continuous motion of the same or similar nature (ie. walking fast, body movements and occasional jumping). As mentioned, the sound blaster was used to sample and store data in the computer. This data will be statistically analysed to see the significance of the fades for the particular antenna positions.

Once the measurement was taken we could view the sound blaster signature or by clicking/enlarging a particular spot on the waveform signature we can produce a corresponding wave pattern on the graph to get a visual of the wave (sinusoid) pattern. Using the sound blaster is a very useful way to show the characteristics of the measurements. By viewing either the wave pattern from the graph or the wave signature, we can see how movement of people causes fading to occur in a channel. The greater the sine wave amplitude the more movements occurred.

Next, statistical analysis of the data samples was required. The results of these statistical analysis are shown in sections 6 and 7. The analysis considered includes the level crossing rate and the average fade duration for each of the fading data samples and fade depth. The measurement environment, system and procedure have been described, it is now time to examine the results and develop statistical models for the fading data samples. This will be carried out in chapter 6.

Chapter 6

RESULTS AND ANALYSIS

6.1 Introduction

The 20 second recordings of the narrowband temporal fading data is analysed extensively and the results are presented in the following sub-sections. The results will be divided in their specific sections so that understanding can be facilitated.

All the results were produced in Matlab 4.2c.1, as it was the most efficient and reliable software available at the time to produce the results and their statistical analysis. The procedure and software used to produce the fading patterns and the cumulative distribution functions will be presented in the following sub-section (section 6.2). The procedure and software used to produce the measurement system calibration data (Figure 5.6) for the fading measurements, as mentioned in section 5.5, will also be shown.

6.2 Procedure and Software Code

The code which was written in Matlab, was used to produce the fading patterns as shown in section 6.3 and also for the system calibration data (figure 5.6). After the measurements were concluded, the post analysis was started. To produce the fading patterns, the 100 Hz amplitude modulated carrier was sampled and saved by the sound blaster as its .wav file format. Next, a procedure which is similar to demodulating an AM signal using a rectifier detector was implemented. The rectifier detection is a noncoherent method of AM demodulation. After this procedure was finished, the data is imported into Matlab, where code is written to produce the fading graphs. I will discuss how the fading patterns were produced in a step by step format, starting with the procedure and, than I will show and explain the software code used to produce the fading patterns.

The first step of this procedure consisted of finding a program (software) which would convert the fading information which is stored in the .wav file format and convert it into

a more useful form of information, such as a data file. A program called Sox was found on the internet to serve the purpose of converting the .wav file format into a useful data file. This Sox program converts the sound blasters .wav file format (eg. crc.wav) into a data file format (eg. atri.dat). When the Sox program is used on the .wav file format, the resultant is a table of data. This data table consists of two columns, one time column (in seconds) and one voltage column (in volts). The time column represents the measurement period of about 20 seconds and the voltage column represents the information of the fading data samples.

Each fading data file represented about 8 megabytes of data, when conversion was done from a .wav file format to a .dat file format by the program. The command which was used to convert the .wav file format to the .dat file format using the Sox program at the MS-DOS prompt, is as follows (this is an example of the command used):-

```
C:\> sox -t.wav test.wav -t.dat record.dat
```

where,

Sox = the Sox.exe command which is used to convert the formats.

-t.wav = is the input file switch in the .wav file format from the sound blaster.

test.wav = is the input file name, which is named prior to the commencement of the measurements.

-t.dat = is the output file switch in the .dat file format, which is converted to the data file.

record.dat = is the name of the output file, which is the file with the data of time vs voltage.

The result of the Sox command is to produce a table of time versus voltage for various ranges of the data. The data basically shows, that at a certain time period there is an equivalent voltage level which is shown and this voltage level directly corresponds to the amplitude of the sinusoid wave for that particular time. This table of data is needed, so that software can be written to produce the fading graphs. From this fading graphs, statistical analysis can be conducted. Before, I go any further, I will mention that due to the large amounts of data which are produced when the above conversion is carried out, it is impossible to present these data files in this report as one data file alone takes up

about 8 megabytes of hard disk space. It is regretted that the files take up so much space, but it is worth it because if we had sampled the 100 Hz frequency at a lower sampling rate, then we might not have produced the entire fading envelope with all its peaks showing.

The next step which was implemented in this procedure was to suppress the positive half of the amplitude modulated 100 Hz carrier frequency. A rectifier detector works in the similar manner. The reason that the positive half is suppressed and not the negative half is because the negative and positive halves of the sinusoid are mirror images of each other. The negative half was chosen because the program used to suppress the sinusoid works easier with negative values. The program which was used to collect all the negative halves of the sinusoid was Turbo Grep version 3.0, produced by Borland International (1991). At the time of retrieving the information, this program proved to be the best solution to the problem at hand. The command used to retrieve the information sought after consisted of applying the following command at the MS-DOS prompt. An example is illustrated,

```
C:\> grep "-" record.dat > record.m
```

where

grep = the program used to retrieve the necessary information

record.dat = is the file, which contains the data of time vs voltage

record.m = is the output file which contains only the negative voltage values

which has been saved with a different prefix (.m) as this is needed by Matlab in this format.

Once this procedure was completed, it was time to write code in Matlab to produce the fading information graphs. The code written to produce the fading patterns was as follows:-

```
load record.m; (line 1)
```

```
recordT = record(:,1); (line 2)
```

```
recordL = record(:,2); (line 3)
```

```

[b,a] = butter(5,40/5512.5);                                (line 4)
fade = filter(b,a,recordL);                                (line 5)
m = mean(fade);                                           (line 6)
lm = 72.5 * m - 63;                                       (line 7)
y = 72.5 * fade - 63;                                       (line 8)
n = -1 * (lm - y);                                           (line 9)
plot(recordT,n)                                           (line 10)

```

I will explain the meaning of each line number, as it used to produce the fading patterns. The rectified data values are loaded into Matlab using the load command, which is represented by line 1. Line 2, is to define an array called *recordT* (which is an example in this case) and this array is equated to the time column of the data file which is called record. Line 3, is to define another array called *recordL*, and this array is equated to the voltage (level) column of the data file.

Line 4, is where a 5th order Butterworth filter with a 3 dB cut-off frequency at 40 Hz divided by half the sampling rate (5512.5 Hz) is created or used on the sampled data to filter out the modulated 100 Hz carrier frequency. This is done because we want to regain the original fading envelope produced when the measurement was carried out. This Butterworth filter with its inputs is then equated to two vectors *b* and *a* (examples in this case). A 5th order Butterworth filter was decided on as it has a sharp cut-off frequency and we want to eliminate the 100 Hz to regain the original fading envelope.

Line 5, is where we apply the Matlab filter function with the inputs of the newly created vectors *[b,a]* of the Butterworth filter and the voltage column array *recordL*, to create a new array variable called *fade*. The filter function uses a digital filter which filters the data in *recordL* (the voltage data file) with the filter described by vectors *a* and *b* to create the filtered data which is *fade*.

Line 6, is where we take the mean of the newly created and filtered array *fade*. This mean represents a one number linear mean of the entire array. Since, Line 6 represents a linear mean, we need to convert this linear mean (in volts) to a logarithmic mean (dBm) to view the fading envelope in more detail. Line 7, creates the logarithm of the mean *m*

and the equation which represents Line 7 was calculated from our calibration curve, Figure 5.6. The received level of -63 dBm was chosen as the starting level because we wanted to have a 30 dB margin, so that if any deep fades occurred within the channel during propagation, they could have been clearly distinguished as a deep fade without being affected by noise and interference.

Line 8, creates a new variable y using our calibration data, to convert the $fade$ variable to a logarithmic function. The variable y represents a non-normalised logarithmic value. Line 9, creates a normalised value n , whereby the log of the mean lm is subtracted from y and the product is multiplied by -1. The product is multiplied by -1 to provide the correct sign sense when the fading envelope is produced. If the product is not multiplied by -1, the fading envelope will be inverted and it will show the wrong fading. Line 10, plots the two variables and the fading envelope or graph is produced. Section 6.3, shows the various fading envelopes for the measurements conducted.

The calibration data curve was produced using the same procedure as explained above, but the code written to produce the calibration curve was a little bit different than the code written to produce the fading envelopes. A few lines were excluded from the code. The curve was produced using the following lines of code:-

```
load calibration.m;
recordL = record(:,2);
[b,a] = butter(5,40/5512.5);
fade = filter(b,a,recordL);
y = 72.5 * fade - 63;
plot (y)
```

The lines for the code above are exactly the same as the lines of code used to produce the fading envelope. The explanation for each line of the code used to produce the calibration curve has been discussed above, as the lines of code are exactly the same. The procedure and software code used to produce the fading patterns has been discussed in length and it is time to present the fading envelopes and their corresponding statistics. These fading envelopes are shown in the following section.

6.3 Results of The Statistical Analysis: Fading Envelopes and Statistical Data

The 20 seconds recordings of the narrowband temporal fading data were analysed thoroughly and their results presented in this section. As mentioned in section 5.6, the measurements were conducted in a systematic order for all the antenna positions as described in section 5.6, but only ten results for different antenna positions are presented in this section. This is due to the relatively tight time constraints which had to be worked with and also the large amounts of data which had to be analysed for each particular measurement. But, the results which are presented accurately represent the entire laboratory for the transmit and receive antenna positions used in the measurements.

The outlook of the presentation will follow a format, whereby the fading envelopes will be presented for the various transmit and receive antenna positions and this will be followed by the statistical properties of that particular fading envelope. Following the presentation of the figures and tables, a discussion for that particular figure and table will be conducted. This format, thus ensures a clear understanding of the statistical analysis of the particular fading envelope and their relevance to the project.

Figures 6.1 to 6.10, displays the envelope fading waveforms for the different transmit and receive positions at the ATRI laboratory. Tables 6.1 to 6.10, present the statistical properties for each of their corresponding figures. The statistical parameters presented include the number of crossings, the level crossing rates (LCR) and the average duration of fades (ADF) for each particular level or threshold (dB). These parameters show the characteristics of fading for each particular figure. See sections 4.7.1 and 4.7.2 to refresh your memory on the level crossing rates and the average duration of fades, and the formulas which are used to represent these statistics. The values for the LCR and ADF were calculated using equations (4.18) and (4.20), respectively.

By viewing the fading envelopes one by one, now, we can see the typical fading patterns which are produced, when a channel is affected by temporal variations. There are no

surprises at this point. Some deep fades are seen on some fading envelopes, while on others the fades are relatively straight forward.

6.3.1 Transmitter Position E and Receiver position A

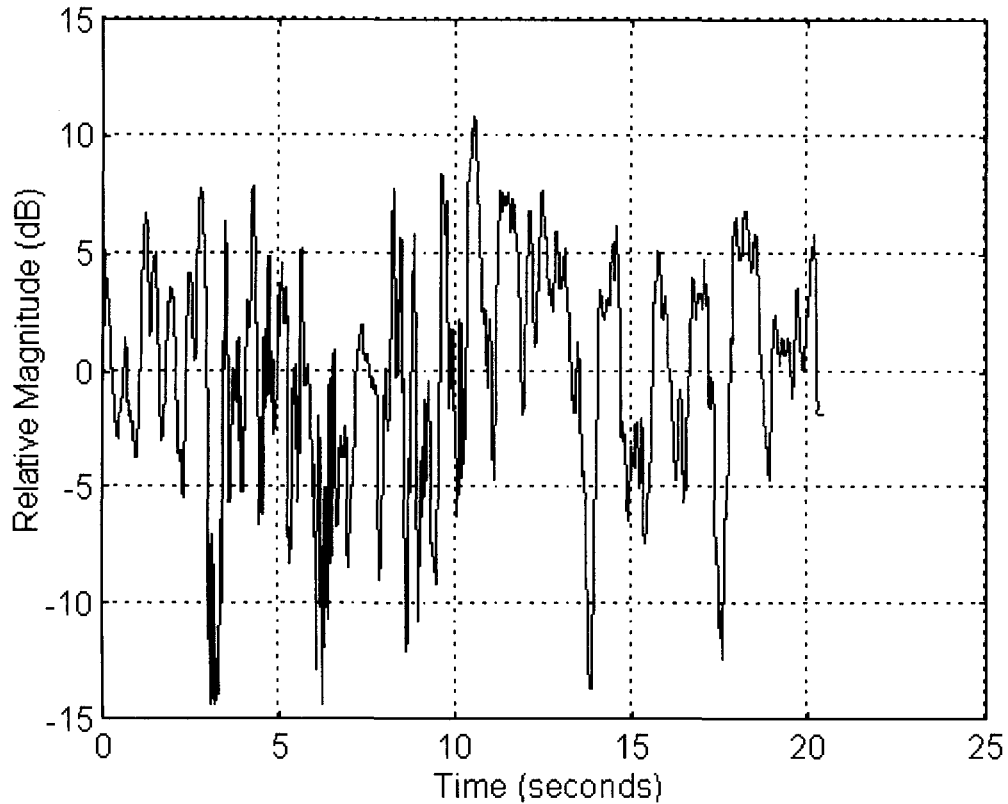


Figure 6.1 Temporal fading envelope for Tx position E and Rx position A

Table 6.1: Statistical parameters of Figure 6.1

Level (dB)	Total Number of Crossings	Level Crossing Rates (crossings / second)	Average Duration of Fades (seconds)
6	13	0.7508	1.1839
3	37	1.8050	0.3786
-3	35	1.7075	0.2525
-6	20	0.9757	0.1196
-9	13	0.0463	0.0793
-12	8	0.3903	0.0489

Figure 6.1, shows the fading envelope for the transmit antenna position E and the receive antenna position A, when the measurement was conducted. See Figure 5.1 for the antenna placements in the laboratory. As we can see from the fading envelope, there are various constructive and destructive interferences which occur within the 20 second measurement period, which are caused by temporal variations due to motion of people or objects. See section 4.3 for explanations of interferences in relation to signal fading.

In the measurements conducted, majority of the motion was initiated or conducted by myself and my colleague. Motion which was contributed by other people working within the room at any particular time was minimal. Motion which was conducted included walking briskly, waving of arms and occasionally jumping around the antennas. These movements are shown in the fading envelopes as constructive or destructive interferences. The line of sight path was blocked a few times during the 20 second measurement period.

Figure 6.1, shows a typical fading envelope, with rapid movements occurring within the first 12 seconds of recording. After 12 seconds less rapid movement can be visualised from the fading envelope. A dynamic fading range for this measurement is about 25 dB. Deep fades of around 14 dB below the mean value can be seen from Figure 6.1. A big enhancement of 11 dB can be seen at the 10.5 second mark, this signal enhance could possibly be due to intermittence which may have been caused by either my colleague or I standing in the way (blocking) of a major out of phase propagation path within the propagation channel.

Examining the statistical parameters of Table 6.1, we can see that there are more crossings around the -3 dB and 3 dB levels of Figure 6.1. This is due to the fact that, when motion was being conducted, during the measurement period, we were not affecting any important propagation paths for the 20 seconds of data recording. The important propagation paths include the LOS path and the major reflected paths within a channel. This thus, shows a greater LCR for the -3 dB and 3 dB levels, when compared to the other levels. The LCR can be directly related to activity (motion), with lots of activity being conducted the LCR increases at all levels. The 0 dB level has the most number of crossings for Figure 6.1 with 38.

The LCR of Table 6.1 represent statistical values for the 20 seconds of measurement. These values are statistically valid if we have a long enough sampling period. Our measurements were conducted for a 20 second period and this measuring period is valid, as we can clearly present fading envelopes and their statistical analysis for the measuring period with 40 to 80 fades as mentioned by [32].

For example, for the -3 dB level we got a LCR of 1.7075 crossings per second, this means that on average there are 1.7075 crossings per second which cross the -3 dB level with a positive slope within the 20 second measurement period. Although, we cannot get 1.7075 of a crossing, these LCR represent statistical values for a valid measuring period of 20 seconds. We may get, say, 2 crossings or 3 crossings in any particular second within the 20 seconds, but this is not what the LCR represents. The LCR just represents an average which is statistically valid for a particular level, of the total measuring period of 20 seconds.

The average duration of fades (ADF) also shows a direct relationship to the activity being conducted within the propagation channel during the measurement period. The greater the activity the greater the value of the ADF, in general. The ADF is related to the rate of the temporal variations, how fast the temporal variations are occurring within the propagation channel. It is basically in relation with the velocity of the physical changes which are occurring in the propagation channel (i.e. people moving, trolleys moving, people running, fans switched on etc.).

From Table 6.1, we can see that the 6 dB level has the highest ADF value 1.1839 seconds, when compared with the other levels. It must be stipulated that the values for the ADF are just averages for a particular level, of the 20 second measuring period. For the -12 dB level the ADF is about 0.05 seconds, as the fading envelope crosses this level 8 times.

As can be seen from Figure 6.1, there are medium to wide duration's between the negative and positive slopes of the 6 dB level. Thus, by adding these individual duration's and dividing them by the total number of crossings we would get a larger value for the ADF at that particular level of 6 dB. For the -12 dB level, there are only a

handful of fades which cross the this level and with relatively smaller duration's between individual fades, when computed we would get a smaller ADF for this particular level.

6.3.2 Transmitter position D and Receiver position A

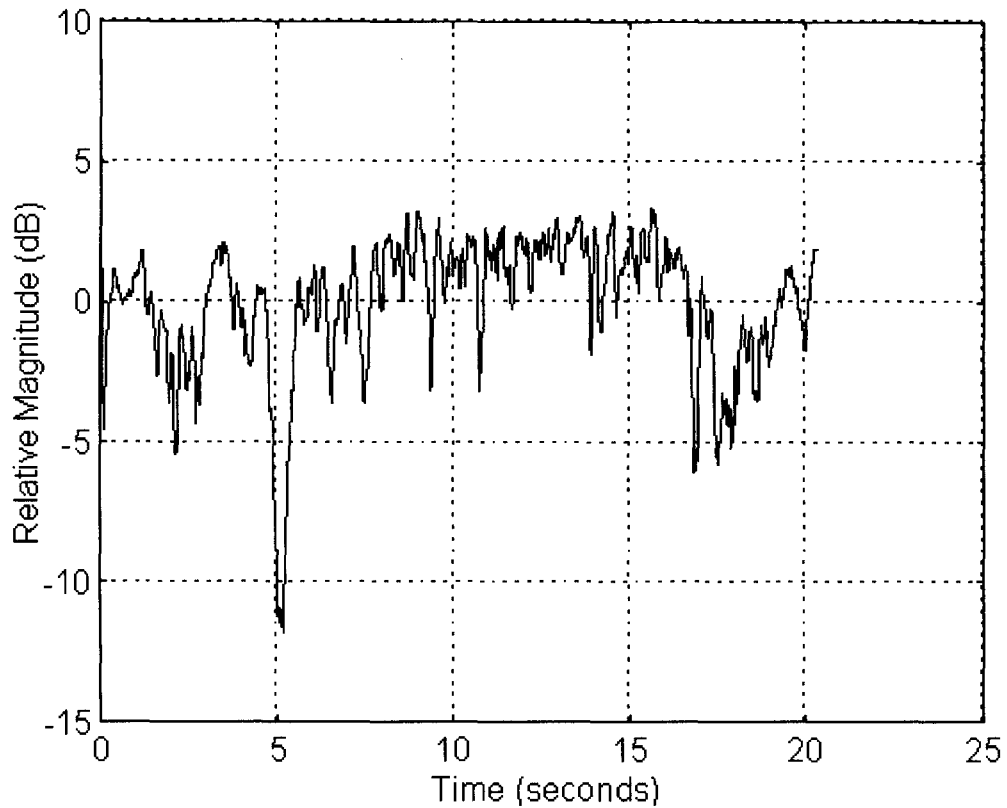


Figure 6.2 Temporal fading envelope for Tx position D and Rx position A

Table 6.2: Statistical parameters of Figure 6.2

Level (dB)	Total Number of Crossings	Level Crossing Rates (crossings / second)	Average Duration of Fades (seconds)
3	9	0.4391	0.7489
-3	16	0.7806	0.1428
-6	3	0.1463	0.1556
-9	1	0.0488	0.2750

From Figure 6.2, we can straight away see a relatively medium fade around the 5 second mark. This could have been due to many waves which may have been reflected, edge scattered of objects or our body parts, or diffracted, and thus combined at the receive antenna to produce the destructive interference seen in the figure. The other fades are relatively small or shallow.

The dynamic range of the fading envelope is around 15 dB, thus showing that in this measurement there weren't any deep fades, only one relatively medium fade around the 5 second mark.

The LCR once again shows a greater number of crossings at the - 3 dB and 3 dB levels when compared to the other levels. The 0 dB level has got the most number of crossings with 26. For the 0 dB level the LCR was calculated to be 1.27 crossings per second. The number of crossings, the LCR and the ADF for each level is presented in Table 6.2.

6.3.3 Transmitter position C and Receiver position A

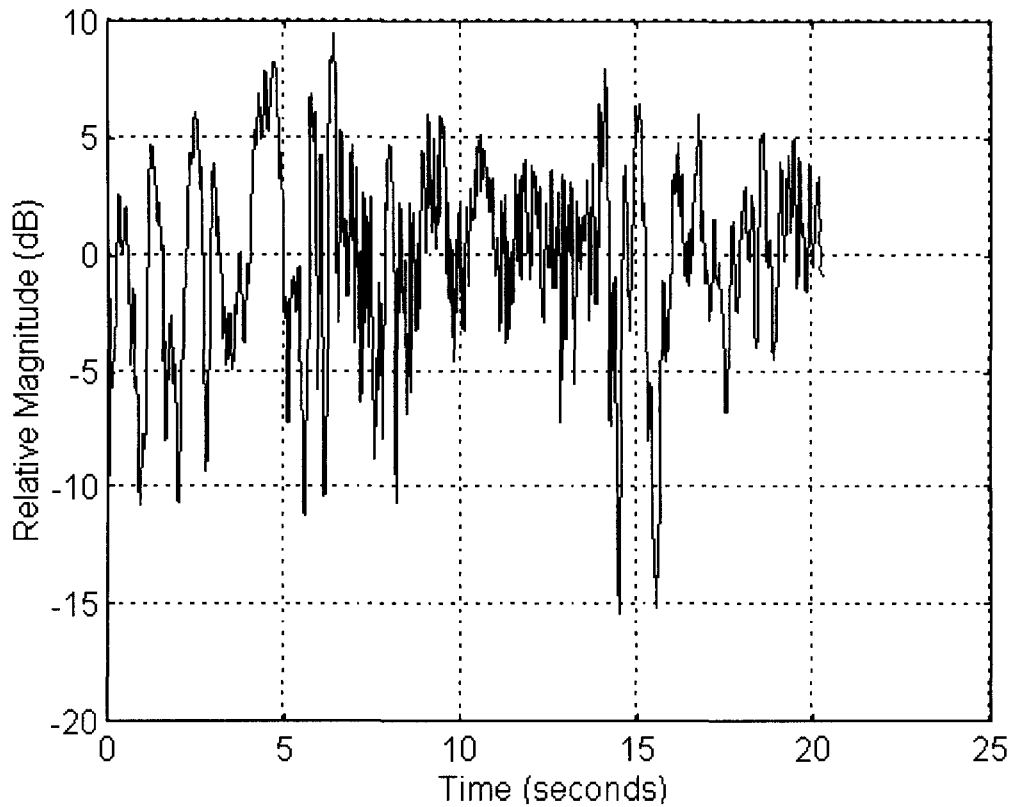


Figure 6.3 Temporal fading envelope for Tx position C and Rx position A

Table 6.3: Statistical parameters of Figure 6.3

Level (dB)	Total Number of Crossings	Level Crossing Rates (crossings / second)	Average Duration of Fades (seconds)
6	13	0.6343	1.0388
3	45	2.1955	0.3068
-3	43	2.0979	0.0940
-6	21	1.0246	0.0772
-9	10	0.4879	0.0683
-12	2	0.0976	0.1212

Figure 6.3 shows use the fading envelope of the particular antenna positions. As we can see, there was lots of activity within the 5 to 15 second mark, as me and my colleague would have really started getting into our motions (especially me) with brisk walking, arm movements and jumping occasionally. This motion is clearly represented on the fading envelope as there are more rapid fades within this particular 10 second period than any other period. Couple of deep fades happened around the 15 second mark and also a few enhancements around the 6 second mark.

By looking at the envelope, a dynamic fading range of about 24 dB can be inferred for Figure 6.3. Figure 6.3 represents a good fading envelope with lots of rapid fades and occasional deep fades. The statistical parameters of Figure 6.3 are presented in Table 6.3. There were 43 crossings and 45 crossings for the -3 dB and 3 dB levels respectively. Most of this crossings would have occurred within the 5 and 15 second marks. There were 64 crossings at the 0 dB level, with a LCR of 3.1225 crossings per second for the 0 dB level.

The ADF for the levels are basically consistent with the number of times a particular fade crosses a level. For example, the duration of each fade in the -3 dB level is relatively small, and there are a lot of crossings through the -3 dB level, thus we have a small value for the ADF for the entire 20 second period in relation to the -3 dB level. But at the -12 dB level, because there are only two crossings at this level, we get a slightly bigger ADF when compared to the -3 dB level.

As can be seen from the number of crossings for each individual level, we can see that the number of crossings get less and less as the we move further away from the 0 dB level. This is because medium to deep fades do not occur as often as the shallower fades for any particular fading envelope analysed. Deep fades only occur when a significant propagation path is affected by motion of people or objects. Deep fades are unwanted in any propagation channel as they produce very high bit error rates (BER).

6.3.4 Transmitter position B and Receiver position A

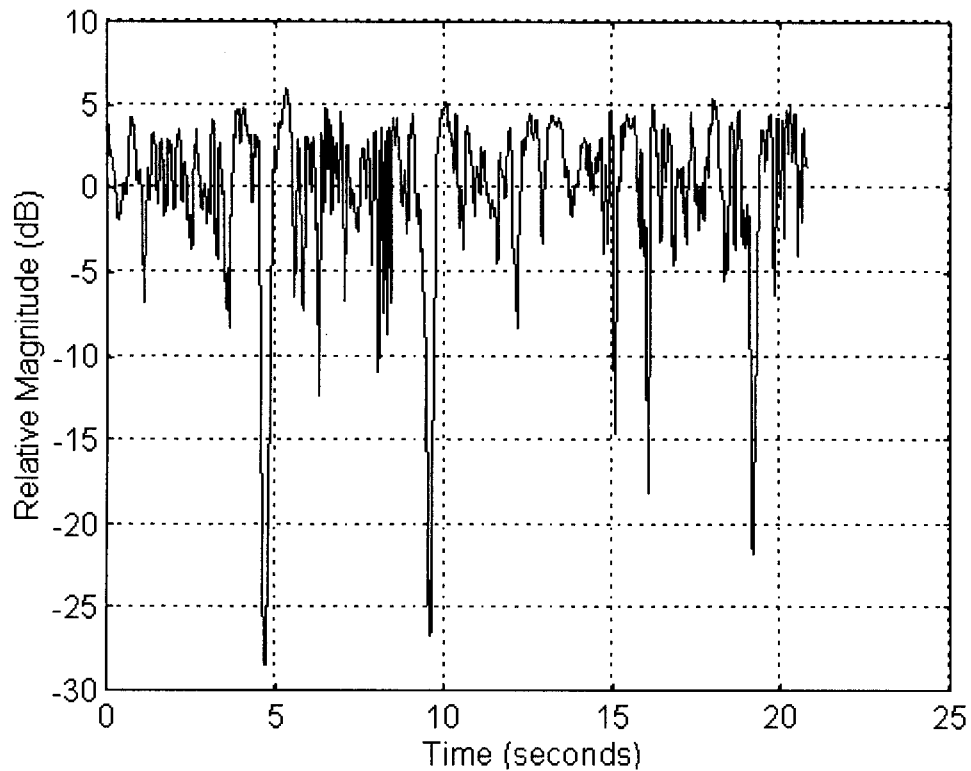


Figure 6.4 Temporal fading envelope for Tx position B and Rx position A

Table 6.4: Statistical parameters of Figure 6.4

Level (dB)	Total Number of Crossings	Level Crossing Rates (crossings / second)	Average Duration of Fades (seconds)
3	50	2.2812	0.2909
-3	38	1.8097	0.0775
-6	18	0.8572	0.0883
-9	7	0.3334	0.1434
-12	6	0.2857	0.0924
-15	4	0.1905	0.1477
-18	4	0.1905	0.1120
-21	3	0.1429	0.1157
-24	3	0.1429	0.0813
-27	2	0.0953	0.0446

On first inspection of Figure 6.4, we can see a number of medium to deep fades. The two deepest fades occurring around the 5 second and 10 second mark. As mentioned in section 6.3.3, deep fades are unwanted in any wireless system. They cause the fades to enter the noise region and any information which is within these information carrying signals will be affected by these deep fades in the noise region. These deep fades will produce very high BER (produce thousands of errors). These fades which start to get close or are within the noise region, will degrade the signal to noise ratio (S/N). Basically, these deep fades causes a very poor S/N to be encountered. Fades which are 20 dB below the mean value are of concern due to the fades approaching the noise region. At -27 dB, the fades are well into the noise region and can be very costly in relation to information lost.

As can be expected the dynamic fading range for this envelope is around 35 dB, thus telling us that deep fades have occurred. Deep fades can be cause by absorption of the waves by our bodies, intermittence, waves being edge scattered of our bodies and reflections. The two almost similar deep fades which occurred around the 5 and 10 second marks, can be contributed to the intermittence effect caused by blocking of important paths by standing within the propagation paths. They were produced by our bodies being in a similar position when the waves were encountered.

From Table 6.4, we can see that more crossings occurred around the -3 dB and 3 dB levels, with 26 crossings and 50 crossings respectively. The greatest number of crossings occurred at the 0 dB level, with 66 crossings. The LCR for the 0 dB level is 3.1432 crossings per second. From visual inspection of Figure 6.1, 3 crossings per second is a statistically valid value for the 20 second measurement period, at 0 dB. The ADF for each level is also shown in Table 6.4, and these values show no surprises on inspection.

6.3.5 Transmitter position F and Receiver position A

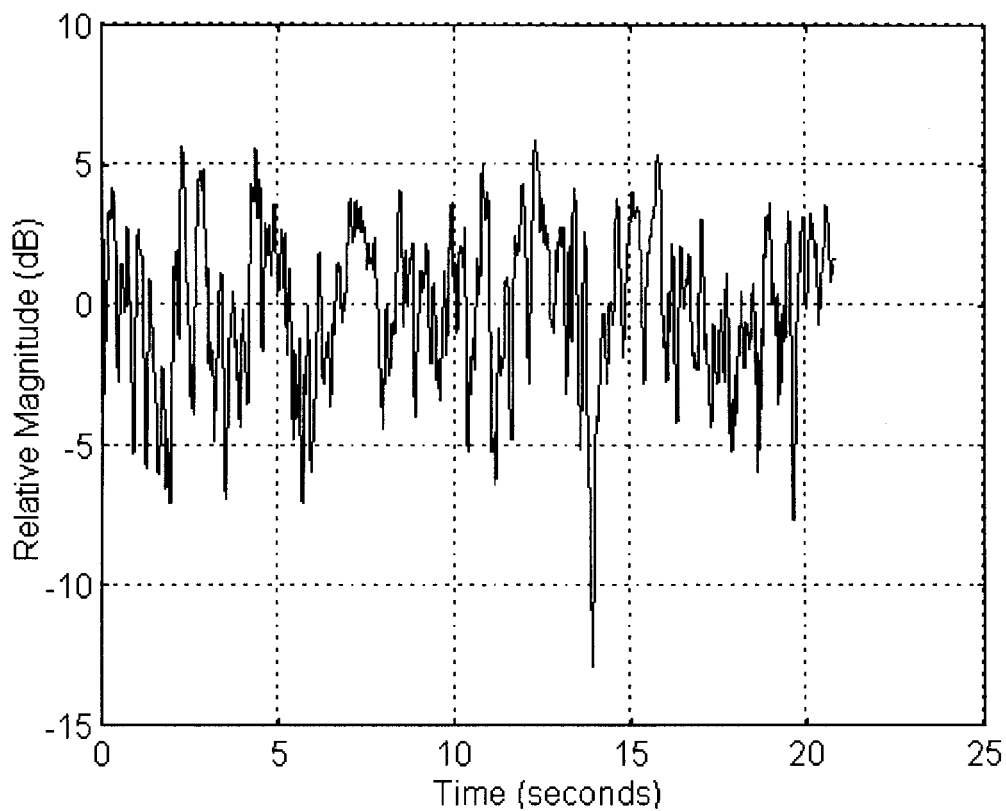


Figure 6.5 Temporal fading envelope for Tx position F and Rx position A

Table 6.5: Statistical parameters of Figure 6.5

Level (dB)	Total Number of Crossings	Level Crossing Rates (crossings / second)	Average Duration of Fades (seconds)
3	26	1.2382	0.6487
-3	35	1.6668	0.0894
-6	10	0.4762	0.0493
-9	1	0.0476	0.0874
-12	1	0.0476	0.0390

Figure 6.5, represents constant rapid motion for the 20 second measurement period. A noticeable, medium fade down to the level of 14 dB can be seen around the 14 second mark of the measurement period. The other fades are fairly shallow with not much variations in their fading.

The dynamic range for the fading envelope of Figure 6.5 is about 19 dB, thus concluding that there are no deep fades present on the fading envelope. Figure 6.5, represents a fairly constant rapid motion fading envelope with lots of constant activity happening throughout the 20 seconds of measurement time.

On viewing Table 6.5, we can see once again that more number of crossings which are occurring around the -3 dB and 3 dB levels, with 0 dB having the highest number of crossings. The number of crossings at the 0 dB level is 53, while at the -3 dB and 3 dB level there 35 and 10 crossings per second, respectively. There is only one crossing at the -9 dB and -12 dB levels, as would be expected because this levels represent the one medium fade which occurs around the 14 second mark of Figure 6.5.

The LCR of the 0 dB level consists of 2.5241 crossings per second, on inspection of the fading envelope, this represents a statistically realistic value for the LCR. The LCR for the 3 dB level is 1.2382 crossings per second and at the -3 dB level the LCR is 1.6668 crossings per second.

The ADF of each level is also presented in Figure 6.5, they represent typically valid values for the fading envelope in consideration. For the 3 dB level, the average duration of fades is around the 0.65 seconds, while at the -12 dB level the ADF is lower in its value. For a statistically valid length of measurement period the statistical parameters of Table 6.1, accurately represent the fading envelope.

6.3.6 Transmitter position H and Receiver position A

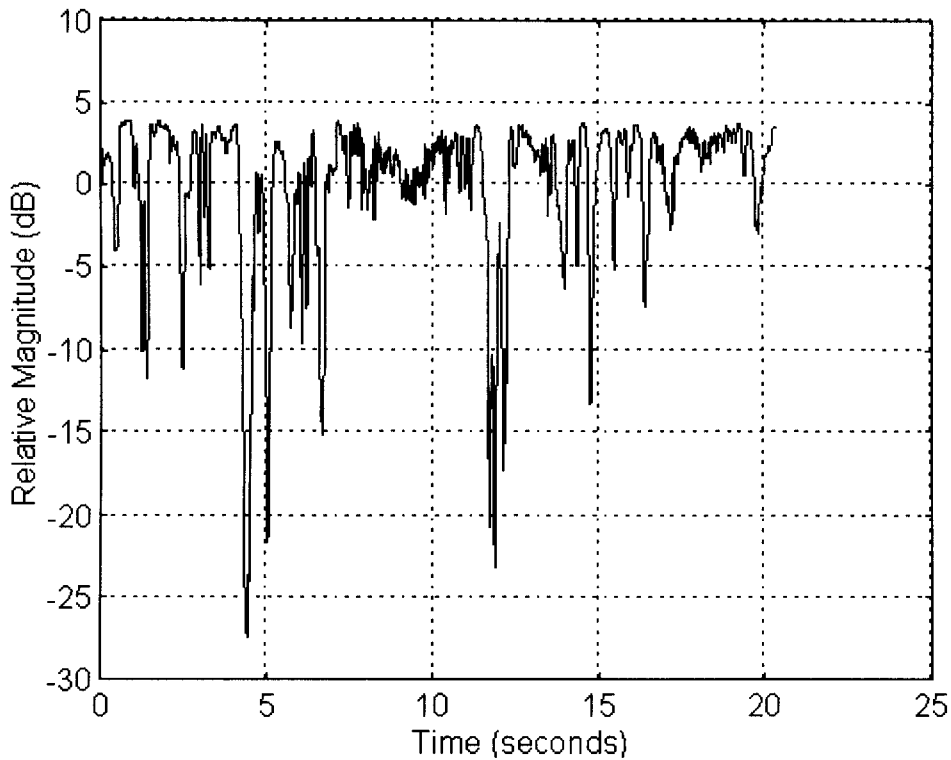


Figure 6.6 Temporal fading envelope for Tx position H and Rx position A

Table 6.6: Statistical parameters of Figure 6.6

Level (dB)	Total Number of Crossings	Level Crossing Rates (crossings / second)	Average Duration of Fades (seconds)
3	43	2.0979	0.2107
-3	19	0.9270	0.1604
-6	16	0.7806	0.1214
-9	10	0.4878	0.1286
-12	9	0.4391	0.0985
-15	6	0.2927	0.0850
-18	4	0.1952	0.0907
-21	4	0.1952	0.0603
-24	2	0.0976	0.0689
-27	1	0.0488	0.0312

Figure 6.6 shows a few medium and also deep fades which have occurred during the 20 second measurement period. As mentioned in section 6.3.4, deep fades are unwanted in a communication system, but they are not preventable from occurring in a channel. Deep fades can only be reduced to lesser fades depths by introducing special techniques which utilise intelligent antenna systems and space diversity techniques, working in combination with each other.

A deep fade occurred around the 5 second mark and also the 12 second mark of the fading envelope. Around the 7 to 11 second marks there were rapid motions occurring as represented by the shorter more rapid fades. Prior to this rapid fades, medium fades and then 2 deep fades occurred from the 0 to 7 second mark. More medium to deep fades occurred from the 11 second mark to the 16 second mark. As mentioned earlier they, can be produced by single affects or a combination of affects such as absorption of the waves by our bodies, intermittence, waves edge scattering off our bodies and reflections.

The statistical parameters of Figure 6.6 are presented in Table 6.6. As we can see there are lots of crossings at the 3 dB level with 43 crossings and also at the 0 dB level with 44 crossings. This would be predicted as there are more constant rapid motions crossing these two levels, then any other levels. As mentioned in section 5.6, the transmit antenna was positioned at position H, which was close to a computer terminal which always had one individual working at the terminal, thus we can suffice that some of these medium to deep fades could have been caused by this person working at his terminal, in combination with my colleague and I introducing motion in a controlled manner.

The dynamic fading range for this envelope fading is 31 dB, which tells us that fairly deep fades occurred in the system during the measurement period. For any wireless system with typical worst case receive levels of -88 dB or more will be affected by medium and also deep fades as the system will be approaching the noise region and these fades will degrade the S/N ratio severely, thus producing very high BER. For a system designer, fades of -20 dB or less below the mean receive value should not be

acceptable values and must be improved for the system to function properly when errors are introduced in the systems channel.

6.3.7 Transmitter position E and Receiver position C

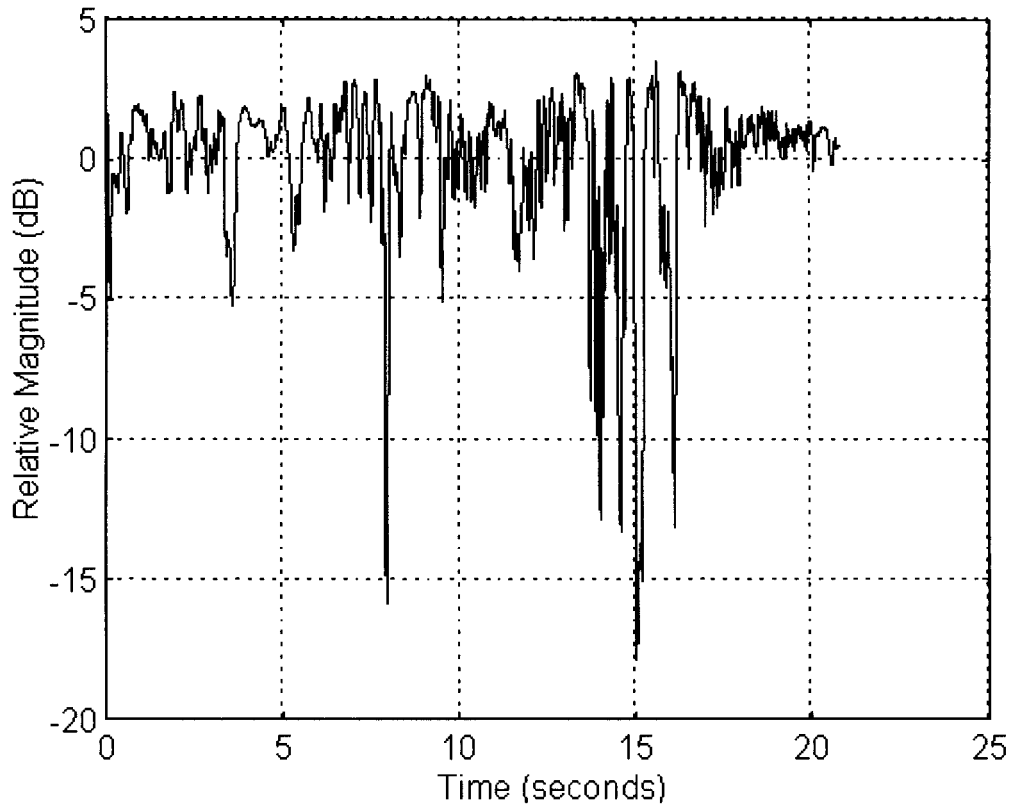


Figure 6.7 Temporal fading envelope for Tx position E and Rx position C

Table 6.7: Statistical parameters of Figure 6.7

Level (dB)	Total Number of Crossings	Level Crossing Rates (crossings / second)	Average Duration of Fades (seconds)
3	8	0.3810	0.8959
-3	23	1.0953	0.1013
-6	9	0.4286	0.0953
-9	7	0.3333	0.0795
-12	6	0.2857	0.0606
-15	3	0.1429	0.0383
-18	1	0.0476	0.0027

Figure 6.7, represents a different kind of fading envelope. At the start there are constant slower motions in progress, after the 9 second mark of the measurement period more rapid motion was initiated, with a medium fade occurring around the 8 second mark, while a whole string of medium to deep fades occurred from the 13 to 16 second marks. Towards the end of the period we see very small fades produced, as this would have represented the end of the measurement, an we would have toned down our motion. From the 10 to 16 second mark, there would have been brisk motion which would have affected important propagation paths, thus producing a whole string of medium to deep fades.

The dynamic range of the fading envelope is 21 dB, which shows that there were some medium to deep fades which occurred within the system during the measurement period. The statistical properties of Figure 6.7, are presented in Table 6.7. Once again, the 0 dB level has the most number of crossings with 58. The LCR for -3 dB is 23 crossings, while the 3 dB level only has 8 crossings. This is because there are more fades occurring below the mean value, and only a few enhancements above the mean value for this particular measurement. There are 2.76 crossings per second at the 0 dB level and about 1.1 crossings per second at the -3 dB level.

At the -18 dB level the deep fade crosses this level once, with a relatively small LCR and ADF. The ADF for the 3 dB level is about 0.9 seconds, while the -3 dB level has an ADF of 0.1 seconds. This is due to the lesser number of crossings crossed for the 3 dB level and with relatively small duration's between the crossings , we have a ADF close to 1 second. While at the -3 dB level, we have smaller duration of fades for each individual fade but a larger number of crossings at this level, thus we have a smaller ADF value, which is close to 0.1 seconds.

6.3.8 Transmitter position G and Receiver position C

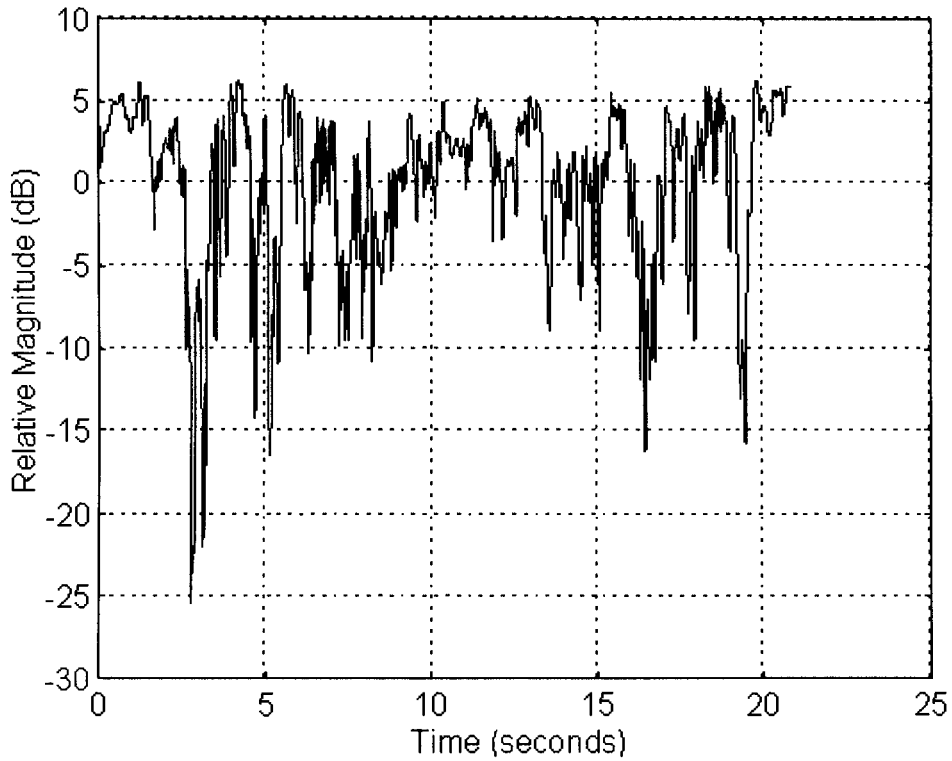


Figure 6.8 Temporal fading envelope for Tx position G and Rx position C

Table 6.8: Statistical parameters of Figure 6.8

Level (dB)	Total Number of Crossings	Level Crossing Rates (crossings / second)	Average Duration of Fades (seconds)
6	6	0.2857	3.229
3	42	2.0002	0.4148
-3	36	1.7144	0.1336
-6	29	1.3811	0.0890
-9	22	1.0477	0.0630
-12	9	0.4286	0.4068
-15	6	0.2857	0.0314
-18	2	0.0952	0.0803
-21	2	0.0952	0.0635
-24	1	0.0476	0.0285

Figure 6.8 represents the fading envelope for the antenna positions mentioned above. The fading envelope represents medium and a couple of deep fades around the 3 to 4 second mark of the measurement period. There are small fades which occurred for the first 2 seconds followed by the two deep fades, and then the envelope tapered off to medium fades and then onto a few enhancements around the 10 second mark. Following this the envelope exhibited smaller fades, then progresses onto medium fades continuing on to the finish. This shows how our movements varied within the 20 seconds of measurement. Rapid motion occurred, constant motion occurred at times and also intermittent affects occurred throughout the measurement period.

The dynamic range of fades for this envelope is similar to that of Figure 6.6, with a range of 31 dB. The deepest fade depth occurred at -25 dB below the mean value. This dynamic fading range once again tells us that, deep fading occurred within the system during measurement time. The dynamic fading range represents a good indication of the amount of fading which is produced within a system when motion is present.

Table 6.8, represents the statistical parameters of Figure 6.8. The number of crossings of the 0 dB level is 52, while the -3 dB and 3 dB levels show 36 and 42 crossings, respectively. The LCR for the 0 dB level was 2.5 crossing per second, while the -3 dB and 3 dB levels had LCR of about 1.7 and 2.0 crossings per second, respectively.

As shown in Table 6.8, the ADF for the 6 dB level was fairly large at 3.23 seconds. As can be seen from Figure 6.8, the duration's of each individual fade at this level is fairly large, some even having duration's of up to 10 seconds long. Due to this large duration's of individual fades and the small number of crossings at this level, we are presented with a large ADF for this particular level. As we progress down the levels, at -24 dB the deep fade only crosses this level once, with a small duration of fade, thus producing a relatively small ADF.

6.3.9 Transmitter position G and Receiver position D

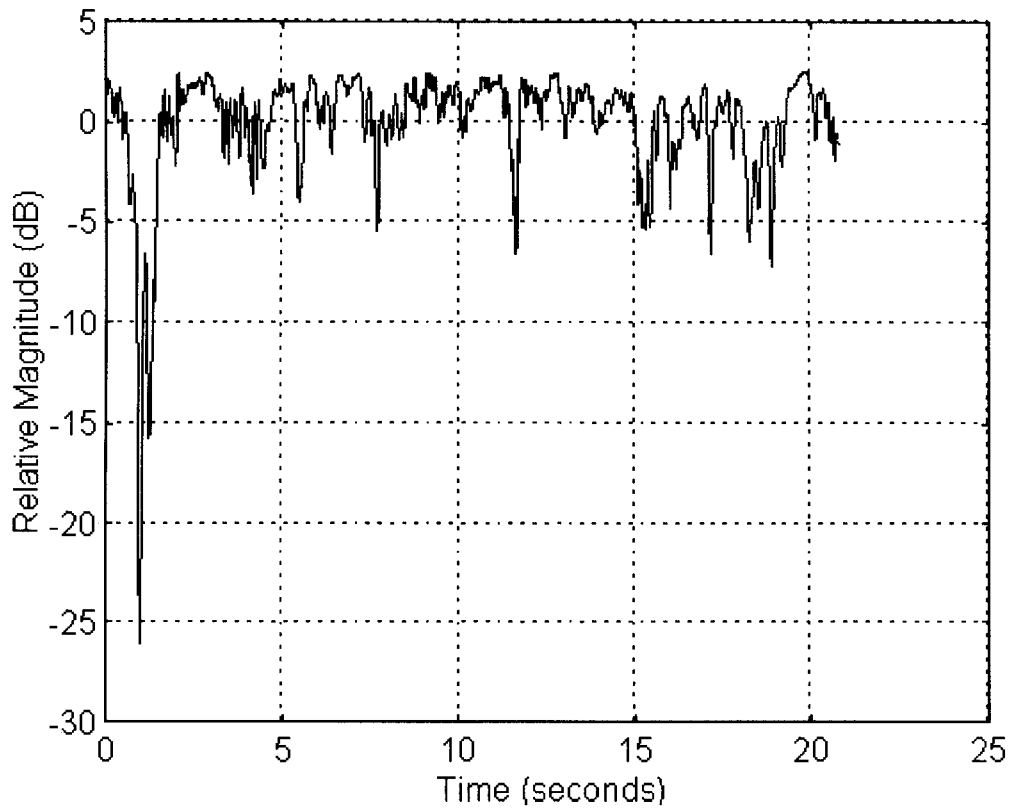


Figure 6.9 Temporal fading envelope for Tx position G and Rx position D

Table 6.9: Statistical parameters of Figure 6.9

Level (dB)	Total Number of Crossings	Level Crossing Rates (crossings / second)	Average Duration of Fades (seconds)
-3	13	0.6191	0.1626
-6	4	0.1905	0.1665
-9	3	0.1429	0.1241
-12	2	0.0953	0.1308
-15	2	0.0953	0.0755
-18	1	0.04763	0.0959
-21	1	0.04763	0.0744
-24	1	0.04763	0.0569

On first sight of Figure 6.9, one thing is clear, there is a deep fade at the initial stages of the measurement period., around the 1.5 second mark. Next to this deep fade there is a medium fade which also occurred around the 1 to 2 second mark. The rest of the envelope fades represent constant motion, showing very little deviation form the mean value.

This deep fade which crossed the -25 dB level could have been myself blocking the LOS path at that instant of time and then moving away and partially blocking this important path again. This is possible, because the way the antennas are positioned they are directly facing each other with a distance of about 1 to 1.5 meters. Most of the motion is around the antennas which are in close proximity to each other, blocking LOS paths did happen once or twice during the measurement period. This kind of motion is good in the context of measurements being conducted, as they show how a WLAN or WPBX system will operate, when the system is introduced to severe motion and/or intermittence effects produced by people in the way of propagation paths carrying important information to the receive terminal.

Table 6.9 represents the statistical properties of Figure 6.9. The number of crossings at the 0 dB level is 47. There are no crossings at the 3 dB level and there are 13 crossings at the -3 dB level. This shows that most of the fades deviated 1 or 2 dB on either side of the mean value. The LCR for the 0 dB level is 2.2 crossings per second, which is fairly accurate. The ADF of the fades at each individual level do not pose any baffling values to surprise the reader.

6.3.10 Transmitter position G and Receiver position E

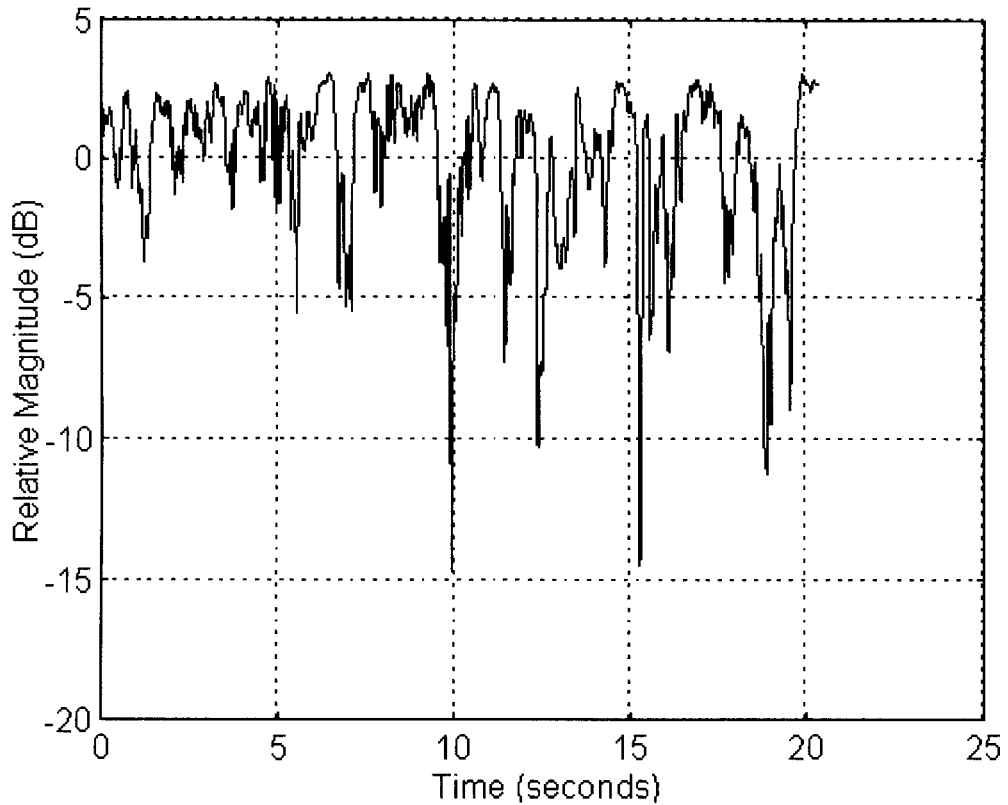


Figure 6.10 Temporal fading envelope for Tx position G and Rx position E

Table 6.10: Statistical parameters of Figure 6.10

Level (dB)	Total Number of Crossings	Level Crossing Rates (crossings / second)	Average Duration of Fades (seconds)
3	4	0.1951	3.1832
-3	23	1.1221	0.1259
-6	11	0.5366	0.0790
-9	5	0.2439	0.0709
-12	2	0.0976	0.0404

Figure 6.10, shows the constant to rapid motion occurring during the measurement period. Medium fades occurred around the 10 to 20 second marks of the measurement period. This could have been my colleague or myself walking more briskly or waving our arms more intensively during this period, with occasional blocking of propagation paths which are important.

The dynamic range for this envelope fade is around 18 dB, thus telling us that medium fades occurred during the measuring time. Table 6.10 shows the statistical parameters of Figure 6.10. The number of crossings at the 0 dB level is 36 and the crossings at the -3 dB level is 23. There weren't many crossings at the 3 dB levels as majority of the fades occurred just above the mean value and lots of fades occurred below the mean value.

The ADF for the 3 dB level is thus quite large, due to the small number of crossings and the large number of duration's between fades. There is a 11 second duration in the last enhancement at the 3 dB level, this would have contributed greatly to the large value of the total individual fade duration's for the 3 dB level.

This, thus concludes the discussion of the fading envelopes and their statistical parameters. To see a better pictorial representation of the number of crossings and the LCR for each of the figures in more detail, I have presented them graphically using Microsoft Excel 5.0 in section 7, as they contribute to the important conclusions which are drawn from the results and statistical analysis of this section.

Before, proceeding to section 7, I mentioned in section 4.6 that the cumulative distribution functions for each of the fading envelopes presented in this section will be compared to the known theoretical distributions as mentioned in section 4.6. Unfortunately, due to time consuming efforts which was needed to analysis these fading statistics and the time constraints involved in getting this report ready on time, I regret to say that the comparison of the data with known theoretical distributions was not possible. This is very unfortunate, as we would have seen how closely our fading envelopes relate to known theoretical distributions and which distribution matches our data most accurately.

Chapter 7

SIGNIFICANCE OF RESULTS

7.1 Introduction

The results and analysis of the fading envelopes and their statistical parameters have been discussed in section 6. The importance of these parameters when critically analysing fading envelopes are very important, as they give a good indication of how a system will perform under multipath fading conditions with temporal variations introduced in the channel. These results can show important system properties which need to be considered for fading conditions when a system is to be designed. The important properties of the fading envelopes will be discussed in this section. Pictorial representations of the number of crossings and the LCR, and the mean statistical parameters of the combined fading envelopes for the various levels will be shown graphically to facilitate understanding.

Following this a discussion of various aspects of the fading envelopes and their parameters in relation to BER and S/N ratio for wireless systems will be conducted. This is to show how these parameters of the fading envelopes can be used in consideration when designing WLAN's and other wireless systems for the ISM band of 2.4 GHz.

7.2 Graphical Representation of the Number of Crossings

The graphical representation of the number of crossings of each of the fading envelopes is shown in this section, it basically, lets the reader interpret the values which are presented in Tables 6.1 to 6.10 pictorially. This shows the importance of the number of crossings at each level and its relationships with BER. The number of crossings for each threshold as represented in Tables 6.1 to 6.10 (see section 6.3), are shown in Figures 7.1 to 7.4. I grouped them together, so that there would less graphs to be presented and thus ease understanding.

As can be seen from Figure 7.1 to 7.4, the values generally start off at lower crossings and then rise sharply to the 0 dB level and then taper off towards the positive dB values. This is the general shape for all the number of crossings of Tables 6.1 to 6.10. The shape kind of follows a Gaussian distribution or a bell curve shape. This is to be expected depending on whether or not an envelope has deep fades or medium fades, there will be less crossings at the deep fades and slightly more at the medium fades and majority around the smaller or shallower fades, which are around the -3 dB and 3 dB levels. All the fading envelopes of section 6.3, have the greatest number of crossings at the 0 dB level, as can be seen when inspecting Figures 7.1 to 7.4. This should be expected, because the fading envelopes were normalised to a mean value of 0 dBm. Most of the fades or enhancements will occur above or below the mean value of 0 dBm.

One important conclusion which can be drawn from Figures 7.1 to 7.4, in respect to the number of crossings, is that if a wireless system (say a WLAN), was operating at the typical worst case receive level of -88 dBm and this typical worst case receive level was set to equal our 0 dB threshold, we would have a maximum fade margin of typically 7 dB before our receive system enters the noise region. At this level of -95 dB, our S/N ratio would be almost zero and the system would be running thousands of errors (very high BER) as the system is completely degraded. If there was information within these deep fades they would be unrecognisable by a detector at the receiver terminal and the information will be decoded as noise as it closely resembles the noise of the typical front end receiver. Thus, deep fades or even medium fades can be very costly in regards to information being propagated across wireless channels depending on the receive levels being used.

This is the case with mobile phones, whereby, they have typical receive levels of -88 dBm and if any fades occur 7 to 8 dB below this mean value, the system will be in the noise region and we can sometimes experience this by the hissing noise which is apparent in the phone. Thus, when we move slightly to the left or right this noise disappears, and we get a clearer signal. We can increase this receive level, by increasing the power level at the transmit terminal. With a greater receive level this will ensure a greater fade margin before a signal enters the noise region and thus better reception. But, the down side of raising the power is that, the battery of the mobile phone needs to

operate at a higher rate, as we are using more of the batteries power and thus, decreasing its life expectancy before recharging is required. Raising the power level, would also be regarded unfavourably by the Spectrum Management Agency, as it may interfere with safety regulations. When designing systems, a balance must be resolved, to ensure the best system is designed with all aspects considered. The number of crossings are shown below in Figure 7.1 to 7.4, with information from Tables 6.1 to 6.10 from section 6.3.

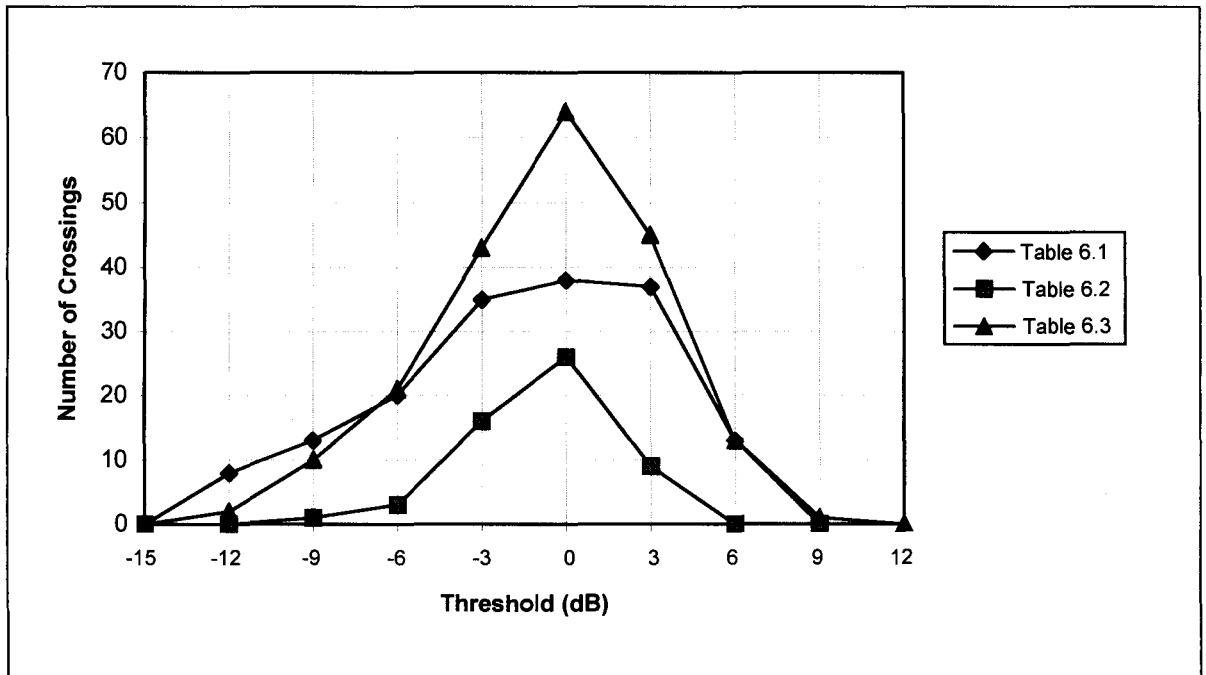


Figure 7.1 Number of crossings of Table 6.1, Table 6.2 and Table 6.3 for the different threshold levels

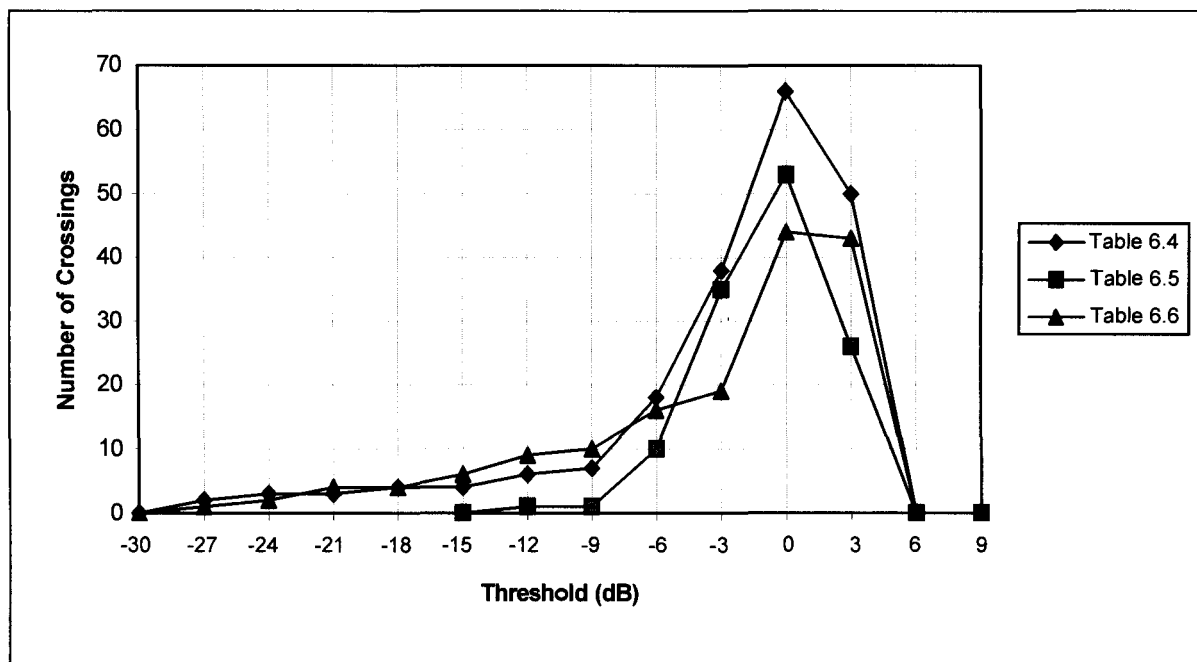


Figure 7.2 Number of crossings of Table 6.4, Table 6.5 and Table 6.6 for the different threshold levels

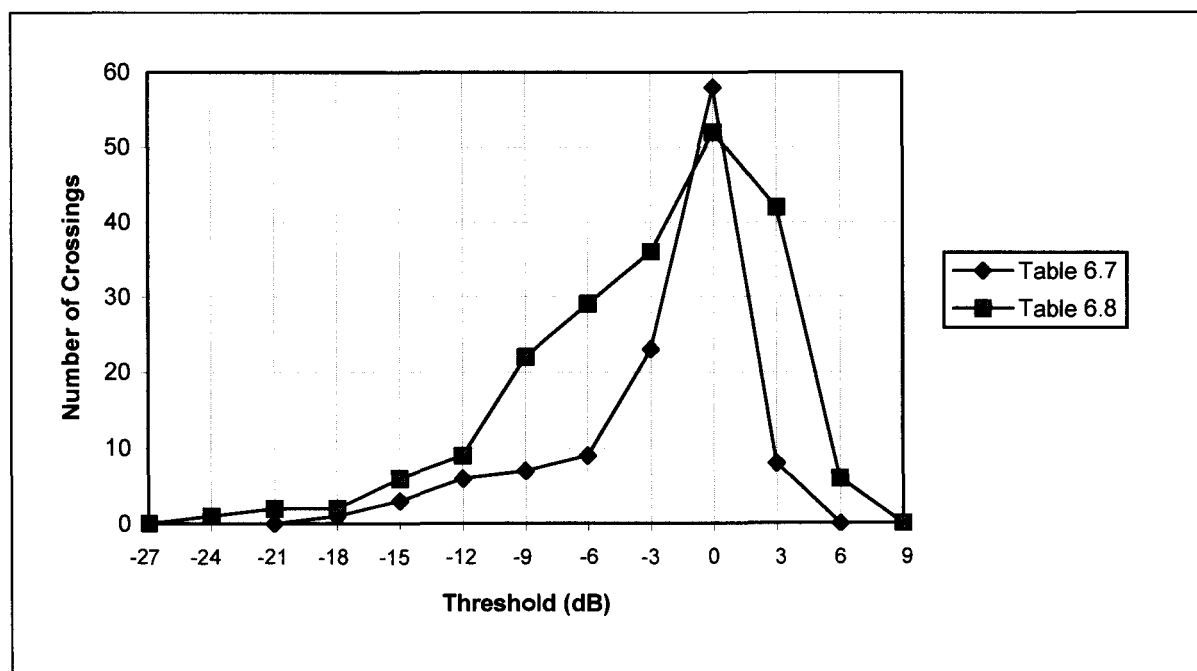


Figure 7.3 Number of crossings of Table 6.7 and Table 6.8 for the different threshold levels

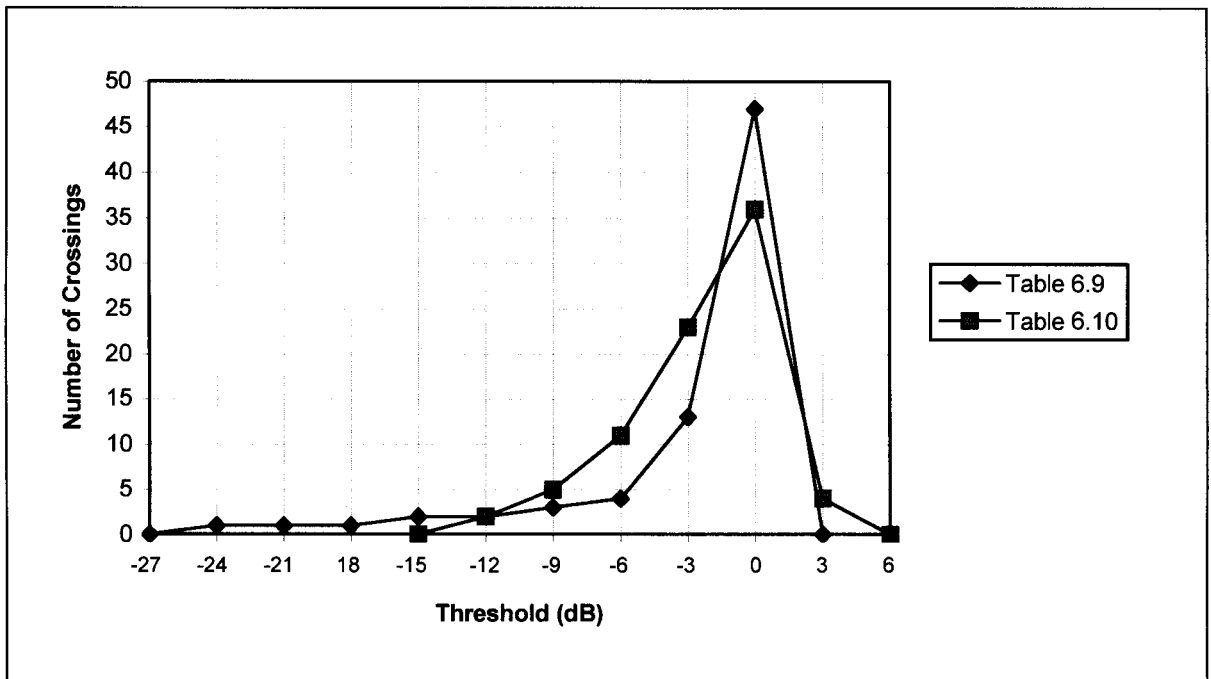


Figure 7.4 Number of crossings of Table 6.9 and Table 6.10 for the different threshold levels

7.3 Graphical Representation of the Level Crossing Rates

The graphical representation of the LCR for each of the fading envelopes are displayed in Figures 7.5 to 7.8. On viewing these figures we can conclude that the LCR have exactly the same shapes as the number of crossings as presented in Figures 7.1 to 7.4. This should be of no surprise, as the LCR is the total number of crossings for each level divided by the total measurement period. Therefore, they show the same shapes as their counterparts, the number of crossings, displayed in Figures 7.1 to 7.4. The LCR are presented pictorial as they show an easier picture or an overall picture of the crossings per second for a specific threshold of a fading envelope. The discussion of the LCR has been conducted in section 6.3, for each fading envelope.

On viewing Figures 7.4 to 7.8, we can see that the 0 dB threshold possess the most crossings per second for the measurement period of 20 seconds. As mentioned in section 7.2, this is expected as the fades or enhancements occur above or below the

mean value. Thus for fades to occur and enhancement to happen they, must swing above of below the mean value, and thus we have more crossings per second for this threshold.

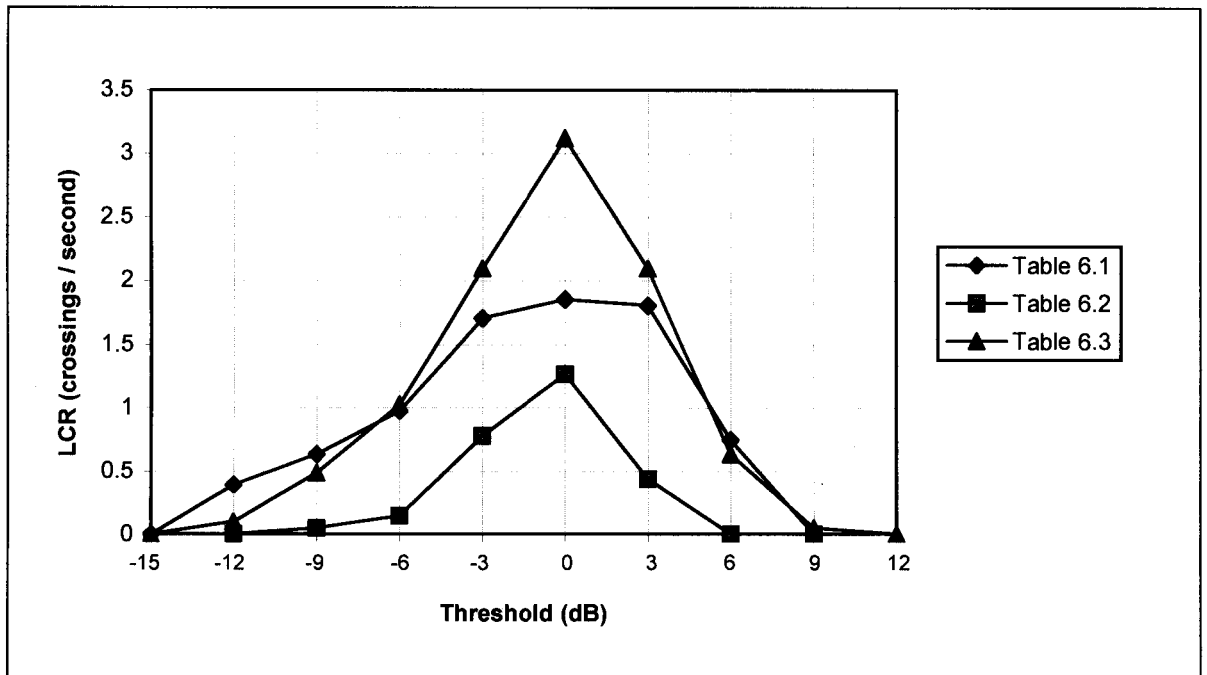


Figure 7.5 Level crossing rates of Table 6.1, Table 6.2 and Table 6.3 for the different threshold levels

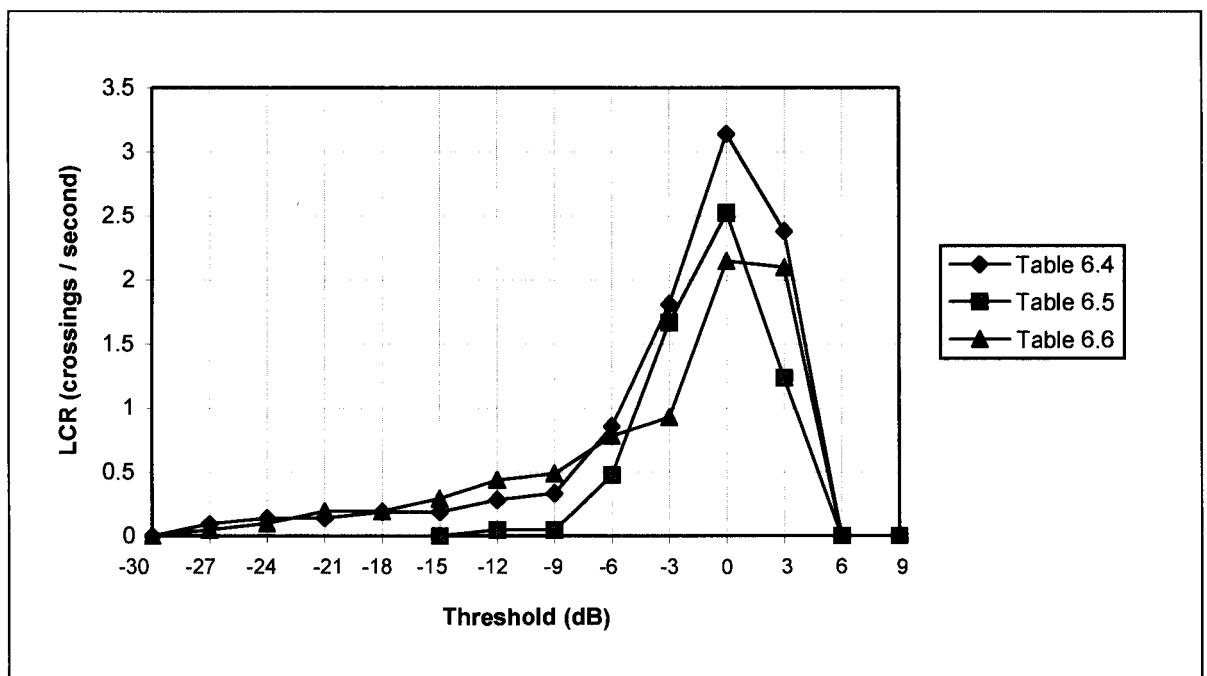


Figure 7.6 Level crossing rates of Table 6.4, Table 6.5 and Table 6.6 for the different threshold levels

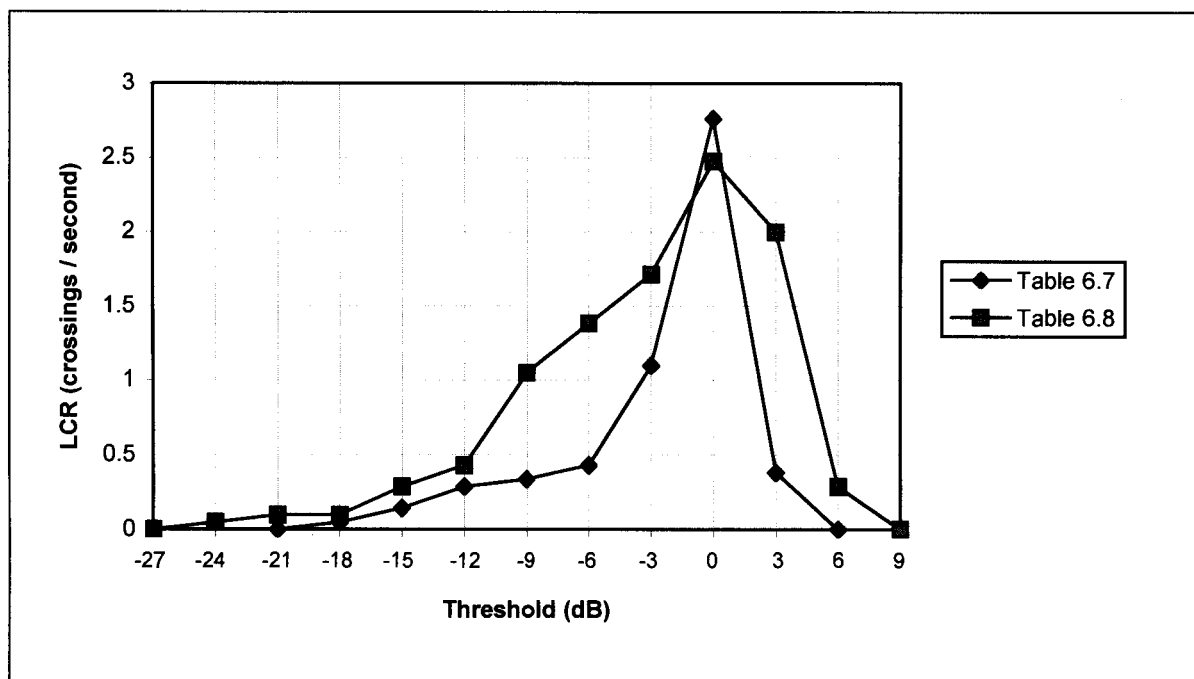


Figure 7.7 Level crossing rates of Table 6.7 and Table 6.8 for the different threshold levels

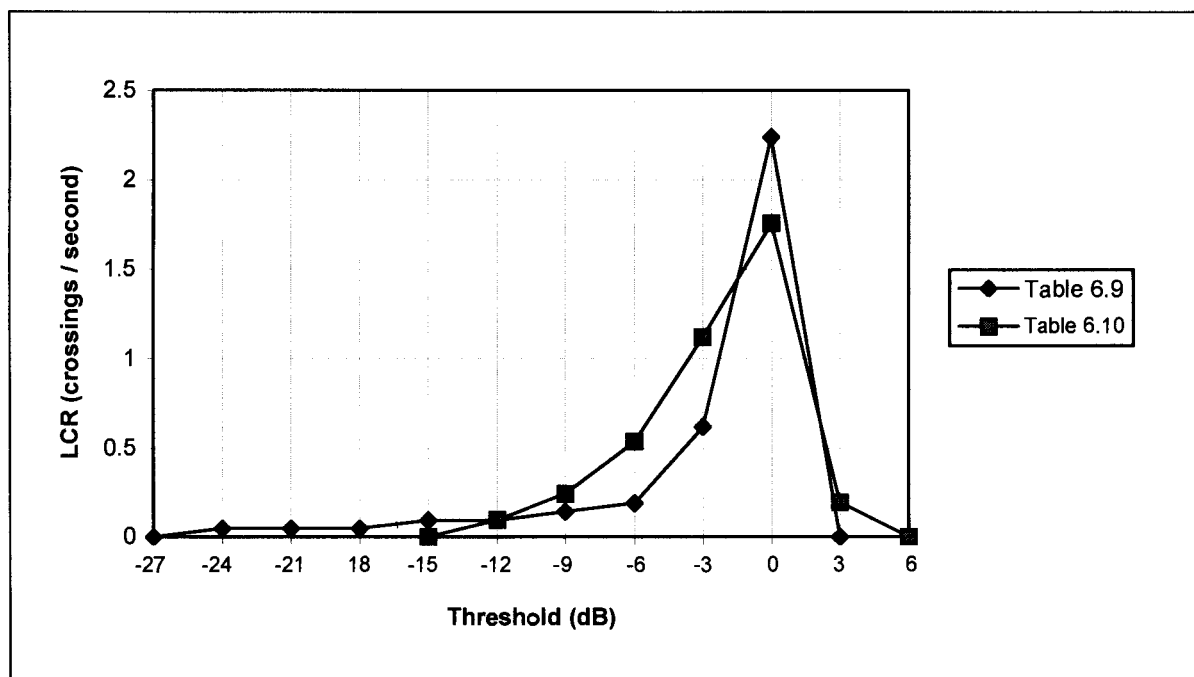


Figure 7.8 Level crossing rates of Table 6.9 and Table 6.10 for the different threshold levels

7.4 Mean Statistical Parameters for Combined Fading Envelopes

This section deals with the mean of the total number of crossings of each threshold for the ten fading envelopes. This mean values for the number of crossings of each level is presented in Table 7.1 and is represented graphically by Figure 7.9. On inspecting Table 7.1 or Figure 7.9, we can clearly see that for the ten measurements which were conducted at the stated antenna positions, an average of about 48 crossings occurred at the 0 dB level. This is expected as mentioned above in section 7.2, the fades and enhancements swing above or below the mean value, thus the 0 dB level has the greatest number of crossings.

We can also see, that on average there were 28 crossings and 26 crossings at the -3 dB and 3 dB thresholds respectively for the combined fading envelopes. This thus, implies that while motion was being created in the channel, we were not affecting many important propagation paths by our motion around the antennas, as we were only moving in one half of the laboratory, basically around the antennas.

Table 7.1 Mean number of crossings for each threshold for the combined fading envelopes

Level (dB)	Mean Number of Crossings
6	3.20
3	26.4
0	48.4
-3	28.3
-6	14.1
-9	7.9
-12	4.5
-15	2.1
-18	1.2
-21	1
-24	0.7
-27	0.3

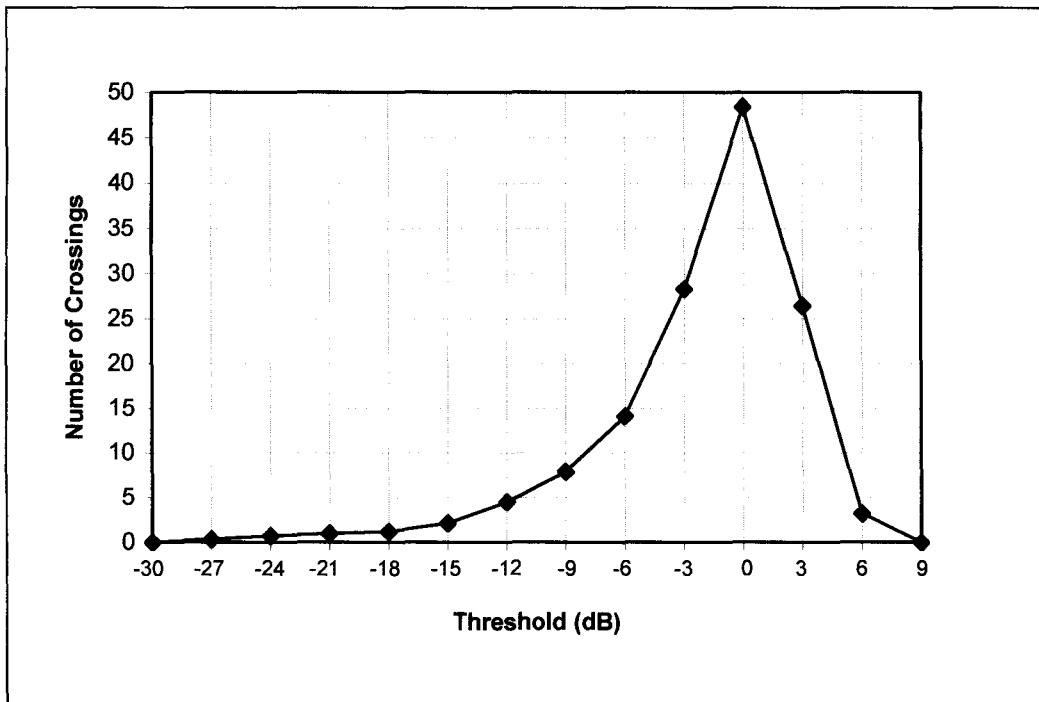


Figure 7.9 Mean number of crossings at each threshold of the combined fading envelopes

Medium or deeper fades occurred less frequently, as can be seen from Table 7.1 or Figure 7.9. This can also be expected, as deeper fades can occur when we block important propagation paths within the channel by our bodies in the way, it can also be caused by our bodies absorbing some the waves, edge scattering the waves off our heads, shoulder, fingers, elbows, watches and also reflections of objects and walls. As mentioned deep fades are unwanted in any system, but they are not preventable but they can be reduced through special techniques.

Table 7.1 and Figure 7.9, show the mean number of crossings of our ten measurements. If new measurements were conducted at the same antenna positions, they would represent different number of crossings, LCR and ADF for each level, as fading is a phenomenon which is very hard to predict. But, with motion introduced in a controlled fashion, under the same environmental conditions as our measurements were conducted, these new measurements would closely relate to our conducted measurements within the laboratory, in a typical cluttered office space.

In designing wireless systems, engineers must conduct these kinds of measurements to see how a newly introduced system will react under fading conditions. The ultimate test would be, if a wireless system could withstand severe fading conditions. In designing new systems, measurements must be conducted for that particular environment to ensure that the environment (office building, factories, supermarkets etc.) can function efficiently under fading conditions. There are many considerations which come into context when designing wireless systems, eliminating or reducing fading is one important factor which must be considered, as a system which is susceptible to deep fades is not a very efficient system.

Mean values for the LCR of the combined fading envelopes are presented in Tables 7.2 and shown graphically in Figure 7.10. As it is apparent from Table 7.2 and Figure 7.10, the highest LCR once again happens at the 0 dB threshold and gradually decreases on either side of the mean value. The mean number of crossings, Figure 7.9, and the mean LCR, Figure 7.10, closely resemble each other. This is expected as mentioned in section 7.3. The mean LCR of all the ten fading envelopes represent statistically valid values for the measurement period of 20 seconds. The mean of the ADF is not presented, as the duration of fades are already averages for a particular threshold of each individual fading envelope. For inspection of the ADF we must look up the values for each fading envelope from Tables 6.1 to 6.10.

Table 7.2 Mean level crossing rates for each threshold for the combined fading envelopes

Level (dB)	Mean Level Crossing Rates (crossings / second)
6	0.1671
3	1.1067
0	2.3292
-3	1.3540
-6	0.6807
-9	0.3220
-12	0.2168
-15	0.1007
-18	0.0576
-21	0.0481
-24	0.0336
-27	0.0144

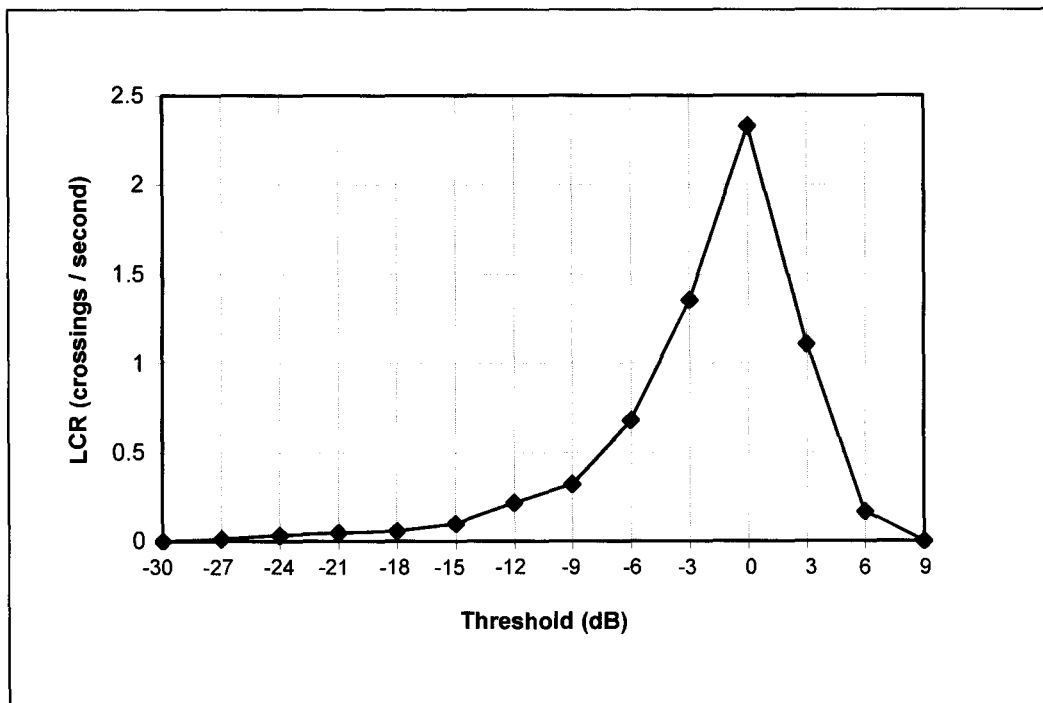


Figure 7.10 Mean level crossing rates at each threshold of the combined fading envelopes

7.5 Discussion of Fading and Bit Error Rates

Section 7.2, briefly mentioned the extent of typical worst case receive levels of around -88 dBm and the relatively small fade margin which is needed before a wireless system enters the noise region and causes irreducible BER due to multipath fading in a temporally varying environment. The example of the mobile phone was mentioned as a typical system which can be affected by severe fading conditions.

As mentioned in section 7.2, if the typical worst case receive level of -88 dBm, was set to our threshold of 0 dB for our fading envelopes, we would only have 7 or 8 dB of fade margin to play with before a system starts to enter the noise region and produce errors. The level of -95 dBm is the typical front end receiver noise level. As our measurements utilised a simplistic quarter wave monopole antenna, we needed to operate our system with worst case receive levels of around -65 dBm, to provide an adequate S/N ratio under fading conditions as shown from the measurement analysis. This was proved by our calibration curve, Figure 5.6 of section 5.5, as we can see from Figure 5.6, the system is affected by the noise region around the -90 dBm level. Therefore wireless systems which are operating at typical worst case receive levels of -88 dBm **must** be able to counter medium to deep fades effectively or else any information which is being sent over the propagation channel will not be recognisable at the receive terminal.

One important conclusion which can be drawn from Figures 7.1 to 7.10, is that for our measurement environment, if wireless system are to be designed, and they are operating at receive levels of -65 dBm, the worst case receive level before the system will start running errors is typically around -88 dBm, therefore, we want to make certain that the deep fades don't go below this typical value of -88 dBm, because the system will then be degraded by these deep fades and will cause a significant BER probability to occur. Basically, we can keep in mind that, the deeper the fade the greater the probability of error occurring in a wireless system.

For example, lets take the highest ADF at a particular level, say -12 dB level, of the fading envelopes, from Tables 6.1 to 6.10 and compare this value with the BER performance. The highest value at the -12 dB threshold is represented in Table 6.8 (see

section 6.3) as 0.4068 seconds for the 9 crossings at this level. This implies that while the fade condition is occurring, for that fade duration, the S/N ratio is being degraded by -12 dB or more, and thus the BER is also increasing. The BER is directly proportional to the S/N ratio degradation in a wireless channel affected by medium to deep fades.

Now, if we were sending a modulated signal across the channel, which is being affected by multipath fading through temporal movement of people, this received signal in relation to ADF will cause a large number of error bursts for the system. For example, if we used the same value for the -12 dB level for the ADF of 0.4068 seconds at that antenna position, and modulate a signal using BPSK at 4 million symbols per second, we can count the number of symbols which would be affected by these fades. This calculation is shown below,

$$\text{Number of Symbols degraded} = \text{symbol rate} \times \text{ADF of that threshold}$$

For our example, it follows that the symbols degraded per second is,

$$\begin{aligned} \text{Number of Symbols degraded} &= (4 \times 10^6) \times 0.4068 \\ &= 1.63 \times 10^6 \text{ symbols} \end{aligned}$$

This shows, that the -12 dB fade causes 1.63 million bits to be affected by this fade duration. This does not mean that 1.63 million bits are in error, but rather 1.63 million bits can be affected by this fade. This directly leads to the degradation of the S/N ratio for this ADF and consequently affecting the BER. Therefore in the 20 second measurement period, the BER will be constantly changing depending on the fades depths of the fading envelope. For the -3 dB or 3 dB levels there will be less probability of a bit error being produced per bit and for say -15 dB level, there would be a greater probability of an error occurring per bit and for the -27 dB level there would be a large probability of errors occurring per bit for a fading envelope.

This clearly shows that modulated information is affected tremendously by medium to deep fades. At different time periods within the measurement time, the S/N ratio of the system will also be continuously changing depending on the how deep a signal fades to. If the typical worst case receive level of -88 dBm is used, fades of 7 dB to 8 dB below the mean value will result in a BER probability that would produce thousands of errors in a system and information sent across the channel will be deeply affected by these fades. Fades at the -27 dB level, would be producing continuous errors and the system will be severely affected by these deep fades.

As mentioned earlier, one way to increase the typical worst case receive level is to increase the transmit power at the transmit terminal and thus give the system a greater fade margin before entering the noise region, which is around -95 dBm. Unfortunately, by increasing the transmit power the receive terminal will also have to operate at a higher power level, and this directly affects any equipment running in the wireless system or network as they require greater amounts of power to operate at a higher receive level. If, we are using a laptop computer in the WLAN, this would mean that the laptop will be utilising more of its battery power and thus shortening its life and this will thus, lead to quicker recharge periods. This is not very favourable, in the context of power usage, as we don't want to keep recharging the battery every 1 to 2 hours. This would also disrupt any work being conducted at a terminal, as we would have more computer crashes due to more errors being introduced into the system by these medium to deep fade conditions.

Designing wireless systems is a complicated process, there are many conditions or aspects which must be considered before introducing the most efficient system for a particular environment, whereby users will benefit from the efficiency of the system to work effectively. Multipath fading in systems, especially medium to deep fades must be reduced to ensure that less errors are introduced into the system at any given time and thus improve the efficiency of the system.

Chapter 8

CONCLUSION

The main objectives of this report have been accomplished without to many problems. The strategy which was followed to accomplish this report proved to be very effective. The literature search was conducted prior to any measurements being conducted. The literature research revealed that although there has been numerous research and work being conducted on wireless communication channels for various frequency ranges, there has not been any published research or findings which deal with the ISM band of 2.4 to 2.5 GHz for wireless systems. Therefore, the results and statistical analysis conducted in this project report can be used to design wireless indoor radio communication systems.

The theory presented in sections 3 and 4 was a direct result of this literature search. Although, the theory presented in this report may seem trivial at times, but it is the building block of the entire report as it provides the reader with an insight into the characteristics of wave propagation and the phenomenon of multipath fading. This is very important in the context of this report, as a good understanding of the nature of fading in the wireless channel needs to be grasped before any further involvement is proceeded.

Once, a good understanding of fading is grasped, the further involvement into this project can be appreciated. Section 5, presented the main core of the system measurements. Important, consideration have been put forward in this section. The main thrust, being the measurement equipment used, the measurement environment where the recordings were conducted and the measurement system used to collect the results. This is basically, the heart of the project, whereby the measurements were conducted in a typical cluttered environment with controlled motion introduced for the entire measurement period. This measurement environment makes this report feasible, as it represents a cluttered laboratory with motion being introduced for the 20 second measurement period. If, wireless systems are to be designed and commissioned, they would be working in a similar environment with motion always present within the channel.

Section 6 presented the findings of the measurements conducted. The results and their statistical analysis can be considered when wireless systems for the similar frequency band need to be designed. The results provided important information regarding the envelope fades at the different antenna locations within the laboratory. With the multipath nature of fading and the introduction of motion within the channel, the direct consequences of this motion can be viewed on the fading envelopes. The envelopes provide vital information, such as the depth of a fade, is it a shallow, medium or deep fade. Other information can also be deduced from the envelopes, we can see at what times there was rapid motion, constant motion or relatively slow and constant motion. These envelopes provided, the systems engineer with vital clues as to how a newly designed and commissioned system will work with typical motion within the propagation channel in progress.

The statistical analysis, also provides important information. It tells us, the number of crossings, level crossing rates (LCR) and the average duration of a fade (ADF). From this we can see how many times a particular fade crosses a particular level and how long the fade duration is for. This is important, as we want to try to eliminate medium to deep fades from a channel to ensure good reception of information. By viewing the statistical parameters of the fading envelopes for their particular antenna positions, we can predict for a specific location within a room or office space and with the same motion in progress we will receive similar fades for that location. This gives engineers clues on designing a system for a particular environment with the same motion present at different times.

Section 7 considered the significance of the results and its relationship to bit error rates caused by fading. This section also graphically presented the information pertaining to the statistical parameters of the fading envelopes. The relationship of medium to deep fades can be outlined. By having deep fades within a system, the system will produce errors. The deep the fade the worst the S/N degradation and consequently the higher the probability of an error occurring within a system at a particular time. This is an aspect which, systems designers must try to reduce or eliminate, the medium to deep fades. The antenna system used in this project deliberately consisted of a simplistic design, and thus did allow measurements of medium to deep fades for some envelope fading

waveforms to occur. But, with more intelligent antenna systems, medium to deep fades can be either reduced or substantially eliminated. This simplistic antenna would provide a good system if only voice communication is required across a wireless system. But, with WLAN's the main transfer of information will be data and thus better, more sophisticated antenna systems need to be designed.

The results and statistical analysis can also be used for simulation purposes. Whereby, the data presented can be used to specify the characteristics for a simulation system which would be operating with an intelligent antenna system. The results for this simulation can be compared with our experimental results to see how feasible these simulation results are. Would they be significantly better, moderately better or marginally better than our experimented results and statistical analysis. If these results show a mark improvement for the environment under consideration, then these intelligent antenna systems can be designed for use within the WLAN. This would be a recommendation for future research

Other techniques which could improve BER performance with the S/N ratio degradation of a system being affected by medium to deep fades can be Code Division Multiple Access (CDMA). The uses of intelligent antenna systems working in combination with diversity techniques, such as space diversity, can also be used to improve the S/N ratio degradation which is affected by deep fading within a wireless channel.

Finally, the measurements and their consequent statistical analysis completed within this project, present data that can be used as a basis for further research and design of efficient antenna systems. The need for an intelligent antenna system for WLAN's has been clearly identified as a requirement necessary to achieve acceptable BER performances over the indoor radio propagation channel.

REFERENCES

- [1] Anderson, J.B., Rappaport, T.S. and Yoshida, S., "Propagation measurement and models for wireless communications channels", *IEEE Communications Magazine*, January 1995, pp. 42-49.
- [2] Bultitude, R.J.C., Mahmoud, S.A. and W.A. Sullivan, "A comparison of the indoor radio propagation characteristics at 910 MHz and 1.75 GHz," *IEEE Journal on Selected Areas in Communications*, vol. 7, no. 1, January 1989, pp. 20-30.
- [3] Bultitude, R.J.C., Melancon, P., Zaghoul, H., Morrison, G. and Prokki, M., "The dependence of indoor radio channel multipath characteristics on transmit/receive ranges," *IEEE Journal on Selected Areas in Communications*, vol. 11, no. 7, September 1993, pp. 979-989.
- [4] Carr, J.J., (1988), "The Fundamentals of Antenna Design", Prentice-Hall Inc., Englewood Cliffs, New Jersey.
- [5] Couch II, L.W., "Digital and Analog Communication Systems", Fourth Edition, Macmillan Publishing Company, New York.
- [6] Elbert, B.R., (1987), "Introduction to Satellite Communication", Artech House Inc., Massachusetts.
- [7] Feher, Dr. K., (1987), "Advanced Digital Communications: System and Signal Processing Techniques", Prentice-Hall Inc., Englewood Cliffs, New Jersey.
- [8] Ganesh, R. and Pahlavan, K., "On the modelling of fading multipath indoor radio channels", *IEEE*, 1989, pp. 1346-1350.
- [9] Hashemi, H., Lee, D. and Ehman, D., "Statistical modeling of the indoor radio propagation channel - part II", *IEEE*, 1992, pp. 839-843.

- [10] Hashemi, H., "The indoor radio propagation channel," *Proceedings of the IEEE*, vol. 81, no. 7, July 1993, pp. 943-965.
- [11] Hashemi, H., McGuire, M., Vlasschaert, T. and Tholl, D., "Measurements and modelling of temporal variations of the indoor radio propagation channel," *IEEE Transactions on Vehicular Technology*, vol. 43, no. 3, August 1994, pp. 733-737.
- [12] Hislop, J.C., (1996), "Analysis of Background Noise for Wireless Microwave LAN Channels", *Honours Thesis Dissertation*, Department of Computer and Communication Engineering, Edith Cowan University, Joondalup Campus, Western Australia.
- [13] Honcharenko, W., et. al., "Mechanisms governing UHF propagation on single floors in modern office buildings", *IEEE Transactions on Vehicular Technology*, vol. 41, no. 4, November 1992, pp. 996-504.
- [14] Honcharenko, W., Bertoni, H.L. and Dailing, J., "Mechanisms governing propagation between different floors in buildings", *IEEE Transactions on Antennas and Propagation*, vol. 41, no. 6, June 1993, pp. 767-790.
- [15] Ippolito Jr., L.J., (1986), "Radiowave Propagation in Satellite Communications", Van Nostrand Reinhold Company, New York.
- [16] Ivanek, F., (1989), "Terrestrial Digital Microwave Communications", Artech House Inc, Massachusetts.
- [17] Kennedy, G. and Davis, B. (1993), "Electronic Communication Systems", Glencoe Division, Macmillan/McGraw-Hill, Ohio.
- [18] Lee, E.A. and Messerschmitt, D.G., (1988), "Digital Communication", Kluwer Academic Publishers, Massachusetts.

-
- [19] Lee, W.C.Y., (1993), "Mobile Communications Design Fundamentals", Second Edition, John Wiley & Sons Inc., New York.
- [20] Linnartz, J-P., (1993), "Narrowband Land-Mobile Radio Networks", Artech House Inc., Massachusetts.
- [21] Parsons, J.D. and Gardiner, J.G., (1989), "Mobile Communication Systems", Blackie and Sons Ltd., London.
- [22] Proakis, J.G. and Salehi, M., (1994), "Communication Systems Engineering", Prentice-Hall International Edition, Prentice-Hall Inc., Englewood Cliffs, New Jersey.
- [23] Proakis, J.G., (1995), "Digital Communications", Third Edition, McGraw-Hill International Edition, McGraw-Hill Inc., New York.
- [24] Rappaport, T.S. and McGillem, C.D., "UHF fading in factories", *IEEE Journal on Selected Areas in Communications*, vol. 7, no. 1, September 1993, pp. 40-48.
- [25] Rappaport, T.S. and Sandhu, S., "Radio-wave propagation for emerging wireless personal-communication systems", *IEEE Antennas and Propagation Magazine*, vol. 36, no. 5, October 1994, pp. 14-23.
- [26] Resnick, R., Halliday, D. and Krane, K.S. (1992), "Physics: volume 1", Fourth Edition, John Wiley & Sons Inc, New York.
- [27] Roden, M.S., (1988), "Digital Communication Systems Design", Prentice-Hall Inc., Englewood Cliffs, New Jersey.
- [28] Sadiku, M.N.O., (1994), "Elements of Electromagnetics", Second Edition, Harcourt Brace College Publishers, Florida.

- [29] Tam, W.K. and Tran, V.N., "Propagation modelling for indoor wireless communication", *Electronics & Communication Journal*, October 1995, pp. 221-228.
- [30] Tomasi, W., (1988), "Electronic Communications Systems: Fundamentals Through Advanced", Prentice-Hall Inc., Englewood Cliffs, New Jersey.
- [31] Walker, E.A., (1996), "Modelling the indoor radio propagation channel as a physical medium for high speed data transmission," *Progress PhD Thesis*, Department of Computer and Communication Engineering, Edith Cowan University, Joondalup Campus, Western Australia.
- [32] Lee, W.C.Y., (1989), "Mobile Cellular Telecommunications Systems", McGraw-Hill Book Company, New York.

APPENDIX

The following glossary presents the standard terms and definitions used in chapter 1. These standards and terms are referenced from, IEEE (1993), "The New Institute of Electrical and Electronics Engineers (IEEE) Standard Dictionary of Electrical and Electronics Terms", Fifth Edition, IEEE Inc., New York. It is based on the IEEE standard 100-1992. The following terms and definitions deal with radiowave propagation only. The definitions and terms explained here are only very basic, for more definitions and terms in relation to radiowave propagation, please look up the IEEE standards dictionary.

Absorption. The irreversible conversion of energy of an electromagnetic wave into another form of energy as a result of wave interaction with matter.

Diffraction. The deviation of the direction of energy flow of a wave, not attributable to reflection and/or refraction, when it passes an obstacle, a restricted aperture, or other inhomogeneities in a medium.

Electromagnetic radiation (antennas). The emission of electromagnetic energy from a finite region in the form of unguided waves

Fading. The temporal variation of received signal power caused by changes in the transmission medium or path(s).

Fresnel zone. In general, any surface or region bounded by adjacent Fresnel ellipses or ellipsoids. For instance, any plane through both antennas will intersect Fresnel ellipses and define Fresnel zones in that plane.

Free space. Free of obstructions and characterised by the constitutive parameters of a vacuum.

Microwaves (data transmission). A term used rather loosely to signify radiowaves in the frequency range from about 1000 megahertz (MHz) upwards.

Multipath propagation. The propagation phenomenon that results in signals reaching the receiving antenna by two or more paths. When two or more signals arrive simultaneously, the wave interference results. The received signal fades if the wave interference is time varying or if one of the terminals is in motion.

Refraction. Of a travelling wave, the change in direction of propagation resulting from the spatial variation of refractive index of the medium

Reflection. For two media, separated by a plane interface, that part of the incident wave which is returned to the first medium. The direction of propagation of the reflected wave is given by Snell's Law.

Scattering. A process in which the energy of a travelling wave is dispersed in a direction by means other than reflection and refraction.